

Delineating Sources of Groundwater Recharge in an Arsenic-Affected Holocene Aquifer in Cambodia Using Stable Isotope-Based Mixing Models

Laura A. Richards^{1*}, Daniel Magnone², Adrian Boyce³, Maria J. Casanueva-Marenco⁴, Bart E. van Dongen¹, Christopher J. Ballentine⁵, David A. Polya¹

¹School of Earth and Environmental Sciences and Williamson Research Centre for Molecular Environmental Science, The University of Manchester, Williamson Building, Oxford Road, Manchester, M13 9PL, UK

²Present address: School of Geography, University of Lincoln, Brayford Pool, Lincoln, Lincolnshire, LN6 7TS, UK

³Scottish Universities Environmental Research Centre, East Kilbride, G75 0QF, UK

⁴Present address: Department of Analytical Chemistry, Institute of Biomolecules, Faculty of Sciences, University of Cádiz, Cádiz, Spain

⁵Present address: Department of Earth Sciences, University of Oxford, South Parks Road, Oxford OX1 3AN, UK

*Corresponding author: laura.richards@manchester.ac.uk

HYDROL23862R1

Highlights

-
- Stable isotopes (δD and $\delta^{18}\text{O}$) and Cl/Br distinguish As-affected groundwater bodies
 - Relative extent of evaporation of groundwater sources estimated using mixing models
 - Chemical signatures of high As groundwaters indicate varying recharge contributions

Delineating Sources of Groundwater Recharge in an Arsenic-Affected Holocene Aquifer in Cambodia Using Stable Isotope-Based Mixing Models

Laura A. Richards^{1*}, Daniel Magnone², Adrian Boyce³, Maria J. Casanueva-Marenco⁴, Bart E. van Dongen¹, Christopher J. Ballentine⁵, David A. Polya¹

¹School of Earth and Environmental Sciences and Williamson Research Centre for Molecular Environmental Science, The University of Manchester, Williamson Building, Oxford Road, Manchester, M13 9PL, UK

²Present address: School of Geography, University of Lincoln, Brayford Pool, Lincoln, Lincolnshire, LN6 7TS, UK

³Scottish Universities Environmental Research Centre, East Kilbride, G75 0QF, UK

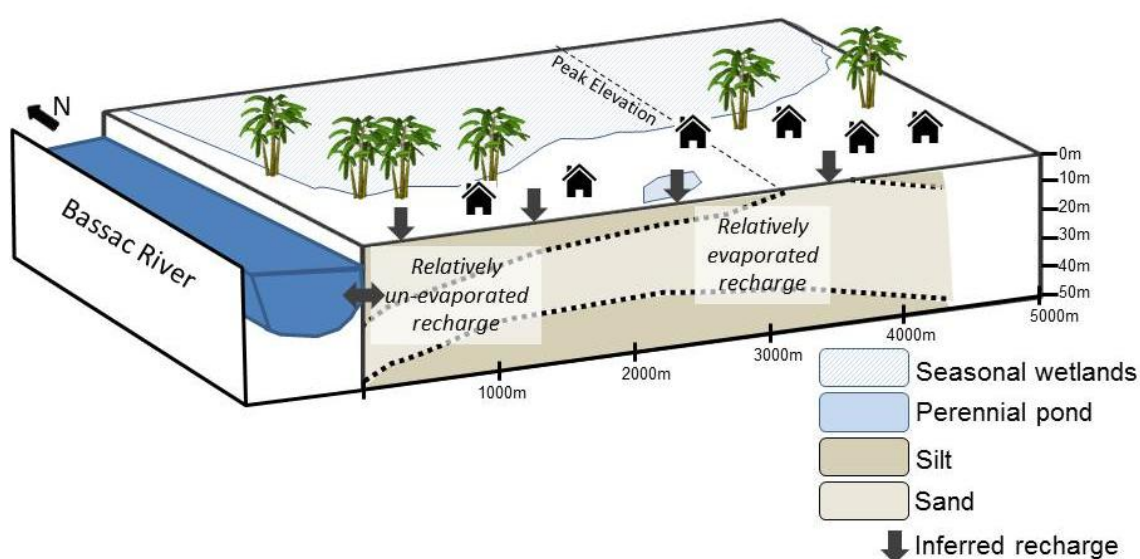
⁴Present address: Department of Analytical Chemistry, Institute of Biomolecules, Faculty of Sciences, University of Cádiz, Cádiz, Spain

⁵Present address: Department of Earth Sciences, University of Oxford, South Parks Road, Oxford OX1 3AN, UK

*Corresponding author: laura.richards@manchester.ac.uk

HYDROL23862R1

Graphical Abstract



Delineating Sources of Groundwater Recharge in an Arsenic-Affected Holocene Aquifer in Cambodia Using Stable Isotope-Based Mixing Models

Laura A. Richards^{1*}, Daniel Magnone², Adrian Boyce³, Maria J. Casanueva-Marengo⁴, Bart E. van Dongen¹, Christopher J. Ballentine⁵, David A. Polya¹

¹School of Earth and Environmental Sciences and Williamson Research Centre for Molecular Environmental Science, The University of Manchester, Williamson Building, Oxford Road, Manchester, M13 9PL, UK

²Present address: School of Geography, University of Lincoln, Brayford Pool, Lincoln, Lincolnshire, LN6 7TS, UK

³Scottish Universities Environmental Research Centre, East Kilbride, G75 0QF, UK

⁴Present address: Department of Analytical Chemistry, Institute of Biomolecules, Faculty of Sciences, University of Cádiz, Cádiz, Spain

⁵Present address: Department of Earth Sciences, University of Oxford, South Parks Road, Oxford OX1 3AN, UK

*Corresponding author: laura.richards@manchester.ac.uk

HYDROL23862R1 Revisions for *Journal of Hydrology*

2017

Abstract

Chronic exposure to arsenic (As) through the consumption of contaminated groundwaters is a major threat to public health in South and Southeast Asia. The source of As-affected groundwaters is important to the fundamental understanding of the controls on As mobilization and subsequent transport throughout shallow aquifers. Using the stable isotopes of hydrogen and oxygen, the source of groundwater and the interactions between various water bodies were investigated in Cambodia's Kandal Province, an area which is heavily affected by As and typical of many circum-Himalayan shallow aquifers. Two-point mixing models based on δD and $\delta^{18}O$ allowed the relative extent of evaporation of groundwater sources to be estimated and allowed various water bodies to be broadly

distinguished within the aquifer system. Model limitations are discussed, including the spatial and temporal variation in end member compositions. The conservative tracer Cl/Br is used to further discriminate between groundwater bodies. The stable isotopic signatures of groundwaters containing high As and/or high dissolved organic carbon plot both near the local meteoric water line and near more evaporative lines. The varying degrees of evaporation of high As groundwater sources are indicative of differing recharge contributions (and thus indirectly inferred associated organic matter contributions). The presence of high As groundwaters with recharge derived from both local precipitation and relatively evaporated surface water sources, such as ponds or flooded wetlands, are consistent with (but do not provide direct evidence for) models of a potential dual role of surface-derived and sedimentary organic matter in As mobilization.

Keywords

stable isotopes, mixing models, recharge sources, arsenic, groundwater

1. Introduction

The chronic exposure to groundwater containing dangerous concentrations of naturally-occurring As is a major threat to public health affecting millions of people in South and Southeast Asia (Smedley and Kinniburgh, 2002; Charlet and Polya, 2006; Ravenscroft et al., 2009; World Health Organization, 2011). In the shallow groundwaters typical to this region, the primary mechanism of As release is widely thought to be the reductive dissolution of As-bearing Fe(III) minerals driven by metal-reducing bacteria and fuelled by bioavailable organic matter (Bhattacharya et al., 1997; Islam et al., 2004; van Geen et al., 2004; Charlet and Polya, 2006; Postma et al., 2007; Rowland et al., 2009). However, the comprehensive understanding of the nature of the organic matter implicated in As-release remains limited. Various inputs are generally thought to contribute in some proportion to As mobilization, including: (i) plant-derived organic matter internal to the sediment aquifers (Nickson et al., 1998; McArthur et al., 2001; McArthur et al., 2004); (ii) external, modern surface-derived organic matter, largely from ponds, rivers and rice paddies and/or wastewater inputs (Harvey et al., 2002; Kocar et al., 2008; Papacostas et al., 2008; Polizzotto et al., 2008;

Neumann et al., 2010; McArthur et al., 2012; Lawson et al., 2013; Lawson et al., 2016), which may be exacerbated by large-scale groundwater abstraction (Harvey et al., 2002; Aggarwal et al., 2003; Harvey et al., 2003; van Geen et al., 2003; Sengupta et al., 2008; Neumann et al., 2010; McArthur et al., 2011; Lawson et al., 2013; Mailloux et al., 2013); and/or (iii) petroleum-derived hydrocarbons from thermally mature sediments (Rowland et al., 2007; van Dongen et al., 2008; Rowland et al., 2009; Al Lawati et al., 2012; Al Lawati et al., 2013). The nature of the organic matter implicated in As release is inherently linked to the sub-surface location where As release occurs and the subsequent controls on As mobility (Nickson et al., 1998; Harvey et al., 2002; McArthur et al., 2004; Gault et al., 2005; Rowland et al., 2007; van Dongen et al., 2008; Neumann et al., 2009; Rowland et al., 2009; Fendorf et al., 2010; Mladenov et al., 2010; Datta et al., 2011; McArthur et al., 2011; Neumann et al., 2011; Al Lawati et al., 2012; Al Lawati et al., 2013; Lawson et al., 2013; Neumann et al., 2014; Lawson et al., 2016; Schaefer et al., 2016; Stuckey et al., 2016). Thus, determining the relative importance of the various potential organic matter inputs is critical in predicting how As hazard may change in the future (Harvey et al., 2002; Polya and Charlet, 2009; Lawson et al., 2016).

The stable isotopes of hydrogen (H, D) and oxygen (^{16}O , ^{18}O) have been used extensively in hydrological studies, including but not limited to the context of As mobilization, to assess groundwater recharge processes, **determine sources of** groundwaters and identify interactions between different water bodies (Aggarwal et al., 2000; Stuben et al., 2003; van Geen et al., 2003; Harvey et al., 2005; Zheng et al., 2005; Klump et al., 2006; Mukherjee et al., 2007; Berg et al., 2008; Sengupta et al., 2008; Datta et al., 2011; Lawson et al., 2013; Lawson et al., 2016). In As-based studies, $\delta^{18}\text{O}$ and δD data have been used to suggest that pond water does not significantly recharge (and thus contribute organic matter) to As-bearing groundwater (van Geen et al., 2003; Sengupta et al., 2008; Datta et al., 2011), whereas others have argued that surface-derived organic matter is an essential driver in As mobilization (Harvey et al., 2002; Kocar et al., 2008; Papacostas et al., 2008; Polizzotto et al., 2008; Neumann et al., 2010; Lawson et al., 2013; Lawson et al., 2016). Stable isotopes are a powerful tool because they are chemically inert (*e.g.* fully conservative) and are directly incorporated into the water molecule, providing robust evidence of direct hydrological processes. In addition, the Cl/Br ratio is a conservative chemical tracer, which has been

used to distinguish different water sources and as an indicator of water-rock interactions (particularly halite dissolution), leaching or wastewater influence on a groundwater (e.g. Davis et al., 1998; Alcalá and Custodio, 2005; Cartwright et al., 2006; McArthur et al., 2012; Xie et al., 2012; Majumder et al., 2016; McArthur et al., 2016) and references within.

The variation in the $\delta^{18}\text{O}$ and δD isotopic signature of natural waters is largely controlled by thermodynamic fractionation, occurring because of physical processes such as evaporation and condensation. The thermodynamic fractionation results in water bodies with isotopically distinct signatures and also produces a defined relationship between δD and $\delta^{18}\text{O}$ for global meteoric precipitation known as the Global Meteoric Water Line (GMWL) (Craig, 1961). The extent of deviation of the isotopic signature of a natural water from the GMWL along evaporation lines reflects the magnitude of the kinetic effect, with greater deviations indicating more extensive evaporation (Craig and Gordon, 1965; Gat, 1971). The isotopic composition varies geographically due to the latitude, amount, elevation and continental effects (Dansgaard, 1974; Clark and Fritz, 1997). Temporal variations can be significant particularly in tropical areas such as Southeast Asia where the isotopic depletion correlates well with the amount of precipitation (Araguás-Araguás and Froehlich, 1998; Araguás-Araguás et al., 2000). These processes determine the isotopic signature of precipitation as well as the evolution of the isotopic signature of surface waters, both of which may contribute to groundwater recharge.

In the shallow aquifers of Kandal Province, Cambodia, in the Lower Mekong Basin, groundwater concentrations of As are well known to be highly heterogeneous and far exceed health-based guidelines (Appelo and Postma, 1993; Polyá et al., 2003; Polyá et al., 2005; Tamura et al., 2007; Benner et al., 2008; Kocar et al., 2008; Polizzotto et al., 2008; Rowland et al., 2008; van Dongen et al., 2008; Polyá and Charlet, 2009; Lawson et al., 2013; Lawson et al., 2016; Richards et al., 2017a). Here, As mobilization seems to be affected by complex, site-specific surface-groundwater interactions as well as in-aquifer interactions which lead to a potential dual role for both surface and sedimentary organic carbon in As mobilization (Lawson et al., 2013; Lawson et al., 2016). The interpretation of the stable isotope and Cl/Br signatures of these As-bearing groundwaters allows for the characterization of recharge mechanisms and systematics, which may assist in improving the understanding of the potential controls on the nature and/or relative contributions of

organic matter affecting As mobilization (Nickson et al., 1998; Harvey et al., 2002; McArthur et al., 2004; Gault et al., 2005; Rowland et al., 2007; van Dongen et al., 2008; Neumann et al., 2009; Rowland et al., 2009; Fendorf et al., 2010; Mladenov et al., 2010; Al Lawati et al., 2012; Al Lawati et al., 2013; Lawson et al., 2013; Neumann et al., 2014; Lawson et al., 2016). The aim of this study is thus to characterize the source of As-affected groundwater in two high-resolution profiles along inferred groundwater flowpaths, with the following objectives: (i) to assess the recharge sources of the groundwater; (ii) to categorize the systematics of surface waters (ponds, rivers, precipitation); and (iii) to differentiate between groundwater bodies within the aquifer via mixing models derived from stable isotope ($\delta^{18}\text{O}$ and δD) signatures to determine the relative extent of evaporation of groundwater sources, as well as by using the conservative tracer Cl/Br.

2. Methods and Materials

2.1 Field Site Description

The field sites are located in the Kien Svay district of northern Kandal Province, Cambodia, an area heavily affected by groundwater As (Appelo and Postma, 1993; Poly a et al., 2003; Poly a et al., 2005; Charlet and Poly a, 2006; Tamura et al., 2007; Benner et al., 2008; Kocar et al., 2008; Polizzotto et al., 2008; Rowland et al., 2008; van Dongen et al., 2008; Poly a and Charlet, 2009; Lawson et al., 2013; Lawson et al., 2016; Richards et al., 2017a; Richards et al., 2017b). Field sites (**Figure 1**) are located along two distinct transects, called here “T-Sand” and “T-Clay” and which are dominated by sand and clay lithologies respectively, and both oriented to be broadly parallel to inferred major groundwater flowpaths (Richards et al., 2017a). The local geology is typical to floodplains in the Lower Mekong Basin, with elevated levees along the Mekong and Bassac River banks which retreat inland towards a seasonally saturated wetland basin (Kocar et al., 2008). Sedimentological attributes and a geomorphological framework for the study area are provided elsewhere (Magnone et al., 2017), and basic hydrogeological parameters such as hydraulic conductivities for a nearby field area are also published elsewhere (Benner et al., 2008). The annual monsoon season drives changes in the horizontal hydraulic head gradient, with groundwater flowing from the rivers inland during the monsoon season and in the opposite direction during the dry season

(Benner et al., 2008; Richards et al., 2017a). Groundwater abstraction in the area is limited and thus the field sites are representative of minimally-influenced, pre-development conditions, also noting that both population density (~ 360 people/km²) (Cambodia Investment, 2014) and sanitation coverage (~ 25 %) (Water and Sanitation Program, 2015) is relatively low.

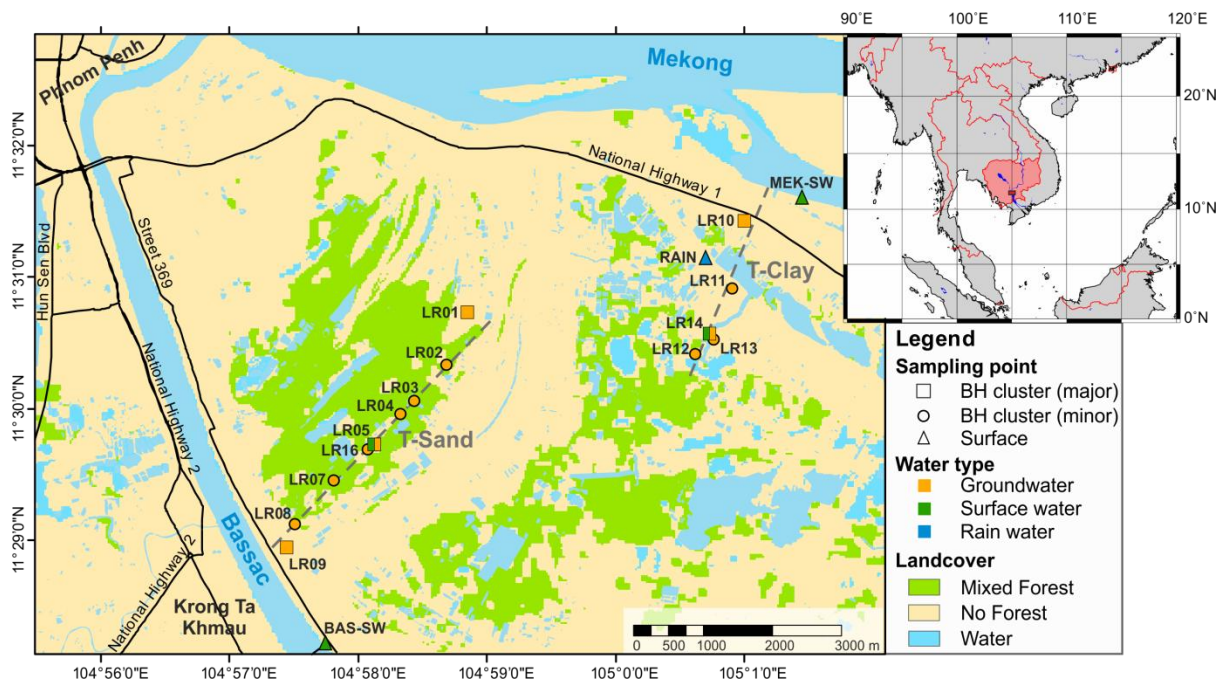


Figure 1. Map of field area and sampling locations in northern Kandal Province, Cambodia (adapted from Richards et al., 2017a; Uhlemann et al., 2017).

2.2 Sample Collection and Characterization

Groundwater from depths of 6 to 45 meters and surface waters were sampled (i) pre-monsoon in May – June 2014; and (ii) post-monsoon in November – December 2014 using methods previously described (Richards et al., 2015; Richards et al., 2017a). Samples for stable isotopes (δD and $\delta^{18}O$) were not filtered nor chemically preserved and were collected in 60 mL acid-washed and furnace-dried amber glass Schott bottles with polyseal caps, placed in field coolers within 60 minutes of collection and in refrigerated storage ($\sim 4^\circ C$) generally within several hours. Samples for stable isotope analysis of accumulated weekly precipitation were collected every month between July and November 2014 and stored in 500 mL amber glass bottles with polyseal caps.

Major cations (including Ca and Na) were analyzed on filtered (0.45 μm cellulose and polypropylene syringe filters, Minisart RC, UK) and acidified ($< \text{pH } 2$, trace grade nitric acid, BDH Aristar, UK) using inductively coupled plasma atomic emission spectrometry (ICP-AES, Perkin-Elmer Optima 5300 dual view) at the Manchester Analytical Geochemistry Unit (MAGU, University of Manchester, UK) with inverse variance weighted first order linear calibration models (Miller and Miller, 2010; Polya et al., 2017; Richards et al., 2017a). Chloride and bromide were measured on subsamples of un-acidified and filtered (0.45 μm cellulose and polypropylene syringe filters, Minisart RC, UK) groundwater using ion chromatography (IC; Dionex ICS5000 Dual Channel Ion Chromatograph) at MAGU (Richards et al., 2017a).

Wet sediment cores were collected at the time of drilling (Richards et al., 2015) and a subsample stored in polyethylene bags and frozen until particle size analysis. Particle size analysis was completed at the British Geological Survey (Keyworth, UK) on dried and sieved ($< 2 \text{ mm}$) sediment samples using laser diffraction (LS 13 320 Laser Diffraction Particle Size Analyzer, Beckman Coulter, UK), enabled with Polarization Intensity Differential Scattering (PIDS) to account for the sizing of non-spherical, sub-micron particles. Sediment samples were sonicated for 300 seconds prior to laser particle size analysis. Data interpretation and statistical analysis was completed using the Gradistat_v8 software package (Blott and Pye, 2001). The following particle size classifications were used: (i) clay $< 8 \mu\text{m}$ ($\phi > 7$); (ii) silt $8 \mu\text{m} - 0.063 \text{ mm}$ ($4 < \phi < 7$); and (iii) sand $0.063 - 2 \text{ mm}$ ($-1 < \phi < 4$) (Vandenberghe et al., 1997; Rawlins et al., 2009). Contour plots of grain size were produced without smoothing using OriginPro 2015 and supplemented with drilling logs where particle size analysis was not completed.

2.3 Analysis of Stable Hydrogen and Oxygen Isotopes

Stable isotope analysis (δD and $\delta^{18}\text{O}$) was conducted at the Isotope Community Support Facility (ICSF) at the Scottish Universities Environmental Research Centre (SUERC, UK). For δD analysis, 1 μL standard and sample aliquots were directly injected into a chromium furnace at 800°C , with the evolved H_2 gas subsequently analyzed on-line using mass spectrometry (VG Optima dual-inlet Mass Spectrometer) (Donnelly et al., 2001). For $\delta^{18}\text{O}$

analysis, 200 μL sample aliquots were over-gassed with 1 % CO_2 -in-He for 5 minutes, followed by a 24 hour equilibration period prior to analysis with mass spectrometry (Delta V Plus Isotope Ratio Mass Spectrometer, Thermo Scientific) set at 25 $^{\circ}\text{C}$ using standard techniques (Nelson, 2000). Reproducibility was estimated to be $\pm 3\%$ and $\pm 0.3\%$ for δD and $\delta^{18}\text{O}$, respectively, and is based on within-run replicate analysis of international reference standards Vienna Standard Mean Ocean Water (VSMOW), Greenland Ice Sheet Precipitation (GISP) and the internal standard Lt Std.

The isotopic composition of water is reported as the per mil (‰) deviation from VSMOW, per Equation 1:

$$\delta = \left[\frac{(R_{\text{sample}} - R_{\text{standard}})}{R_{\text{standard}}} \right] \cdot 1000 \quad [1]$$

where $R = {}^2\text{D}/{}^1\text{H}$ for hydrogen and ${}^{18}\text{O}/{}^{16}\text{O}$ for oxygen, the ratio of the heavy to light isotope. Because of the significant geographical and temporal variations in the isotopic composition of precipitation (Dansgaard, 1974; Clark and Fritz, 1997; Araguás-Araguás and Froehlich, 1998; Araguás-Araguás et al., 2000), a local meteoric water line (LWML) was derived from local precipitation to compare the isotopic composition of groundwater and surface water. The deuterium excess (d) is a way to quantify locally-dependent deviation (particularly due to humidity or mixing of different vapour masses), and is given by Equation 2 (Dansgaard, 1974; Araguás-Araguás et al., 2000):

$$d = \delta\text{D} - 8\delta^{18}\text{O} \quad [2]$$

Isotope exchange between groundwater and aquifer minerals is assumed to be negligible (Clark and Fritz, 1997).

2.4 Modelling the Estimated Relative Extent of Evaporation of Groundwater Sources

The degree of groundwater source evaporation was estimated using simple two-component mixing models with end-members representing the most enriched (*e.g.* 100 % evaporated compared to that of the most evaporated water observed) and most depleted (*e.g.* 0 % evaporated) δD and $\delta^{18}\text{O}$ signatures observed in 2014 pond water and local precipitation,

respectively. This was calculated via Equations 3 and 4:

$$X_{GW,\delta^{18}O} = \frac{\delta^{18}O_{GW} - \delta^{18}O_{EMDepleted}}{\delta^{18}O_{EMEvaporated} - \delta^{18}O_{EMDepleted}} \quad [3]$$

$$X_{GW,\delta D} = \frac{\delta D_{GW} - \delta D_{EMDepleted}}{\delta D_{EMEvaporated} - \delta D_{EMDepleted}} \quad [4]$$

where the relative extent of source evaporation (X) of a groundwater sample based on $\delta^{18}O$ or δD is $X_{GW, \delta^{18}O}$ and $X_{GW, \delta D}$, respectively and $\delta^{18}O$ and δD of the groundwater (GW) and depleted or evaporated end-members (EM) are measured. Calculations were made for each groundwater pre- and post-monsoon sample using both the δD and $\delta^{18}O$ signatures, with the median and range reported for the δD and $\delta^{18}O$ -based results to give an estimated degree of relative source evaporation. The difference in evaporation estimate between the independent δD and $\delta^{18}O$ calculations was generally within a few percent. It was assumed that the end-member values for the 2014 sampling season were broadly similar to values typically encountered over previous years, although yearly variation in weather conditions such as rainfall and humidity can occur (Mekong River Commission, 2015). Discussion on the characterization of model end-members, model bias and limitations are found in Section 3.3.

3. Results and Discussion

3.1 Stable Oxygen and Hydrogen Isotopes

The degree of interaction between surface and groundwaters was investigated by comparing the isotopic signature (δD versus $\delta^{18}O$) of groundwaters from T-Sand and T-Clay with Mekong and Bassac River water, isolated pond waters and precipitation (**Figure 2**). The mean isotopic compositions of groundwaters, surface waters and the volumetric-weighted mean of precipitation are shown on **Table 1**. A local meteoric water line (LMWL; $\delta D = 6.4 \delta^{18}O - 1.3$, adjusted $R^2 = 0.99$) was developed from cumulative weekly samples of rainwater. The 2014 LMWL has a slope of 6.4, which is less than the global meteoric water line (GMWL)

slope of 8.17 (Rozanski et al., 1993), less than the 2009 LMWL gradient of 8.3 in the same area (Lawson et al., 2016) and also less than the 2003 – 2005 LMWL gradient of 6.82 – 7.95 for the nearby Kampong Province (Kabeya et al., 2007). The slope of any LMWL is a function of local conditions related to fluctuating weather, relative humidity or mixing of differently sourced vapour masses, and particularly in tropical regions like Cambodia, may differ substantially from the GMWL, with greater deviation reflecting more extensive evaporation (Craig and Gordon, 1965; Gat, 1971; Araguás-Araguás et al., 2000). Indeed, 2014 is the driest year on record from available data (2008 – 2015) (Mekong River Commission, 2015), which is consistent with the more evaporative LMWL observed. The deuterium excess, d , of the local precipitation ranges from 2.6 to 15.6 (relative to a slope of 8), suggesting that local surface waters contribute a kinetically controlled, re-evaporated component to the precipitation, which is characteristic of humid climates (Merlivat and Jouzel, 1979; Clark and Fritz, 1997; Pfahl and Sodemann, 2014). Seasonal differences in d have been shown to vary by more than 10 ‰ in the eastern Asian monsoon region (Kondoh and Shimada, 1997) which is the same broad range observed here.

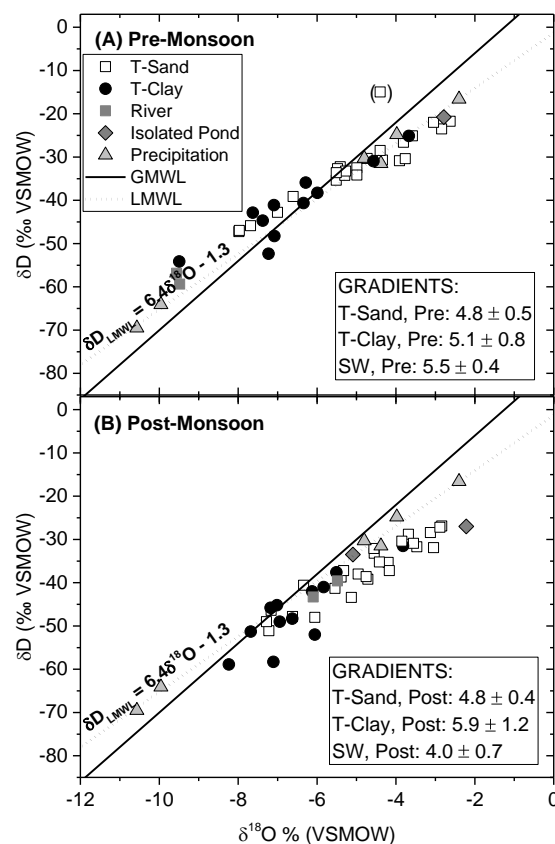


Figure 2. δD versus $\delta^{18}O$ of groundwaters (T-Sand and T-Clay), surface water and precipitation in northern Kandal Province, Cambodia. Groundwater and surface samples

were collected (A) pre-monsoon (May – June 2014) and (B) post-monsoon (November – December 2014) and local precipitation samples were collected as cumulative weekly samples taken the first week of each month from July to November 2014. The local meteoric water line is derived from the precipitation samples. The point marked in parentheses is considered an outlier as δD is beyond two standard deviations of the mean.

264

265 **Table 1.** Mean δD and $\delta^{18}O$ for groundwaters (GW) and surface water (SW) in northern
 266 Kandal Province, Cambodia during pre- and post-monsoon conditions and volumetric-
 267 weighted mean of precipitation. Rainfall data is from the Mekong River Commission
 268 Monitoring Station Phnom Penh Chaktomuk (Bassac) (Mekong River Commission, 2015);
 269 * indicates that only one sample was collected.

Group	δD , Mean (‰ VSMOW)			$\delta^{18}O$, Mean (‰ VSMOW)		
	Pre-Monsoon	Post-Monsoon	Overall	Pre-Monsoon	Post-Monsoon	Overall
T-Sand, GW	-32.3	-36.9	-34.7	-5.0	-4.7	-4.9
T-Clay, GW	-41.3	-46.7	-44.1	-6.6	-6.5	-6.6
River, SW	-58.0	-41.5	-49.8	-9.5	-5.8	-7.7
Ponds, SW	-21.0*	-30.3	-27.1	-2.8*	-3.7	-3.4
Precipitation		-35.7			-5.5	

270

271 Pre-monsoon groundwater (**Figure 2A**) typically falls near the LMWL, with some samples
 272 slightly enriched and some slightly depleted in comparison. Post-monsoon groundwater
 273 (**Figure 2B** and **Table 1**) typically falls on or below the LMWL, and is generally more depleted
 274 in δD (shifting to lighter, more negative values) than pre-monsoon groundwater (*e.g.* mean
 275 δD for T-Sand is -32.3 and -36.9 for pre- and post-monsoon, respectively) ; in contrast $\delta^{18}O$
 276 becomes slightly less depleted during the post-monsoon season (*e.g.* mean $\delta^{18}O$ for T-Sand
 277 is -5.0 and -4.7 for pre- and post-monsoon, respectively). In both pre- and post-monsoon
 278 seasons, groundwater from T-Sand generally trends towards more enriched values as
 279 compared to groundwater from T-Clay. The more enriched isotopic signature of T-Sand
 280 groundwaters indicates the contribution of an evaporated source of recharge to the
 281 groundwater particularly along this transect. This evaporated source could either be from
 282 surface waters or as a result of evaporation of meteoric water during recharge. Broad
 283 comparison of the gradients of the pre-monsoon regression lines for T-Sand (slope = $4.8 \pm$
 284 0.5) and T-Clay (slope = 5.1 ± 0.8) with the surface waters (5.5 ± 0.4) and LMWL (slope = 6.4
 285 ± 0.2) suggest that surface waters are the most likely source of recharge to the groundwater
 286 prior to the onset of the monsoonal rains. In contrast, post-monsoon regression lines for T-
 287 Sand (slope = 4.8 ± 0.4) and T-Clay (slope = 5.9 ± 1.2) with the surface waters (slope = $4.0 \pm$

0.7) and LMWL (slope = 6.4 ± 0.2) suggest that contributions of both surface waters and meteoric water recharge sources may be observed in post-monsoon groundwater. The differences in the gradients of the regression lines for the different transects and seasons indicates that the recharge scenarios for the two aquifers may be different, which is feasible due to the differences in dominant lithology noted for these two transects .

The post-monsoon groundwater regression line for T-Sand intercepts the LMWL at an isotopic composition (*e.g.* at $\delta D = -54 \text{ ‰}$, $\delta^{18}O = -8.3 \text{ ‰}$) consistent with (i) precipitation which falls in between the first week in October 2014 ($\delta D = -64 \text{ ‰}$, $\delta^{18}O = -10 \text{ ‰}$) and the first week in November 2014 ($\delta D = -32 \text{ ‰}$, $\delta^{18}O = -4.4 \text{ ‰}$), as well as (ii) values of west bank Mekong water which are expected to derive from the Tonle Sap during the early post-monsoon period (Kabeya et al., 2008). This intersection point is more depleted than the volumetric-weighted mean of 2014 precipitation ($\delta D = -36 \text{ ‰}$, $\delta^{18}O = -5.5 \text{ ‰}$, shown on **Table 1**). Interestingly, the horizontal groundwater hydraulic gradient changes direction in that same time period between October and November 2014, changing from the gradient in the direction from the rivers towards inland basins before mid-October, to the opposite direction from the inland basins towards the rivers after mid-October. This is an annual effect driven by monsoonal changes in water level (Benner et al., 2008). The fact that the groundwater regression line intersects the LMWL at an isotopic signature reflecting the time that corresponds to the change in direction of groundwater gradient (October/November 2014) rather than the local volumetric precipitation peak in July 2014 (Mekong River Commission, 2015) is indicative that a significant amount of groundwater recharge may be river-derived. This provides evidence for river-groundwater connectivity which may affect the isotopic signatures of affected groundwaters, and may in part explain why a number of the post-monsoon groundwaters are more depleted than the 2014 volumetric-weighted mean of precipitation. Similarly, the LMWL intercepts the *pre*-monsoon groundwater regression lines for groundwaters along both T-Sand and T-Clay at a similar isotopic composition ($\delta D = -28 \text{ ‰}$, $\delta^{18}O = -4.2 \text{ ‰}$ for T-Sand; $\delta D = -32 \text{ ‰}$, $\delta^{18}O = -4.8 \text{ ‰}$ for T-Clay). This isotopic composition of this interception point is again similar to the local precipitation which falls in November 2014 ($\delta D = -32 \text{ ‰}$, $\delta^{18}O = -4.4 \text{ ‰}$) and similarly more depleted than the 2014 volumetric-weighted precipitation mean. Although precipitation data were not collected for the 2013 monsoon season which is what would have directly/most recently

influenced the pre-monsoon samples collected in May/June 2014, the similarity in the intersection point data with the November 2014 precipitation indicates that these interactions are likely to be annual.

The precipitation and surface waters (Mekong River, Bassac River, isolated pond near LR14 on T-Clay and isolated pond near LR05 on T-Sand) show large temporal variations over the period of May 2014 – December 2014 (**Figure 3**). These variations are largely due to (i) Rayleigh fractionation for precipitation; (ii) evaporation for pond water; and (iii) both fractionation and evaporation for river water. The isotopic signature of the precipitation shows very large temporal changes and reaches a peak in evaporative enrichment around August, corresponding to around the time when relative humidity generally also peaks (Kabeya et al., 2007). The monthly rainfall in August 2014 was unusually low as compared to previous years, contributing only ~ 8 % to the total 2014 precipitation (Mekong River Commission, 2015). Rainfall in June, July, August, September and October 2014 volumetrically contributed ~ 16 %, 36 %, 8 %, 23 % and 17 %, respectively, to the total 2014 precipitation recorded (Mekong River Commission, 2015). The isotopic signature of the rivers becomes more enriched (more positive) during the post-monsoon sampling campaign, which is consistent with the contribution of precipitation during the monsoon season and subsequent evaporation, as well as with the flood-pulse recession from the Tonle Sap (Kabeya et al., 2008). Temporal patterns in the isotopic signature of the Mekong River have been previously linked with the monsoonal changes in river water level (Lawson et al., 2013). Conversely to the rivers, the isolated ponds show the opposite overall trend during the same period. The isolated ponds become more depleted (more negative) during the post-monsoon sampling campaign, evolving toward a more groundwater-similar signature. One explanation for this trend is the contribution of precipitation to the pond water. In the period of September and October 2014, temperature decreases but rainfall remains at high volumes (Mekong River Commission, 2015) and water levels in the wetlands significantly increase (Benner et al., 2008), suggesting that dilution of the ponds from mixing with precipitation is responsible for the isotopic depletion in these waters. An alternative explanation for the increasingly depleted ponds in the post-monsoon season is that more depleted groundwater may be influenced by strong upward groundwater flow manifesting as artesian flow in areas of low topography during this time period (Benner et al., 2008;

Lawson et al., 2013), leading to a contribution of groundwater to the ponds and providing evidence for surface-groundwater connectivity.

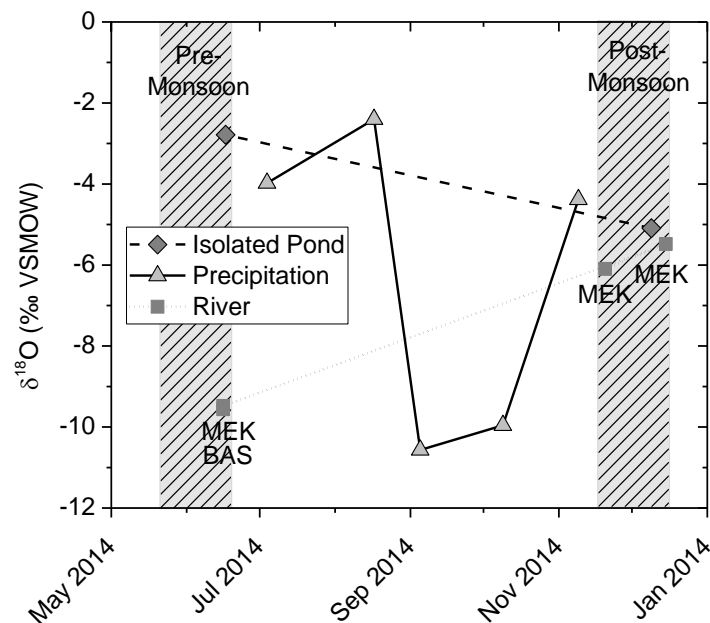


Figure 3. Temporal variability of $\delta^{18}\text{O}$ from May 2014 – December 2014 in local precipitation and surface waters in northern Kandal Province, Cambodia (River = Mekong (MEK) and Bassac (BAS) Rivers; Isolated Ponds = near site LR14 on T-Clay and another near site LR05 on T-Sand). Local precipitation samples were collected each month (as cumulative weekly samples) during the monsoon season and river and pond samples were collected during the pre- and post-monsoon water sampling campaigns, marked as grey boxes.

3.2 The Spatial Distribution of Stable Isotope Composition

The isotopic signatures of groundwater on T-Sand do not show any consistent, overall trend with depth (Figure 4), suggesting that the groundwater at deeper parts of the aquifer was recharged under climatic conditions which are similar to current climatic conditions. This is consistent with the relatively fast recharge rates that can be expected in an area of sand-dominated lithology. The slightly negative correlation between both δD and $\delta^{18}\text{O}$ with depth on T-Clay ($t(21) = -2.61$, $p = 0.016$ and $t(21) = -2.63$, $p = 0.016$ for δD and $\delta^{18}\text{O}$, respectively) indicates that some groundwaters on this transect may have been recharged under different, more depleted conditions. The observed differences between the two

364 transects are broadly consistent with differences in lithology (e.g. sand versus clay
 365 dominant) and other geochemical characterization (Lawson et al., 2013; Lawson et al.,
 366 2016).

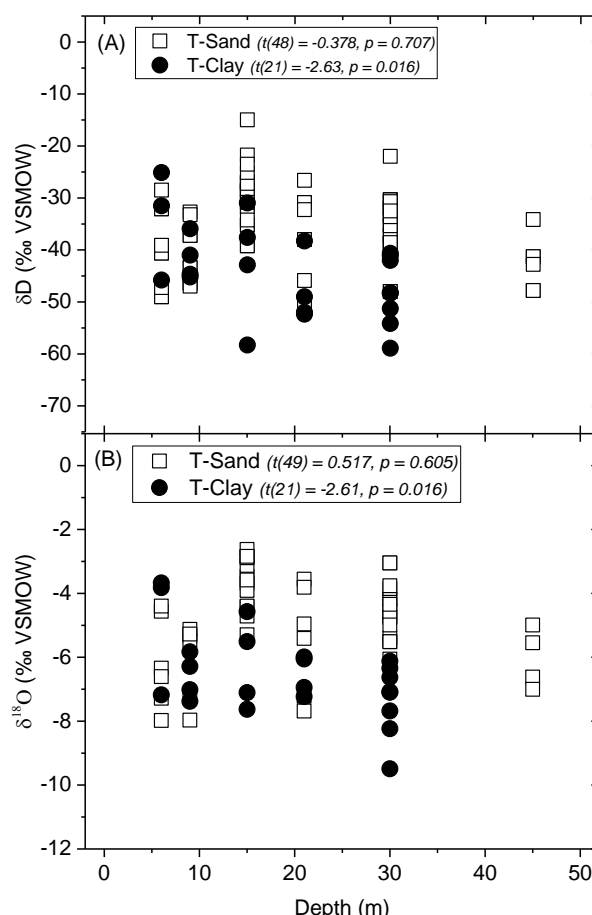


Figure 4. (A) δD and (B) $\delta^{18}O$ and Depth for T-Sand and T-Clay, northern Kandal Province, Cambodia. There is no statistically significant relationship between depth and δD nor $\delta^{18}O$ on T-Sand, suggesting that deep samples on T-Sand were recharged under similar climatic conditions which currently prevail. The slightly negative correlation for T-Clay suggests that some recharge may have occurred under different climatic conditions than currently prevail.

367

368 There are site-specific variations in isotopic signatures, with either depth or increasing
 369 distance from the river (**Figure 5**). For example, the most depleted signatures on T-Sand are
 370 observed with shallow samples located in relative proximity to the Bassac River at site LR09.
 371 Similarly the groundwater is depleted at site LR10, which is in close proximity to the Mekong
 372 River on T-Clay. The most enriched samples are located along T-Sand, particularly in the
 373 central belt of the aquifer from sites LR03 to LR07 which is dominated by sand lithology.
 374 These relatively enriched samples are indicative of an evaporated source of recharge.

Interestingly, at site LR09, the most enriched samples are found at depth indicating the possibility of depth-specific recharge sources or sources which change along groundwater flowpaths. All post-monsoon samples on T-Sand have more enriched $\delta^{18}\text{O}$ signatures than pre-monsoon signatures at the same depth and location, clearly indicating a seasonal timescale on recharge. This same observation cannot be made across T-Clay where monsoonal changes are less variable and more site-specific.

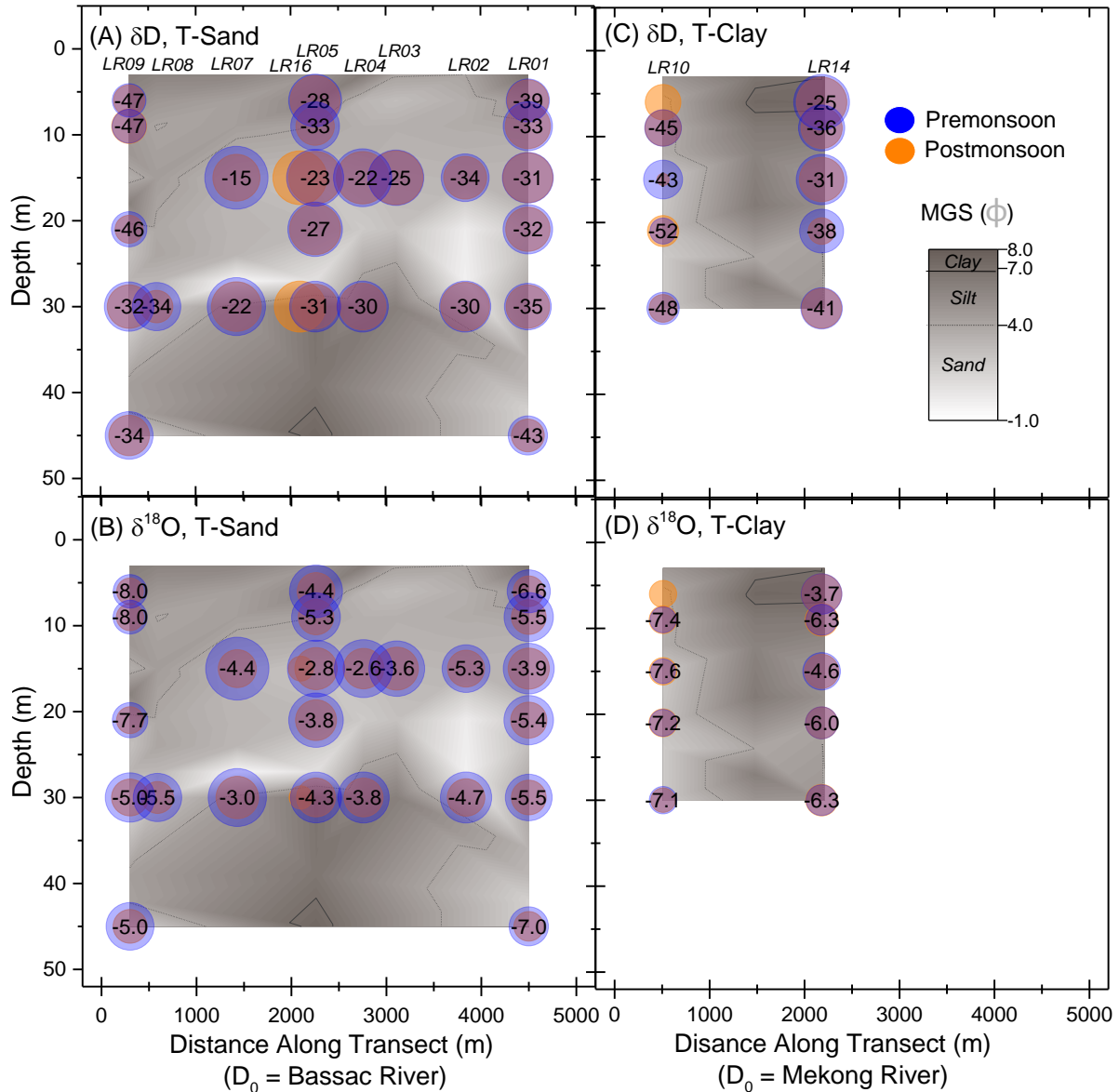


Figure 5. Distribution of (A and C) δD and (B and D) $\delta^{18}\text{O}$ across (A and B) T-Sand and (C and D) T-Clay. More negative isotopic values represent more depleted isotopic signatures and are shown by smaller size bubbles. The underlying contour represents the mean grain size (MGS) in sediments collected from the same locations within the aquifer, with darker colors

representing smaller mean particle size. Labelled datapoints represent pre-monsoon values (blue bubbles) and post-monsoon values (orange bubbles) are unlabelled.

3.3 Estimation of the Relative Extent of Evaporation of Groundwater Sources

Site-specific comparisons of the isotopic signature of various groundwaters with the signatures of isotopically enriched and depleted end-members allow for the relative extent of evaporation of recharge source to be estimated with simple two-point mixing models, and may be indicative of recharge from surface waters in some cases (**Figure 6**). Here, the end-members were assumed to be the 2014 extreme values namely (i) a pond with the most enriched signature representing 100 % relative evaporation (*e.g.* compared to that of the most evaporated water observed) ($\delta^{18}\text{O} = -2.8 \text{ ‰}$; $\delta\text{D} = -20.8 \text{ ‰}$); and (ii) meteoric water with the most depleted signature representing 0 % evaporation ($\delta^{18}\text{O} = -10.6 \text{ ‰}$; $\delta\text{D} = -69.5 \text{ ‰}$). The dashed line shown on **Figure 6** represents the modelled relative evaporation (65 %) for the 2014 annual, volumetric-weighted mean of precipitation, so anything falling to the right or left of that line is considered to be more or less evaporated, respectively, than mean precipitation. Local and small-scale variations are very important for understanding groundwater provenance and identifying recharge mechanisms. For example, at site LR09 (**Figure 6A**), which is near the Bassac River, the deeper groundwaters are more isotopically enriched (and thus have a more evaporated source) than shallow, relatively un-evaporated groundwater sources at the same location (*e.g.* approximately 70 % versus 40 % relative source evaporation, respectively). This suggests that deep and shallow groundwaters may have contributions from different recharge sources, and specifically that deeper groundwaters may be recharged by more relatively evaporated, surface-water derived sources, possibly derived from the nearby Bassac River with connectivity from a deep sand lens. A mechanism such as mixing of locally-derived recharge with relatively depleted river water (**Table 1**) in the riparian zone is plausible and modelling of groundwater mixing regimes is the subject of a separate manuscript. Site LR01 (**Figure 6B**), which is located several kilometers from the river, shows a different evaporative pattern. Here, the mid-depth LR01-15 groundwater source shows a peak in relative evaporative enrichment around 85 %, which could reflect an increasing source of

evaporated surface waters at shallow to mid depths, possibly deriving from seasonal wetlands and transporting via near-surface sand windows. The most evaporated signatures are seen at site LR05 (**Figure 6C**), which is located near a permanent pond and sand window on T-Sand. The comparatively high relative evaporative signature (averaging around 80 % with a maximum > 95 %) indicates that highly evaporated recharge is likely at this site, probably as a result of connectivity with the nearby pond. Site LR14 (data not shown) is also located near a pond and exhibits similarly high evaporative signatures. Finally, the least relative evaporative signatures overall are seen at site LR10 (**Figure 6D**), averaging around 40 %. This site is located in close proximity to the Mekong River, and the lesser extent of evaporation could foreseeably be attributed to the large contribution of precipitation to the Mekong River and subsequent surface-groundwater interaction. Trends are generally very similar between pre- and post-monsoon sample sets. Along T-Sand (**Figure 6A, B, C**), pre-monsoon isotopic signatures are typically slightly more evaporated than post-monsoon, which is consistent with a contribution of recharge occurring during the (more evaporated) dry season. The stable isotopic composition of these groundwaters is indicative of surface-groundwater interactions at sites particularly near rivers (*e.g.* LR09, LR10), ponds (*e.g.* LR05) and/or sand windows (*e.g.* LR01). When the overall dataset is considered (**Figure 7**), groundwater sources from T-Sand generally have higher relative evaporation as compared to T-Clay, and the associations with transect are more apparent than with depth.

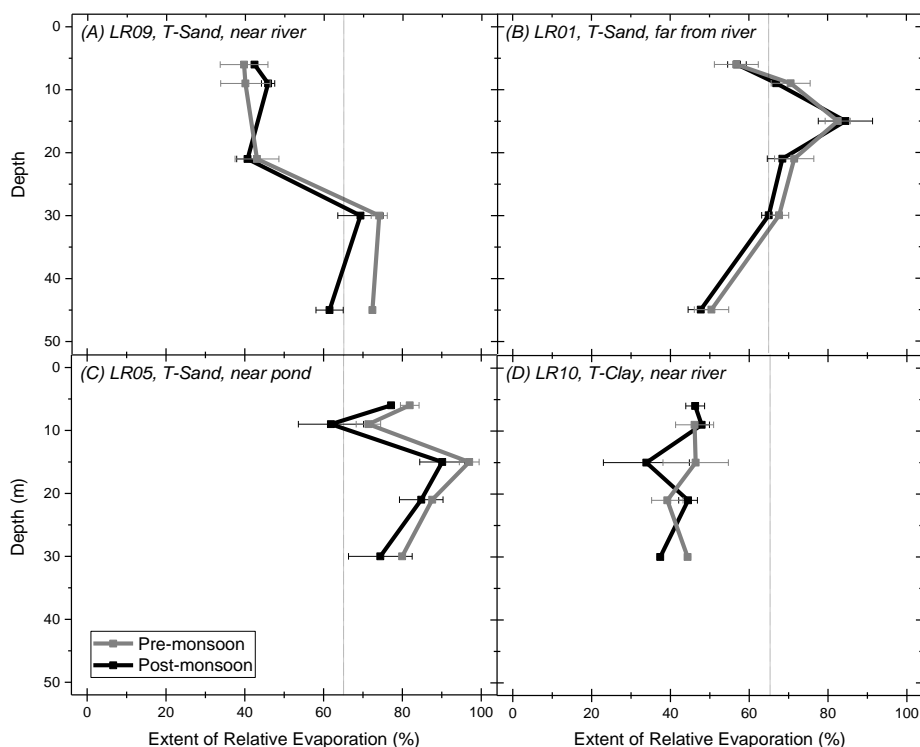


Figure 6. Estimated extent of relative recharge source evaporation with depth and site for groundwaters from northern Kandal Province, Cambodia using simple two-point mixing models assuming end-members of (i) a pond with the most enriched signature representing 100 % evaporation compared to that of the most evaporated water observed; and (ii) meteoric water with the most depleted signature from September 2014 representing 0 % evaporation. Reported values represent the mean of relative evaporation calculated from both $\delta^{18}\text{O}$ - and δD -based mixing models with error bars representing the range. The dashed line indicates the relative evaporation estimate calculated from the isotopic signature of the annual, volumetric-weighted mean of precipitation. Major well clusters on T-Sand are: (A) LR09; (B) LR01; (C) LR05; and T-Clay: (D) LR10. Sites LR09 and LR10 are located near the Bassac and Mekong rivers, respectively; site LR05 is near a pond; sites LR01 and LR05 are near sand windows.

431

432

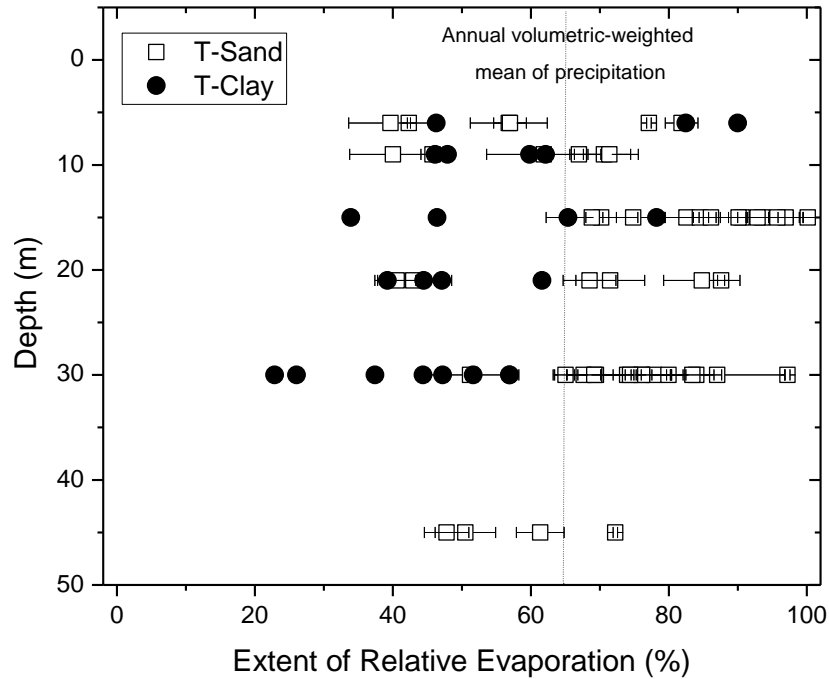


Figure 7. Estimated extent of relative source evaporation with depth and site for groundwaters from northern Kandal Province, Cambodia using simple two-point $\delta^{18}\text{O}$ - and δD -based mixing models for the overall groundwater dataset from T-Sand (open squares) and T-Clay (filled circles). The dashed line indicates the relative evaporation estimate calculated from the isotopic signature of the annual, volumetric-weighted mean of 2014 precipitation.

The modelled extent of relative groundwater source evaporation as qualitatively compared to mean, volumetric-weighted precipitation shows spatial patterns generally consistent with the proximity to surface water bodies (Figure 8). This suggests differing surface-groundwater interactions are occurring at various locations across both transects. For example, groundwater sources that are less evaporated than the mean precipitation are observed in locations near rivers (*e.g.* LR09 and LR10), whereas the majority of T-Sand has groundwater sources which are more evaporated than the mean precipitation. Some sites are variable with depth (*e.g.* LR14) which plausibly could be linked to local interactions with the nearby pond.

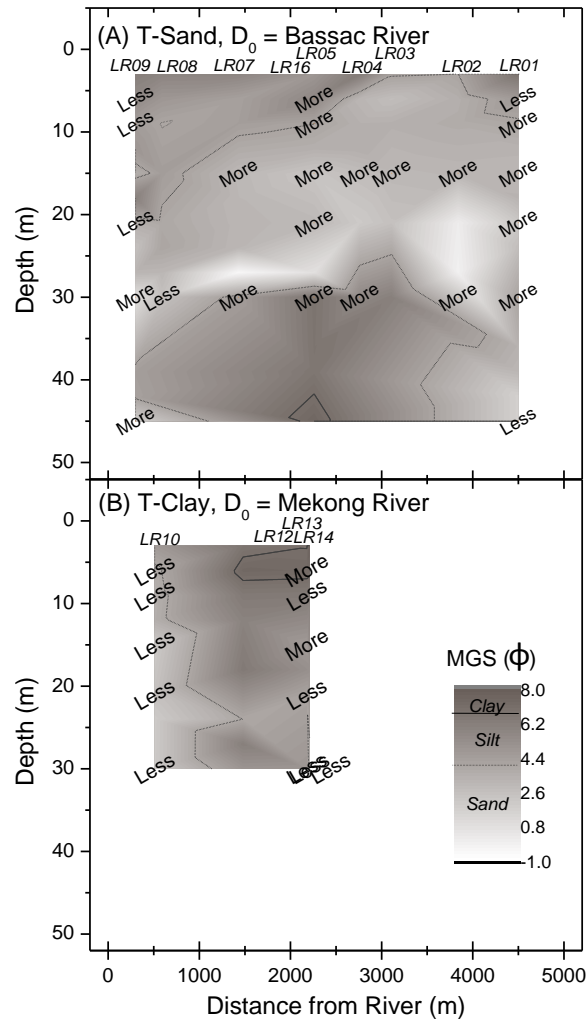


Figure 8. The modelled extent of relative groundwater source evaporation based on simple two-point $\delta^{18}\text{O}$ - and δD -based mixing models as compared to the relative extent of evaporation of the 2014 annual, volumetric-weighted mean of precipitation (65 %) for groundwater on (A) T-Sand and (B) T-Clay. “More” and “Less” refer to groundwater samples (mean of pre- and post-monsoon) with more and less evaporated sources as compared to the annual, volumetric-weighted mean of 2014 precipitation.

444

445 These comparisons should be considered indicative rather than absolute due to the
 446 assumptions inherent in the mixing models, particularly since the modeled extents of
 447 groundwater source evaporation are relative to the selected extreme end-members rather
 448 than absolute values. The pre- and post-monsoon sampling campaigns represent two
 449 “snap-shots” in time of a non-equilibrium and highly heterogeneous system, where non-
 450 linear flowpaths, mixing of recharge sourced from different locations and time, and high
 451 degrees of small-scale local variability are likely. The use of 2014 annual averages as mixing
 452 model end-members inputs may not be sufficient. Realistically all samples will be recharged

by bulk and mixed sources over time, and thus a singular mean input for precipitation, ponds and rivers will not account for all recharge conditions. Furthermore, this mean value may not be suitable for all depths, as it assumes that recharge is the same throughout the entire depth profile and that recharge occurred under similar climatic conditions to 2014, which may not be the case particularly on T-Clay (as discussed on **Figure 4**) as well as because 2014 was the driest year in the study area from recent records (2008 – 2015) (Mekong River Commission, 2015). Regardless of these limitations, these comparative models still provide a useful tool for broadly differentiating between groundwater bodies within the aquifer.

The extent of relative groundwater source evaporation and the chloride concentration of the evaporative endmembers can be used to reconstruct a modelled chloride concentration of the groundwater samples (**Figure 9**). Distinct populations appear to be largely associated with the depth of the groundwater as well as with transect. One depth grouping, consisting of relatively deep (> 15 m depth) groundwaters, is poorly correlated with a weakly positive gradient of approximately 0.05:1 ($t(17) = 0.07$, $p = 0.95$; note this is not statistically significant). In contrast, the grouping of shallow (≤ 15 m depth) groundwaters has a weakly negative but statistically significant gradient of approximately -0.1:1 ($t(17) = -2.70$, $p = 0.02$). If the model were to reasonably describe the interactions in this system, it would be expected that the fit for all samples would be reasonably close to a 1:1 gradient. The observation that there are distinct populations, neither which is well-described by the model, suggests that other processes in addition to evaporation may also be important in some cases and/or that the selected end-members may not sufficiently describe the entire system. Evaporative processes are co-variant with the end-member parameters; for example evaporation will lead to linear changes in the concentration of the conservative tracer chloride but non-linear changes in isotopic compositions. In the case of the deep groundwater, the reconstructed chloride concentration exceeds the measured chloride in every case, which could suggest that the stable-isotope models overestimate the relative degree of source evaporation of these deeper groundwater samples. In contrast the reconstructed chloride concentration underestimates the chloride measured in shallow groundwater samples. This emphasizes the heterogeneity of the system. These differences may be attributed, in part to the co-variance of evaporation with the end-member

parameters, as well as the simplification of end-members selected to represent a complex and changing system (e.g. the end-member values selected only represent one point in time, and will change both spatially and temporally). Some small variations may be due to the presence of additional sources of chloride in the groundwater from natural and/or anthropogenic influences but this impact is likely to be minor compared to evaporative processes.

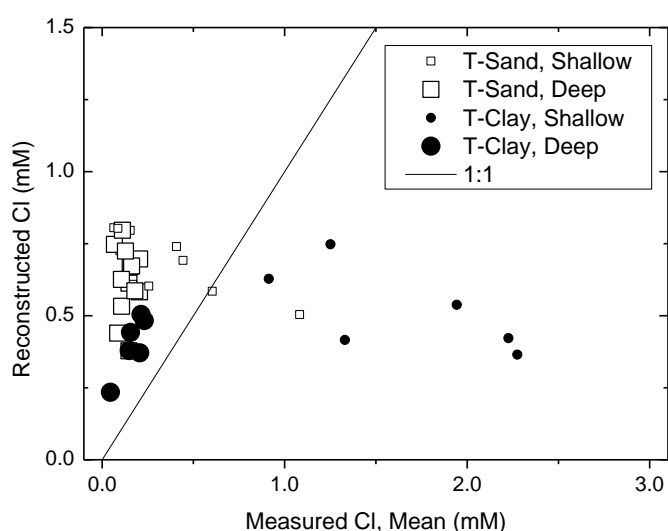


Figure 9. Calculated reconstructed chloride concentrations using the evaporative end-member chloride concentrations and relative extent of evaporation of recharge sources predicted by two-component mixing models against measured chloride (mean of post-and pre-monsoon samples) in groundwater samples from T-Sand (open square) and T-Clay (filled circle). Symbol size indicates if the groundwater is shallow (≤ 15 m depth) or deep (> 15 m depth).

The relationship between Cl/Br and chloride indicates distinct trends for T-Sand and T-Clay groundwaters (**Figure 10**). Water-rock interactions and/or leaching are indicated by a trend of higher chloride and higher Cl/Br ratios; this is particularly evident in the T-Clay groundwater samples. At sites LR10 and LR14 this might be consistent with their proximity to nearby pond and river, respectively, but the elevated chloride concentrations (**Figure 9**) are not consistent with the compositional variation being largely explained by rain water – river/pond water mixing. Instead LR10 and LR14 samples tend to fall between mixing lines calculated between the most dilute groundwater found in this study and West Bengal urine and seawater mixing as adapted from (McArthur et al., 2012). Although they tend in this

direction for these comparatively elevated (in Cl and Cl/Br) samples, the volumetric contributions of urine and/or seawater required to obtain the measured values are very small and are roughly < 0.2 % for seawater and < 2 % for urine as estimated from basic mixing models. This shows that inputs from urine or seawater are likely to be very small but still may influence the local groundwater geochemical signature in some sites. The shallow LR01-6 sample is located near a pig farm which may be plausibly associated with the relatively elevated Cl/Br and chloride observed here; similarly, though, a very small volumetric input of animal or human waste may be enough to shift the geochemical signature. The signature of the T-Clay groundwater is generally consistent with more extensive organic degradation, as organic matter preferentially concentrates Br over Cl, and more evaporation (which increases Cl but leaves Cl/Br unaffected) (McArthur et al., 2012) as compared to T-Sand. Many T-Sand groundwater samples fall along the **apparent** mixing line between rain and river water, with relatively low chloride and increasing Cl/Br. It is expected that rain water would have low chloride and Cl/Br and fall near the most dilute groundwater sample (Xie et al., 2012). The inverse relationship of Cl/Br with depth is apparent (**Figure 11**), with the correlation stronger for T-Clay ($t(13) = -3.23$, $p = 0.007$) than T-Sand ($t(23) = -1.82$, $p = 0.082$; note $p > \text{significance level of } 0.05$). The range of values observed are broadly consistent with other studies elsewhere in circum-Himalayan Asia, for example, in the Bengal Basin (McArthur et al., 2012; Majumder et al., 2016; McArthur et al., 2016) and China (Xie et al., 2012). Human and animal (*e.g.* pig) waste have been distinctively identified by Cl/Br ratios in other studies (Panno et al., 2006; McArthur et al., 2012); given that the field area has low population density and is relatively pristine, it is expected that these contributions are likely to be minimal overall but still may be locally important in some specific sites and/or samples (*e.g.* particularly shallow, sandy areas very near family and/or animal dwellings), which is supported by the typically relatively low Cl observed in groundwater samples here as compared to human and/or animal waste and the discussion above. On a greater regional scale, such as in the Bengal and/or Red River basins (McArthur et al., 2012) or elsewhere in the Mekong basin, it may be important to consider these impacts more broadly (McArthur et al., 2012).

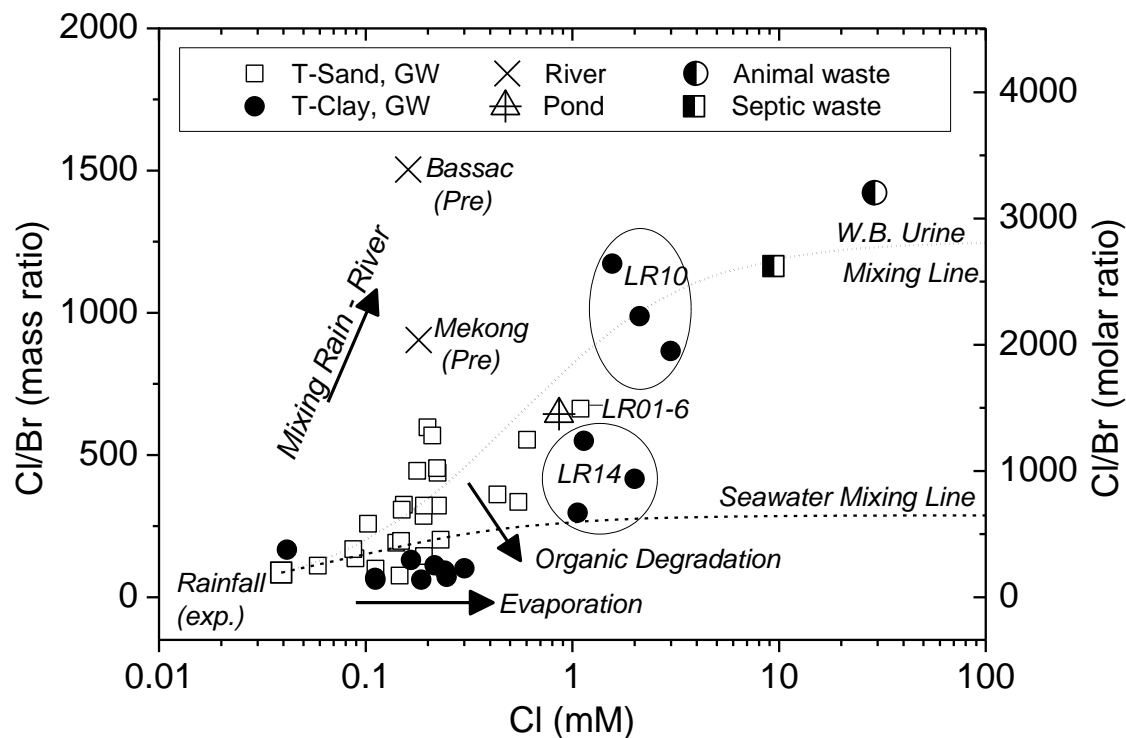


Figure 10. Cl/Br against Cl (mM, logarithmic scale) for groundwater, pond and river water and expected rainwater composition (noting that Br was not detected in the rain water sample so an exact Cl/Br for rainwater could not be calculated) in northern Kandal Province, Cambodia; labels/circles are included for selected samples/sites particularly relevant to discussion. Distinct trends for T-Sand and T-Clay are observed. Mixing lines are adapted (McArthur et al., 2012) for mixing between West Bengal urine and seawater endmembers (McArthur et al., 2012) with the most dilute groundwater sample (this study, LR04-15-PRE, Cl = 0.04 mM Cl, Cl/Br = 87 by mass); septic effluent in USA and animal (hog and horse) (Panno et al., 2006) waste are shown for reference.

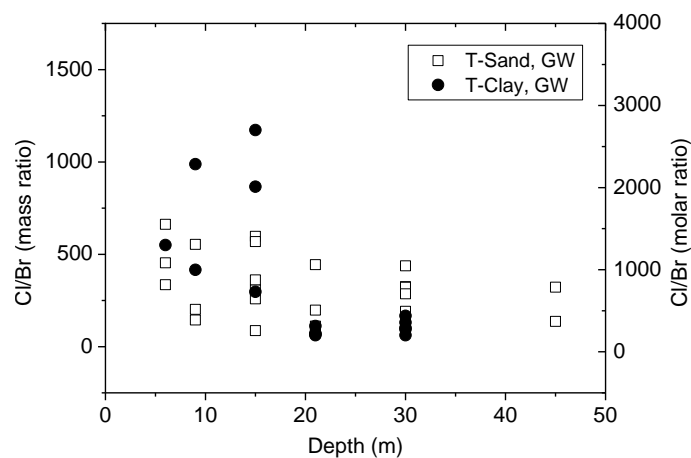


Figure 11. Cl/Br versus depth for groundwater along T-Sand (open squares) and T-Clay (filled circles).

533

534 The relationship between Cl/Br and $\delta^{18}\text{O}$ (**Figure 12**) further shows the distinction between
 535 T-Clay and T-Sand groundwater bodies, with the groundwater from LR10 approaching the
 536 high Cl/Br and low $\delta^{18}\text{O}$ observed in river samples, suggesting that there may be
 537 surface/river-groundwater connectivity near this site. Site LR09 along T-Sand, which is
 538 located near the Bassac River, also trends towards the direction of the river samples,
 539 although to a much lesser extent (particularly with regard to the Cl/Br) than the LR10
 540 groundwater. In addition, the single T-Clay sample falling on the opposite side with
 541 relatively high $\delta^{18}\text{O}$ trends towards a pond-similar signature, and is distinct from the other
 542 T-Clay samples. This groundwater sample is a shallow groundwater (6 m depth) from site
 543 LR14, which is located within meters of the nearby pond. This similarity indicates there may
 544 be surface/pond-groundwater connectivity near this site, consistent with the findings of
 545 Lawson *et al.* (2013).

546

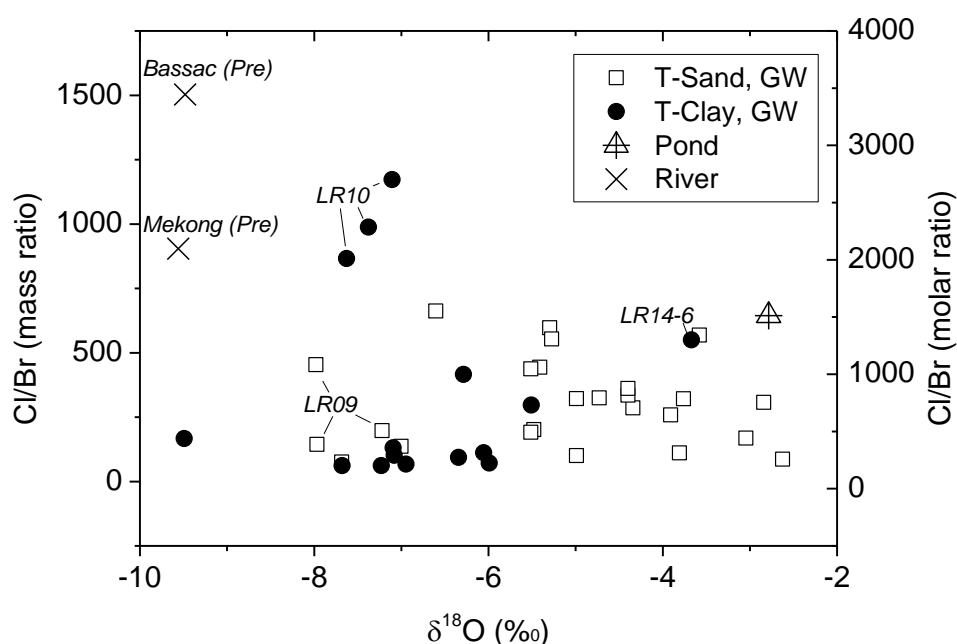


Figure 12. Cl/Br versus $\delta^{18}\text{O}$ for groundwater along T-Sand (open squares) and T-Clay (filled circles), pond (hatched triangle) and river (cross); labels/lines are included for selected samples/sites particularly relevant to discussion.

547

548 The distinct groundwater bodies and the complexity of geochemical interactions within the
 549 aquifer system are further observed when the Ca/Na mass ratio is considered alongside

stable isotope signatures (**Figure 13**). The Ca/Na ratio in natural waters is affected by weathering, sediment-water interactions and cloud type (Carroll, 1962; Khemani, 1968; Frape and Fritz, 1984). The following relative characterizations of various recharge sources and groundwaters can be observed: (i) ponds are characterized by low Ca/Na, and high $\delta^{18}\text{O}$ and δD (data not shown for δD); (ii) rivers are characterized by moderate Ca/Na and low $\delta^{18}\text{O}$ and δD ; and (iii) cumulative precipitation by high Ca/Na and moderate $\delta^{18}\text{O}$ and δD . The Ca/Na ratio of groundwater in T-Clay is generally lower than in T-Sand which could plausibly be attributed to the higher sorption capacity and ion exchange typically observed in clays as compared to sands. The deeper groundwaters in T-Clay tend to have lower $\delta^{18}\text{O}$ and δD and higher Ca/Na than shallower groundwaters, and the opposite trend is observed for T-Sand. These differences highlight that the groundwater populations from T-Clay and T-Sand are geochemically distinct. In general, more extensive water-rock interactions would be expected towards the direction of decreasing Ca/Na and $\delta^{18}\text{O}$ on **Figure 13**. The distinct trends with shallow and deep groundwater populations from both T-Sand and T-Clay indicate different recharge processes and hydrogeological conditions co-occurring within the aquifer.

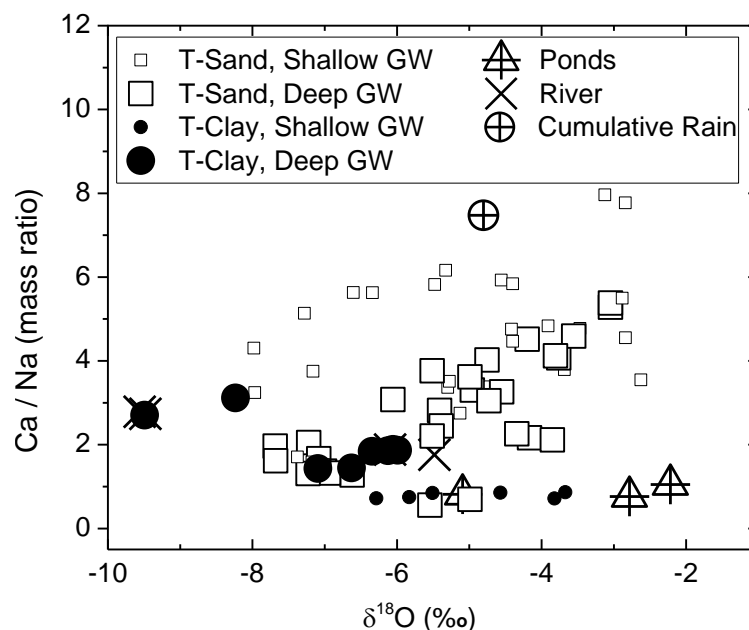


Figure 13. Ca/Na mass ratio against $\delta^{18}\text{O}$ for distinct groupings of shallow (≤ 15 m depth; smaller symbol size) and deep (> 15 m depth; larger symbol size) groundwaters from T-Clay (filled circles) and T-Sand (open squares), pond samples, river samples and cumulative

precipitation from northern Kandal Province, Cambodia. Groundwater from T-Clay typically has lower Ca/Na than groundwater from T-Sand.

3.4 Implications on Arsenic Mobilization

Groundwaters with high As (Richards et al., 2017a) show mixed trends in δD and $\delta^{18}O$ signature in comparison to the LMWL (**Figure 14A**). In a number of cases, high As groundwaters have a much more evaporated signature than the LMWL, which indicates that these groundwaters have been recharged by evaporated surface waters rather than directly by local precipitation. In other cases, high As groundwaters plot near the LMWL. Previously, high As groundwaters were shown to plot along the LMWL in West Bengal, which was used as evidence to suggest that evaporated perennial ponds were not an important source of recharge to shallow, As-affected waters (Datta et al., 2011). Our current data instead suggests that high As groundwaters can plot both near the LMWL as well as along evaporative trend lines, and thus evaporative ponds may be an important source of recharge in some circumstances, as has been suggested by Lawson *et al.* (Lawson et al., 2013; Lawson et al., 2016). The isotopic signatures reported here indicate a non-exclusive contribution of surface water to high As groundwater, consistent with but not conclusive that As release in shallow aquifers is driven in part by ingress of evaporated surface water, plausibly derived from ponds and/or wetlands. Similarly, high bulk DOC groundwaters (Richards et al., 2017a) plot both near the LMWL in some cases and, in other cases, have a much more evaporated signature than the LMWL (**Figure 14B**) indicating that high DOC groundwaters may derive from various recharge sources.

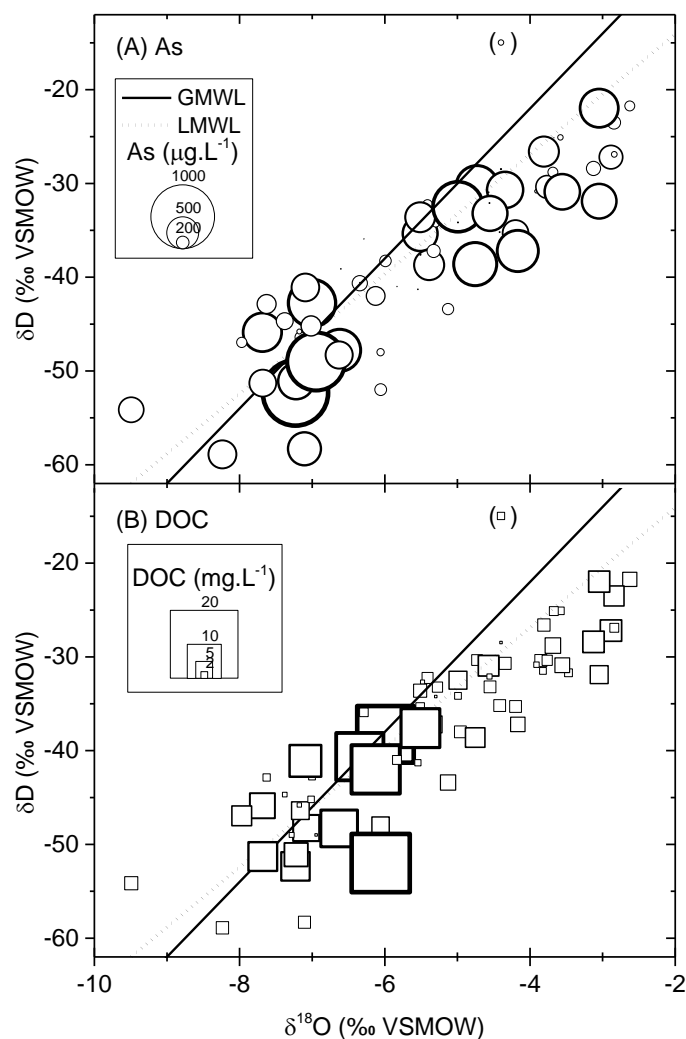


Figure 14. δD versus $\delta^{18}O$ for all groundwater samples in northern Kandal Province, Cambodia with (A) As concentrations and (B) bulk dissolved organic carbon (DOC) represented by bubble size (Richards et al., 2017a). Global Meteoric Water Line (GMWL) and Local Meteoric Water Line (LMWL) shown for comparison.

589

590 Groundwater As plotted against the modelled extent of source evaporation shows that As
 591 concentrations are very high in cases both where relative evaporation is greater or less than
 592 the annual volumetric-weighted mean of precipitation (**Figure 15**). In some cases high As is
 593 associated with evaporated surface water, likely derived from ponds and/or wetlands, and
 594 in other cases high As is associated with more precipitation-similar isotopic
 595 signatures. The high level of heterogeneity in As concentrations is likely to reflect both the
 596 inferred differing sources of organic carbon contributing to As mobilization and originating
 597 from the differing water bodies, as well as transport of released As within the aquifer. The

high heterogeneity observed is reflected also in the characterization of the aqueous inorganic geochemistry of the system (Richards et al., 2017a) and also highlights the difficulties associated with a priori extrapolation of conclusions from one site to another, even within a similar field area. For example, in general, most of the highest concentrations of As occur in more permeable sands along T-Sand, and interestingly the high As, less evaporated outliers observed on T-Clay are from a site (LR10) which is locally sandy despite being located along T-Clay (Richards et al., 2017a). Although δD and $\delta^{18}O$ do not provide direct evidence of the organic matter implicated in As release, their direct incorporation into the water molecule may be indicative of the presence of associated organic matter which is typical of a given recharge source. Thus, the data presented here speculates that mixed sources of organic matter (both surface- and sediment-derived) may be present throughout the shallow aquifers (Lawson et al., 2013; Lawson et al., 2016). The site-specific characterization of the organic matter and its role in As mobilization remains the subject of ongoing work.

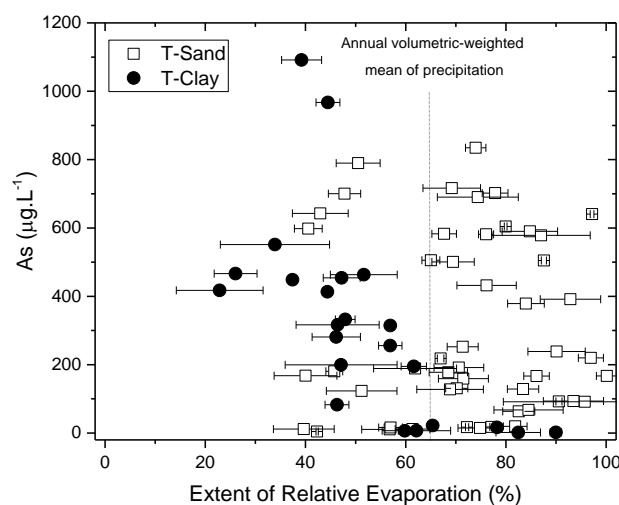


Figure 15. Groundwater As concentrations along T-Sand and T-Clay (Richards et al., 2017a) in northern Kandal Province, Cambodia with the modelled extent of relative evaporation of recharge sources. The estimated relative source evaporation is based on simple two-point mixing models assuming end-members of (i) a pond with the most enriched signature representing 100 % relative evaporation compared to that of the most evaporated water observed; and (ii) meteoric water with the most depleted signature from September 2014 representing 0 % evaporation. The dashed line indicates the relative source evaporation estimate calculated from the isotopic signature of the annual, volumetric-weighted mean of precipitation. Error bars represent the range of relative evaporation calculated using $\delta^{18}O$ - and δD -based mixing models.

4. Conclusions

The δD and $\delta^{18}O$ isotopic signature of groundwater in a heavily As-affected aquifer in Kandal Province, Cambodia in the Lower Mekong Basin was used to characterize the source of groundwater, categorize the systematics of surface waters and to differentiate between various groundwater bodies within the aquifers. Comparisons of groundwater with local precipitation and surface waters indicated varying trends with site, depth, transect and season. The relative extent of evaporation of groundwater sources was estimated based on the end-members showing the most depleted precipitation and most enriched pond signatures. Groundwaters in distinct populations were shown to have varying degrees of relative evaporation of recharge sources, consistent with lithology, locality and other geochemical observations, including the behaviour of the conservative tracer Cl/Br. High As groundwaters demonstrate varying degrees of source evaporation and plot both along the LMWL and along evaporative trend lines, indicating that high As groundwaters likely can be recharged both by local precipitation and by more evaporated surface water sources, consistent with (but not providing direct evidence for) models of a dual role of surface-derived and sedimentary organic matter in As mobilization. Such information, in conjunction with other isotopic and, particularly organic, geochemical measurements, is important to understanding the controls on As release and how As hazard may change in the future.

Acknowledgements

This research was funded by a NERC Standard Research Grant (NE/J023833/1) to DP, BvD and CB, a NERC PhD studentship (NE/L501591/1) to DM and a Leverhulme Trust Early Career Fellowship (ECF2015-657) to LR. Stable isotope analysis was supported by a NERC Isotope Geosciences Facilities award (IP-1505-1114). Sebastian Uhlemann (British Geological Survey and ETH Zurich) is thanked for adapting the site map provided. The following people are gratefully acknowledged for their contributions to the relevant field campaigns: Chansopheaktra Sovann (Royal University of Phnom Penh, Phnom Penh, Cambodia), Chivuth Kong, Pheary Meas and Yut Yann (all Royal University of Agriculture, Phnom Penh,

Cambodia), Chhengngunn Aing, Zongta Sang and Teyden Sok (all Royal University of Phnom Penh), Helen Downie (The University of Manchester) and Lee Chambers (The University of Lancaster). The support of the local landowners and drilling team led by Hok Meas was strongly appreciated. Ann Hall, Marc Hall, Lori Frees, Lori Allen and Dina Kuy (Resources Development International – Cambodia, RDI) are thanked for logistical support and the usage of laboratory facilities. Gren Turner, Barry Rawlins, Oliver Kuras (British Geological Survey) and Lee Chambers are thanked for support and/or advice regarding particle size distribution measurements. Lee Chambers also assisted with particle size measurements. We thank the reviewers whose feedback has improved the manuscript. The views expressed here do not necessarily represent those of any of the funders or individuals whose support is acknowledged.

References

- Aggarwal, P.K., Basu, A.R., Kulkarni, K.M., 2003. Comment on "Arsenic Mobility and Groundwater Extraction in Bangladesh" (I). *Science*, 300: 584b.
- Aggarwal, P.K., Basu, A.R., Poreda, R.J., Kulkarni, K.M., Froehlich, K., Tarafdar, S.A., Ali, M., Ahmed, N., Hussain, A., Rahman, M., Ahmed, S.R., 2000. Isotope hydrology of groundwater in Bangladesh: Implications for characterization and mitigation of arsenic in groundwater. In: BGD/8/016, I.-T.P.R. (Ed.). International Atomic Energy Agency, Vienna.
- Al Lawati, W.M., Jean, J.-S., Kulp, T.R., Lee, M.-K., Polya, D.A., Liu, C.-C., van Dongen, B.E., 2013. Characterisation of organic matter associated with groundwater arsenic in reducing aquifers of southwestern Taiwan. *J. Hazard. Mater.*, 262: 970 - 979.
- Al Lawati, W.M., Rizoulis, A., Eiche, E., Boothman, C., Polya, D.A., Lloyd, J.R., Berg, M., Vasquez-Aguilar, P., van Dongen, B.E., 2012. Characterisation of organic matter and microbial communities in contrasting arsenic-rich Holocene and arsenic-poor Pleistocene aquifers, Red River Delta, Vietnam. *Appl. Geochem.*, 27: 315 - 325.
- Alcalá, F.J., Custodio, R., 2005. Use of the Cl/Br ratio as a tracer to identify the origin of salinity in some coastal aquifers of Spain, 18th Salt Water Intrusion Meeting IGME y IAH, Cartagena, pp. 481 - 497.
- Appelo, C.A.J., Postma, D., 1993. *Geochemistry, groundwater and pollution*. Balkema.
- Araguás-Araguás, L., Froehlich, K., 1998. Stable isotope composition of precipitation over southeast Asia. *J. Geophys. Res.*, 103(D22): 28721 - 28742.
- Araguás-Araguás, L., Froehlich, K., Rozanski, K., 2000. Deuterium and oxygen-18 isotope composition of precipitation and atmospheric moisture. *Hydrol. Proc.*, 14: 1341 - 1355.
- Benner, S.G., Polizzotto, M.L., Kocar, B.D., Ganguly, S., Phan, K., Ouch, K., Sampson, M., Fendorf, S., 2008. Groundwater flow in an arsenic-contaminated aquifer, Mekong Delta, Cambodia. *Appl. Geochem.*, 23(11): 3072-3087.
- Berg, M., Trang, P.T.K., Stengel, C., Buschmann, J., Viet, P.H., Van Dan, N., Giger, W., Stüben, D., 2008. Hydrological and sedimentary controls leading to arsenic contamination of groundwater in the Hanoi area, Vietnam: The impact of iron-arsenic ratios, peat, river bank deposits, and excessive groundwater abstraction. *Chem. Geol.*, 249(1-2): 91-112.
- Bhattacharya, P., Chatterjee, D., Jacks, G., 1997. Occurrence of arsenic contaminated groundwater in alluvial aquifers from delta plains, Eastern India: Options for safe drinking water supply. *Wat. Res. Dev.*, 13: 79-92.
- Blott, S.J., Pye, K., 2001. GRADISTAT: A grain size distribution and statistics package for the analysis of unconsolidated sediments. *Eart. Surf. Proc. Land.*, 26: 1237 - 1248.
- Cambodia Investment, 2014. Municipality and Province Investment Information: Kandal Province (http://www.cambodiainvestment.gov.kh/wp-content/uploads/2014/03/Kandal-Province_eng.pdf, accessed Oct 2017).
- Carroll, D., 1962. Rainwater as a Chemical Agent of Geologic Processes - A Review. Geological Survey Water-Supply Paper 1535-G, U.S. Department of the Interior.
- Cartwright, I., Weaver, T.R., Fifield, L.K., 2006. Cl/Br ratios and environmental isotopes as indicators of recharge variability and groundwater flow: An example from the southeast Murray Basin, Australia. *Chem. Geol.*, 231: 38 - 56.

- Charlet, L., Polya, D.A., 2006. Arsenic in Shallow, Reducing Groundwaters in Southern Asia: An Environmental Health Disaster. *Elements*, 2: 91 - 96.
- Clark, I., Fritz, P., 1997. *Environmental Isotopes in Hydrogeology*. Lewis Publishers, New York.
- Craig, H., 1961. Isotopic Variations in Meteoric Waters. *Science*, 133(3465): 1702 - 1703.
- Craig, H., Gordon, L.I., 1965. Deuterium and oxygen 18 variations in the ocean and the marine atmosphere. 277 -374.
- Dansgaard, W., 1974. Stable isotopes in precipitation. *Tellus*, XVI(4).
- Datta, S., Neal, A.W., Mohajerin, T.J., Ocheltree, T., Rosenheim, B.E., White, C.D., Johannesson, K.H., 2011. Perennial ponds are not an important source of water or dissolved organic matter to groundwaters with high arsenic concentrations in West Bengal, India. *Geophysical Research Letters*, 38(L20404).
- Davis, S.N., Whittemore, D.O., Fabryka-Martin, J., 1998. Uses of Chloride/Bromide Ratios in Studies of Potable Water. *Groundwater*, 36(2): 338 - 350.
- Donnelly, T., Waldron, S., Tait, A., Dougans, J., Bearhop, S., 2001. Hydrogen isotope analysis of natural abundance and deuterium-enriched waters by reduction over chromium on-line to a dynamic dual inlet isotope-ratio mass spectrometer. *Rapid Commun. Mass Spectrom.*, 15: 1297-1303.
- Fendorf, S., Michael, H.A., van Geen, A., 2010. Spatial and temporal variations of groundwater arsenic in south and southeast Asia. *Science*, 328: 1123-1127.
- Frape, S.K., Fritz, P., 1984. Water-rock interaction and chemistry of groundwaters from the Canadian Shield. *Geochim. Cosmochim. Acta*, 48: 1617 - 1627.
- Gat, J.R., 1971. Comments on the Stable Isotope Method in Regional Groundwater Investigations. *Water Resour. Res.*, 7(4): 980 - 993.
- Gault, A.G., Islam, F.S., Polya, D.A., Charnock, J.M., Boothman, C., Chatterjee, D., Lloyd, J.R., 2005. Microcosm depth profiles of arsenic release in a shallow aquifer, West Bengal. *Mineralogical Magazine*, 69(5): 855-863.
- Harvey, C.F., Swartz, C.H., Badruzzaman, A.B.M., Keon-Blute, N., Ali, M.A., Jay, J., Beckie, R., Oates, P.M., Ashfaq, K.N., Islam, S., Hemond, H.F., Ahmed, M.F., 2003. Response to comments on "Arsenic mobility and groundwater extraction in Bangladesh". *Science*, 300: 584d.
- Harvey, C.F., Swartz, C.H., Badruzzaman, A.B.M., Keon-Blute, N., Yu, W., Ali, M.A., Jay, J., Beckie, R., Niedan, V., Brabander, D., Oates, P.M., Ashfaq, K.N., Islam, S., Hemond, H.F., Ahmed, M.F., 2005. Groundwater arsenic contamination on the Ganges Delta: biogeochemistry, hydrology, human perturbations, and human suffering on a large scale. *Comp. Rend. Geos.*, 337(1-2): 285-296.
- Harvey, C.F., Swartz, C.H., Badruzzaman, A.B.M., Keon-Blute, N., Yu, W., Ashraf Ali, M., Jay, J., Beckie, R., Niedan, V., Brabander, D., Oates, P.M., Ashfaq, K.N., Islam, S., Hemond, H.F., Ahmed, M.F., 2002. Arsenic mobility and groundwater extraction in Bangladesh. *Science*, 298: 1602-1606.
- Islam, F.S., Gault, A.G., Boothman, C., Polya, D.A., Charnock, J.M., Chatterjee, D., Lloyd, J.R., 2004. Role of metal-reducing bacteria in arsenic release from Bengal delta sediments. *Nature*, 430: 68-71.
- Kabeya, N., Kubota, T., Shimizu, A., Nobuhiro, T., Tsuboyama, Y., Chann, S., Tith, N., 2008. Isotopic investigation of river water mixing around the confluence of the Tonle Sap and Mekong rivers. *Hydrol. Proc.*, 22(0): 1351 - 1358.

- Kabeya, N., Shimizu, A., Chann, S., Tsuboyama, Y., Nobuhiro, T., Keth, N., Tamai, K., 2007. Stable Isotope Studies of Rainfall and Stream Water in Forest Watersheds in Kampong Thom, Cambodia, Forest Environments in the Mekong River Basin, pp. 125 - 134.
- Khemani, L.T., 1968. Chemical composition of rain water and rain characteristics of Delhi. *Tellus*, 20(2): 284 - 292.
- Klump, S., Kipfer, R., Cirpka, O.A., Harvey, C.F., Brennwald, M.S., Ashfaq, K.N., Badruzzaman, A.B.M., Hug, S.J., Imboden, D.M., 2006. Groundwater dynamics and arsenic mobilization in Bangladesh assessed using noble gases and tritium. *Environ. Sci. Technol.*, 40: 243-250.
- Kocar, B.D., Polizzotto, M.L., Benner, S.G., Ying, S.C., Ung, M., Ouch, K., Samreth, S., Suy, B., Phan, K., Sampson, M., Fendorf, S., 2008. Integrated biogeochemical and hydrologic processes driving arsenic release from shallow sediments to groundwaters of the Mekong delta. *Appl. Geochem.*, 23(11): 3059-3071.
- Kondoh, A., Shimada, J., 1997. The Origin of Precipitation in Eastern Asia by Deuterium Excess. *J. Jap. Soc. Hydrol. Wat. Res.*, 10(6): 627 - 629.
- Lawson, M., Polya, D.A., Boyce, A.J., Bryant, C., Ballentine, C.J., 2016. Tracing organic matter composition and distribution and its role on arsenic release in shallow Cambodian groundwaters. *Geochim. Cosmochim. Acta*, 178: 160 - 177.
- Lawson, M., Polya, D.A., Boyce, A.J., Bryant, C., Mondal, D., Shantz, A., Ballentine, C.J., 2013. Pond-derived organic carbon driving changes in arsenic hazard found in Asian groundwaters. *Environ. Sci. Technol.*, 47: 7085 - 7094.
- Magnone, D., Richards, L.A., Polya, D.A., Bryant, C., Jones, M., van Dongen, B.E., 2017. Biomarker-indicated extent of oxidation of plant-derived organic carbon (OC) in relation to geomorphology in an arsenic contaminated Holocene aquifer, Cambodia. *Sci. Rep.*, 7(13093): DOI:10.1038/s41598-017-13354-8.
- Mailloux, B.J., Trembath-Reichert, E., Cheung, J., Watson, M., Stute, M., Freyer, G.A., Ferguson, A.S., Ahmed, K.M., Alam, M.J., Buchholz, B.A., Thomas, J., Layton, A.C., Zheng, Y., Bostick, B.C., van Geen, A., 2013. Advection of surface-derived organic carbon fuels microbial reduction in Bangladesh groundwater. *PNAS*, 110(13): 5331 - 5335.
- Majumder, S., Datta, S., Nath, B., Neidhardt, H., Sarkar, S., Roman-Ross, G., Berner, Z., Hidalgo, M., Chatterjee, D., 2016. Monsoonal influence on variation of hydrochemistry and isotopic signatures: Implications for associated arsenic release in groundwater. *J. Hydrol.*, 535: 407 - 417.
- McArthur, J., Ravenscroft, P., Safiulla, S., Thirwall, M.F., 2001. Arsenic in groundwater: Testing pollution mechanisms for sedimentary aquifers in Bangladesh. *Water Resour. Res.*, 37(1): 109-117.
- McArthur, J.M., Banerjee, D.M., Hudson-Edwards, K.A., Mishra, R., Purohit, R., Ravenscroft, P., Cronin, A., Howarth, R.J., Chatterjee, A., Talukder, T., Lowry, D., Houghton, S., Chadha, D.K., 2004. Natural organic matter in sedimentary basins and its relation to arsenic in anoxic ground water: the example of West Bengal and its worldwide implications. *Appl. Geochem.*, 19(8): 1255-1293.
- McArthur, J.M., Ghosal, U., Sikdar, P.K., Ball, J.D., 2016. Arsenic in Groundwater: The Deep Late Pleistocene Aquifers of the Western Bengal Basin. *Environ. Sci. Technol.*, 50(7): 3469 - 3476.

792 McArthur, J.M., Ravenscroft, P., Sracek, O., 2011. Aquifer arsenic source. *Nat. Geos.*, 4(10):
793 655 - 656.

794 McArthur, J.M., Sikdar, P.K., Hoque, M.A., Ghosal, U., 2012. Waste-water impacts on
795 groundwater: Cl/Br ratios and implications for arsenic pollution of groundwater in
796 the Bengal Basin and Red River Basin, Vietnam. *Sci. Total Environ.*, 437: 390 - 402.

797 Mekong River Commission, 2015. Historical Records
798 (http://ffw.mrcmekong.org/historical_rec.htm, last accessed 20 October 2015).

799 Merlivat, L., Jouzel, J., 1979. Global Climatic Interpretation of the Deuterium-Oxygen 18
800 Relationship for Precipitation. *J. Geophys. Res.*, 84(C8): 5029 - 5033.

801 Miller, J.N., Miller, J.C., 2010. Chapter 5: Calibration methods in instrumental analysis:
802 regression and correlation, *Statistics and Chemometrics for Analytical Chemistry*.
803 Pearson Education.

804 Mladenov, N., Zheng, Y., Miller, M.P., Nemergut, D.R., Legg, T., Simone, B., Hageman, C.,
805 Rahman, M.M., Ahmed, K.M., McKnight, D.M., 2010. Dissolved Organic Matter
806 Sources and Consequences for Iron and Arsenic Mobilization in Bangladesh Aquifers.
807 *Environ. Sci. Technol.*, 44(1): 123 - 128.

808 Mukherjee, A., Fryar, A.E., Rowe, H.D., 2007. Regional-scale stable isotopic signatures of
809 recharge and deep groundwater in the arsenic affected areas of West Bengal, India.
810 *J. Hydrol.*, 334(1-2): 151-161.

811 Nelson, S.T., 2000. A simple, practical methodology for routine VSMOW/SLAP normalization
812 of water samples analyzed by continuous flow methods. *Rapid Commun. Mass*
813 *Spectrom.*, 14: 1044 - 1046.

814 Neumann, R.B., Ashfaq, K.N., Badruzzaman, A.B.M., Ali, M.A., Shoemaker, J.K., Harvey,
815 C.F., 2010. Anthropogenic influences on groundwater arsenic concentrations in
816 Bangladesh. *Nat. Geos.*, 3(1): 46-52.

817 Neumann, R.B., Ashfaq, K.N., Badruzzaman, A.B.M., Ali, M.A., Shoemaker, J.K., Harvey,
818 C.F., 2011. Aquifer arsenic source reply. *Nat. Geos.*

819 Neumann, R.B., Polizzotto, M.L., Badruzzaman, A.B.M., Ali, M.A., Zhang, Z.Y., Harvey, C.F.,
820 2009. Hydrology of a groundwater-irrigated rice field in Bangladesh: Seasonal and
821 daily mechanisms of infiltration. *Water Resour. Res.*, 45: 14.

822 Neumann, R.B., Pracht, L.E., Polizzotto, M.L., Badruzzaman, A.B.M., Ashraf Ali, M., 2014.
823 Biodegradable Organic Carbon in Sediments of an Arsenic-Contaminated Aquifer in
824 Bangladesh. *Environmental Science and Technology Letters*, 1: 221 - 225.

825 Nickson, R.T., McArthur, J.M., Burgess, W.G., Ahmed, K.M., Ravenscroft, P., Rahman, M.,
826 1998. Arsenic poisoning of Bangladesh groundwater. *Nature*, 395: 338.

827 Panno, S.V., Hackley, K.C., Hwang, H.H., Greenberg, S.E., Krapac, I.G., Landsberger, S.,
828 O'Kelly, D.J., 2006. Characterization and Identification of Na-Cl Sources in
829 Groundwater. *Groundwater*, 44(2): 176 - 187.

830 Papacostas, N.C., Bostick, B., Quicksall, A.N., Landis, J.D., Sampson, M., 2008. Geomorphic
831 controls on groundwater arsenic distribution in the Mekong River Delta, Cambodia.
832 *Geology*, 36(11): 891-894.

833 Pfahl, S., Sodemann, H., 2014. What controls deuterium excess in global precipitation? *Clim.*
834 *Past*, 10: 771 - 781.

835 Polizzotto, M.L., Kocar, B.D., Benner, S.G., Sampson, M., Fendorf, S., 2008. Near-surface
836 wetland sediments as a source of arsenic release to ground water in Asia. *Nature*,
837 454: 505-508.

838 Poly, D.A., Charlet, L., 2009. Rising arsenic risk? *Nat. Geos.*, 2(6): 383-384.

- Polya, D.A., Gault, A.G., Bourne, N.J., Lythgoe, P.R., Cooke, D.A., 2003. Coupled HPLC-ICP-MS analysis indicates highly hazardous concentrations of dissolved arsenic species in Cambodian groundwaters. *Royal Society of Chemistry Special Publication*, 288: 127 - 140.
- Polya, D.A., Gault, A.G., Diebe, N., Feldman, P., Rosenboom, J.W., Gilligan, E., Fredericks, D., Milton, A.H., Sampson, M., Rowland, H.A.L., Lythgoe, P.R., Jones, J.C., Middleton, C., Cooke, D.A., 2005. Arsenic hazard in shallow Cambodian groundwaters. *Mineralogical Magazine*, 69(5): 807-823.
- Polya, D.A., Richards, L.A., Al Bualy, A.N., Sovann, C., Magnone, D., Lythgoe, P.R., 2017. Chapter A14: Groundwater sampling, arsenic analysis and risk communication: Cambodia Case Study. In: Bhattacharya, P., Polya, D.A., Jovanovic, D. (Eds.), *Best Practice Guide for the Control of Arsenic in Drinking Water*. IWA Publishing.
- Postma, D., Larsen, F., Minh Hue, N.T., Duc, M.T., Viet, P.H., Nhan, P.Q., Jessen, S., 2007. Arsenic in groundwater of the Red River floodplain, Vietnam: Controlling geochemical processes and reactive transport modeling. *Geochim. Cosmochim. Acta*, 71(21): 5054-5071.
- Ravenscroft, P., Brammer, H., Richards, K., 2009. *Arsenic pollution - A global synthesis*. Royal Geographical Society with IBG. Wiley-Blackwell, Chichester, 588 pp.
- Rawlins, B.G., Webster, R., Tye, A.M., Lawley, R., O'Hara, S.L., 2009. Estimating particle-size fractions of soil dominated by silicate minerals from geochemistry. *European Journal of Soil Science*, 60: 116 - 126.
- Richards, L.A., Magnone, D., Sovann, C., Kong, C., Uhlemann, S., Kuras, O., van Dongen, B.E., Ballentine, C.J., Polya, D.A., 2017a. High Resolution Profile of Inorganic Aqueous Geochemistry and Key Redox Zones in an Arsenic Bearing Aquifer in Cambodia. *Sci. Total Environ.*, 590 - 591: 540 - 553.
- Richards, L.A., Magnone, D., van Dongen, B.E., Ballentine, C.J., Polya, D.A., 2015. Use of Lithium Tracers to Quantify Drilling Fluid Contamination for Groundwater Monitoring in Southeast Asia. *Appl. Geochem.*, 63: 190 - 202.
- Richards, L.A., Sültenfuß, J., Ballentine, C.J., Magnone, D., van Dongen, B.E., Sovann, C., Polya, D.A., 2017b. Tritium Tracers of Rapid Surface Water Ingression into Arsenic-Bearing Aquifers in the Lower Mekong Basin, Cambodia. *Procedia Earth and Planetary Science*, 17C: 849 - 852.
- Rowland, H.A.L., Boothman, C., Pancost, R.D., Gault, A.G., Polya, D.A., Lloyd, J.R., 2009. The role of indigenous microorganisms in the biodegradation of naturally occurring petroleum, the reduction of iron, and the mobilization of arsenite from West Bengal aquifer sediments. *J. Env. Qual.*, 38(4): 1598 - 1607.
- Rowland, H.A.L., Gault, A.G., Lythgoe, P., Polya, D.A., 2008. Geochemistry of aquifer sediments and arsenic-rich groundwaters from Kandal Province, Cambodia. *Appl. Geochem.*, 23(11): 3029-3046.
- Rowland, H.A.L., Pederick, R.L., Polya, D.A., Pancost, R.D., Van Dongen, B.E., Gault, A.G., Vaughan, D.J., Bryant, C., Anderson, B., Lloyd, J.R., 2007. The control of organic matter on microbially mediated iron reduction and arsenic release in shallow alluvial aquifers, Cambodia. *Geobio.*, 5: 281-292.
- Rozanski, K., Araguás-Araguás, L., Gonfiantini, R., 1993. *Isotopic Patterns in Modern Global Precipitation*. *Climate Change in Continental Isotopic Records*, Geochemical Monograph 78(American Geophysical Union).

- Schaefer, M.V., Ying, S.C., Benner, S.G., Duan, Y., Wang, Y., Fendorf, S., 2016. Aquifer Arsenic Cycling Induced by Seasonal Hydrologic Changes within the Yangtze River Basin. *Environ. Sci. Technol.*, 50(7): 3521 - 3529.
- Sengupta, S., McArthur, J., Sarkar, A., Leng, M.J., Ravenscroft, P., Howarth, R.J., Banerjee, D.M., 2008. Do Ponds Cause Arsenic-Pollution of Groundwater in the Bengal Basin? An Answer from West Bengal. *Environ. Sci. Technol.*, 42: 5156 - 5164.
- Smedley, P.L., Kinniburgh, D.G., 2002. A review of the source, behaviour and distribution of arsenic in natural waters. *Appl. Geochem.*, 17(5): 517-568.
- Stuben, D., Berner, Z., Chandrasekharam, D., Karmaker, J., 2003. Arsenic enrichment in groundwater of West Bengal, India: geochemical evidence for mobilization of As under reducing conditions. *Appl. Geochem.*, 18: 1417-1434.
- Stuckey, J.W., Schaefer, M.V., Kocar, B.D., Benner, S.G., Fendorf, S., 2016. Arsenic release metabolically limited to permanently water-saturated soil in Mekong Delta. *Nat. Geos.*, 9: 70 - 76.
- Tamura, T., Saito, Y., Sieng, S., Ben, B., Kong, M., Choup, S., Tsukawaki, S., 2007. Depositional facies and radiocarbon ages of a drill core from the Mekong River lowland near Phnom Penh, Cambodia: Evidence for tidal sedimentation at the time of Holocene maximum flooding. *J. Asia. Ear. Sci.*, 29(5-6): 585-592.
- Uhlemann, S., Kuras, O., Richards, L.A., Naden, E., Polya, D.A., 2017. Electrical Resistivity Tomography determines the spatial distribution of clay layer thickness and aquifer vulnerability, Kandal Province, Cambodia. *J. Asia. Ear. Sci.*, 147: 402 - 414.
- van Dongen, B., Rowland, H.A.L., Gault, A.G., Polya, D.A., Bryant, C., Pancost, R.D., 2008. Hopane, sterane and n-alkane distributions in shallow sediments hosting high arsenic groundwaters in Cambodia. *Appl. Geochem.*, 23: 3047 - 3058.
- van Geen, A., Rose, J., Thorai, S., Garnier, J.M., Zheng, Y., Bottero, J.Y., 2004. Decoupling of As and Fe release to Bangladesh groundwater under reducing conditions. Part II: Evidence from sediment incubations. *Geochim. Cosmochim. Acta*, 68(17): 3475-3486.
- van Geen, A., Zheng, Y., Stute, M., Ahmed, K.M., 2003. Comment on "Arsenic mobility and groundwater extraction in Bangladesh" (II). *Science*, 300: 584c.
- Vandenbergh, J., Zhisheng, A., Nugteren, G., Huary, L., Van Huissteden, K., 1997. New absolute time scale for the Quaternary climate in the Chinese loess region by grain-size analysis. *Geology*, 25(1): 35 - 38.
- Water and Sanitation Program, 2015. Water Supply and Sanitation in Cambodia: Turning Finance into Services for the Future (<https://www.wsp.org/sites/wsp.org/files/publications/WSP-Cambodia-WSS-Turning-Finance-into-Service-for-the-Future.pdf>, accessed Oct 2017).
- World Health Organization, 2011. Guidelines for Drinking-water Quality: Fourth Edition, Geneva.
- Xie, X., Wang, Y., Su, C., Li, J., Li, M., 2012. Influence of irrigation practices on arsenic mobilization: Evidence from isotope composition and Cl/Br ratios in groundwater from Datong Basin, northern China. *J. Hydrol.*, 424 - 426: 37 - 47.
- Zheng, Y., van Geen, A., Stute, M., Dhar, R., Mo, Z., Cheng, Z., Horneman, A., Gavrieli, I., Simpson, H.J., Versteeg, R., Steckler, M., Grazioli-Venier, A., Goodbred, S., Shahnewaz, M., Shamsudduha, M., Hoque, M.A., Ahmed, K.M., 2005. Geochemical and hydrogeological contrasts between shallow and deeper aquifers in two villages

931 of Araihaazar, Bangladesh: Implications for deeper aquifers as drinking water sources.
932 Geochim. Cosmochim. Acta, 69(22): 5203-5218.

933

934

List of Figures

Figure 1. Map of field area and sampling locations in northern Kandal Province, Cambodia (adapted from Richards et al., 2017a; Uhlemann et al., 2017).

Figure 2. δD versus $\delta^{18}O$ of groundwaters (T-Sand and T-Clay), surface water and precipitation in northern Kandal Province, Cambodia. Groundwater and surface samples were collected (A) pre-monsoon (May – June 2014) and (B) post-monsoon (November – December 2014) and local precipitation samples were collected as cumulative weekly samples taken the first week of each month from July to November 2014. The local meteoric water line is derived from the precipitation samples.

Figure 3. Temporal variability of $\delta^{18}O$ from May 2014 – December 2014 in local precipitation and surface waters in northern Kandal Province, Cambodia (River = Mekong (MEK) and Bassac (BAS) Rivers; Isolated Ponds = near site LR14 on T-Clay and another near site LR05 on T-Sand). Local precipitation samples were collected each month (as cumulative weekly samples) during the monsoon season and river and pond samples were collected during the pre- and post-monsoon water sampling campaigns, marked as grey boxes.

Figure 4. (A) δD and (B) $\delta^{18}O$ and Depth for T-Sand and T-Clay, northern Kandal Province, Cambodia. There is no statistically significant relationship between depth and δD nor $\delta^{18}O$ on T-Sand, suggesting that deep samples on T-Sand were recharged under similar climatic conditions which currently prevail. The slightly negative correlation for T-Clay suggests that some recharge may have occurred under different climatic conditions than currently prevail.

Figure 5. Distribution of (A and C) δD and (B and D) $\delta^{18}O$ across (A and B) T-Sand and (C and D) T-Clay. More negative isotopic values represent more depleted isotopic signatures and are shown by smaller size bubbles. The underlying contour represents the mean grain size (MGS) in sediments collected from the same locations within the aquifer, with darker colors representing smaller mean particle size.

Figure 6. Estimated extent of relative recharge source evaporation with depth and site for groundwaters from northern Kandal Province, Cambodia using simple two-point mixing models assuming end-members of (i) a pond with the most enriched signature representing 100 % evaporation compared to that of the most evaporated water observed; and (ii) meteoric water with the most depleted signature from September 2014 representing 0 % evaporation. Reported values represent the mean of relative evaporation calculated from both $\delta^{18}O$ - and δD -based mixing models with error bars representing the range. The dashed line indicates the relative evaporation estimate calculated from the isotopic signature of the annual, volumetric-weighted mean of precipitation. Major well clusters on T-Sand are: (A) LR09; (B) LR01; (C) LR05; and T-Clay: (D) LR10. Sites LR09 and LR10 are located near the Bassac and Mekong rivers, respectively; site LR05 is near a pond; sites LR01 and LR05 are near sand windows.

Figure 7. Estimated extent of relative source evaporation with depth and site for groundwaters from northern Kandal Province, Cambodia using simple two-point $\delta^{18}\text{O}$ - and δD -based mixing models for the overall groundwater dataset from T-Sand (open squares) and T-Clay (filled circles). The dashed line indicates the relative evaporation estimate calculated from the isotopic signature of the annual, volumetric-weighted mean of 2014 precipitation.

Figure 8. The modelled extent of relative groundwater source evaporation based on simple two-point $\delta^{18}\text{O}$ - and δD -based mixing models as compared to the relative extent of evaporation of the 2014 annual, volumetric-weighted mean of precipitation (65 %) for groundwater on (A) T-Sand and (B) T-Clay. “More” and “Less” refer to groundwater samples (mean of pre- and post-monsoon) with more and less evaporated sources as compared to the annual, volumetric-weighted mean of 2014 precipitation.

Figure 9. Calculated reconstructed chloride concentrations using the evaporative end-member chloride concentrations and relative extent of evaporation of recharge sources predicted by two-component mixing models against measured chloride (mean of post-and pre-monsoon samples) in groundwater samples from T-Sand (open square) and T-Clay (filled circle). Symbol size indicates if the groundwater is shallow (≤ 15 m depth) or deep (> 15 m depth).

Figure 10. Cl/Br against Cl (mM, logarithmic scale) for groundwater, pond and river water and expected rainwater composition (noting that Br was not detected in the rain water sample so an exact Cl/Br for rainwater could not be calculated) in northern Kandal Province, Cambodia; labels/circles are included for selected samples/sites particularly relevant to discussion. Distinct trends for T-Sand and T-Clay are observed. Mixing lines are adapted (McArthur et al., 2012) for mixing between West Bengal urine and seawater endmembers (McArthur et al., 2012) with the most dilute groundwater sample (this study, LR04-15-PRE, Cl = 0.04 mM Cl, Cl/Br = 87 by mass); septic effluent in USA and animal (hog and horse) (Panno et al., 2006) waste are shown for reference.

Figure 11. Cl/Br versus depth for groundwater along T-Sand (open squares) and T-Clay (filled circles).

Figure 12. Cl/Br versus $\delta^{18}\text{O}$ for groundwater along T-Sand (open squares) and T-Clay (filled circles), pond (hatched triangle) and river (cross); labels/lines are included for selected samples/sites particularly relevant to discussion.

Figure 13. Ca/Na mass ratio against $\delta^{18}\text{O}$ for distinct groupings of shallow (≤ 15 m depth; smaller symbol size) and deep (> 15 m depth; larger symbol size) groundwaters from T-Clay (filled circles) and T-Sand (open squares), pond samples, river samples and cumulative precipitation from northern Kandal Province, Cambodia. Groundwater from T-Clay typically has lower Ca/Na than groundwater from T-Sand.

Figure 14. δD versus $\delta^{18}O$ for all groundwater samples in northern Kandal Province, Cambodia with (A) As concentrations and (B) bulk dissolved organic carbon (DOC) represented by bubble size (Richards et al., 2017a). Global Meteoric Water Line (GMWL) and Local Meteoric Water Line (LMWL) shown for comparison.

Figure 15. Groundwater As concentrations along T-Sand and T-Clay (Richards et al., 2017a) in northern Kandal Province, Cambodia with the modelled extent of relative evaporation of recharge sources. The estimated relative source evaporation is based on simple two-point mixing models assuming end-members of (i) a pond with the most enriched signature representing 100 % relative evaporation compared to that of the most evaporated water observed; and (ii) meteoric water with the most depleted signature from September 2014 representing 0 % evaporation. The dashed line indicates the relative source evaporation estimate calculated from the isotopic signature of the annual, volumetric-weighted mean of precipitation. Error bars represent the range of relative evaporation calculated using $\delta^{18}O$ - and δD -based mixing models.

1026 **List of Tables**

1027 **Table 1.** Mean δD and $\delta^{18}O$ for groundwaters (GW) and surface water (SW) in northern
1028 Kandal Province, Cambodia during pre- and post-monsoon conditions and volumetric-
1029 weighted mean of precipitation. Rainfall data is from the Mekong River Commission
1030 Monitoring Station Phnom Penh Chaktomuk (Bassac) (Mekong River Commission, 2015);
1031 * indicates that only one sample was collected.

1032

Delineating Sources of Groundwater Recharge in an Arsenic-Affected Holocene Aquifer in Cambodia Using Stable Isotope-Based Mixing Models

Laura A. Richards^{1*}, Daniel Magnone², Adrian Boyce³, Maria J. Casanueva-Marenco⁴, Bart E. van Dongen¹, Christopher J. Ballentine⁵, David A. Polya¹

¹School of Earth and Environmental Sciences and Williamson Research Centre for Molecular Environmental Science, The University of Manchester, Williamson Building, Oxford Road, Manchester, M13 9PL, UK

²Present address: School of Geography, University of Lincoln, Brayford Pool, Lincoln, Lincolnshire, LN6 7TS, UK

³Scottish Universities Environmental Research Centre, East Kilbride, G75 0QF, UK

⁴Present address: Department of Analytical Chemistry, Institute of Biomolecules, Faculty of Sciences, University of Cádiz, Cádiz, Spain

⁵Present address: Department of Earth Sciences, University of Oxford, South Parks Road, Oxford OX1 3AN, UK

*Corresponding author: laura.richards@manchester.ac.uk

HYDROL23862R1 Revisions for *Journal of Hydrology*
2017

Abstract

Chronic exposure to arsenic (As) through the consumption of contaminated groundwaters is a major threat to public health in South and Southeast Asia. The source of As-affected groundwaters is important to the fundamental understanding of the controls on As mobilization and subsequent transport throughout shallow aquifers. Using the stable isotopes of hydrogen and oxygen, the source of groundwater and the interactions between various water bodies were investigated in Cambodia's Kandal Province, an area which is heavily affected by As and typical of many circum-Himalayan shallow aquifers. Two-point mixing models based on δD and $\delta^{18}O$ allowed the relative extent of evaporation of groundwater sources to be estimated and allowed various water bodies to be broadly

distinguished within the aquifer system. Model limitations are discussed, including the spatial and temporal variation in end member compositions. The conservative tracer Cl/Br is used to further discriminate between groundwater bodies. The stable isotopic signatures of groundwaters containing high As and/or high dissolved organic carbon plot both near the local meteoric water line and near more evaporative lines. The varying degrees of evaporation of high As groundwater sources are indicative of differing recharge contributions (and thus indirectly inferred associated organic matter contributions). The presence of high As groundwaters with recharge derived from both local precipitation and relatively evaporated surface water sources, such as ponds or flooded wetlands, are consistent with (but do not provide direct evidence for) models of a potential dual role of surface-derived and sedimentary organic matter in As mobilization.

Keywords

stable isotopes, mixing models, recharge sources, arsenic, groundwater

1. Introduction

The chronic exposure to groundwater containing dangerous concentrations of naturally-occurring As is a major threat to public health affecting millions of people in South and Southeast Asia (Smedley and Kinniburgh, 2002; Charlet and Polya, 2006; Ravenscroft et al., 2009; World Health Organization, 2011). In the shallow groundwaters typical to this region, the primary mechanism of As release is widely thought to be the reductive dissolution of As-bearing Fe(III) minerals driven by metal-reducing bacteria and fuelled by bioavailable organic matter (Bhattacharya et al., 1997; Islam et al., 2004; van Geen et al., 2004; Charlet and Polya, 2006; Postma et al., 2007; Rowland et al., 2009). However, the comprehensive understanding of the nature of the organic matter implicated in As-release remains limited. Various inputs are generally thought to contribute in some proportion to As mobilization, including: (i) plant-derived organic matter internal to the sediment aquifers (Nickson et al., 1998; McArthur et al., 2001; McArthur et al., 2004); (ii) external, modern surface-derived organic matter, largely from ponds, rivers and rice paddies and/or wastewater inputs (Harvey et al., 2002; Kocar et al., 2008; Papacostas et al., 2008; Polizzotto et al., 2008;

Neumann et al., 2010; McArthur et al., 2012; Lawson et al., 2013; Lawson et al., 2016), which may be exacerbated by large-scale groundwater abstraction (Harvey et al., 2002; Aggarwal et al., 2003; Harvey et al., 2003; van Geen et al., 2003; Sengupta et al., 2008; Neumann et al., 2010; McArthur et al., 2011; Lawson et al., 2013; Mailloux et al., 2013); and/or (iii) petroleum-derived hydrocarbons from thermally mature sediments (Rowland et al., 2007; van Dongen et al., 2008; Rowland et al., 2009; Al Lawati et al., 2012; Al Lawati et al., 2013). The nature of the organic matter implicated in As release is inherently linked to the sub-surface location where As release occurs and the subsequent controls on As mobility (Nickson et al., 1998; Harvey et al., 2002; McArthur et al., 2004; Gault et al., 2005; Rowland et al., 2007; van Dongen et al., 2008; Neumann et al., 2009; Rowland et al., 2009; Fendorf et al., 2010; Mladenov et al., 2010; Datta et al., 2011; McArthur et al., 2011; Neumann et al., 2011; Al Lawati et al., 2012; Al Lawati et al., 2013; Lawson et al., 2013; Neumann et al., 2014; Lawson et al., 2016; Schaefer et al., 2016; Stuckey et al., 2016). Thus, determining the relative importance of the various potential organic matter inputs is critical in predicting how As hazard may change in the future (Harvey et al., 2002; Polya and Charlet, 2009; Lawson et al., 2016).

The stable isotopes of hydrogen (H, D) and oxygen (^{16}O , ^{18}O) have been used extensively in hydrological studies, including but not limited to the context of As mobilization, to assess groundwater recharge processes, determine sources of groundwaters and identify interactions between different water bodies (Aggarwal et al., 2000; Stuben et al., 2003; van Geen et al., 2003; Harvey et al., 2005; Zheng et al., 2005; Klump et al., 2006; Mukherjee et al., 2007; Berg et al., 2008; Sengupta et al., 2008; Datta et al., 2011; Lawson et al., 2013; Lawson et al., 2016). In As-based studies, $\delta^{18}\text{O}$ and δD data have been used to suggest that pond water does not significantly recharge (and thus contribute organic matter) to As-bearing groundwater (van Geen et al., 2003; Sengupta et al., 2008; Datta et al., 2011), whereas others have argued that surface-derived organic matter is an essential driver in As mobilization (Harvey et al., 2002; Kocar et al., 2008; Papacostas et al., 2008; Polizzotto et al., 2008; Neumann et al., 2010; Lawson et al., 2013; Lawson et al., 2016). Stable isotopes are a powerful tool because they are chemically inert (*e.g.* fully conservative) and are directly incorporated into the water molecule, providing robust evidence of direct hydrological processes. In addition, the Cl/Br ratio is a conservative chemical tracer, which has been

used to distinguish different water sources and as an indicator of water-rock interactions (particularly halite dissolution), leaching or wastewater influence on a groundwater (e.g. Davis et al., 1998; Alcalá and Custodio, 2005; Cartwright et al., 2006; McArthur et al., 2012; Xie et al., 2012; Majumder et al., 2016; McArthur et al., 2016) and references within.

The variation in the $\delta^{18}\text{O}$ and δD isotopic signature of natural waters is largely controlled by thermodynamic fractionation, occurring because of physical processes such as evaporation and condensation. The thermodynamic fractionation results in water bodies with isotopically distinct signatures and also produces a defined relationship between δD and $\delta^{18}\text{O}$ for global meteoric precipitation known as the Global Meteoric Water Line (GMWL) (Craig, 1961). The extent of deviation of the isotopic signature of a natural water from the GMWL along evaporation lines reflects the magnitude of the kinetic effect, with greater deviations indicating more extensive evaporation (Craig and Gordon, 1965; Gat, 1971). The isotopic composition varies geographically due to the latitude, amount, elevation and continental effects (Dansgaard, 1974; Clark and Fritz, 1997). Temporal variations can be significant particularly in tropical areas such as Southeast Asia where the isotopic depletion correlates well with the amount of precipitation (Araguás-Araguás and Froehlich, 1998; Araguás-Araguás et al., 2000). These processes determine the isotopic signature of precipitation as well as the evolution of the isotopic signature of surface waters, both of which may contribute to groundwater recharge.

In the shallow aquifers of Kandal Province, Cambodia, in the Lower Mekong Basin, groundwater concentrations of As are well known to be highly heterogeneous and far exceed health-based guidelines (Appelo and Postma, 1993; Polyá et al., 2003; Polyá et al., 2005; Tamura et al., 2007; Benner et al., 2008; Kocar et al., 2008; Polizzotto et al., 2008; Rowland et al., 2008; van Dongen et al., 2008; Polyá and Charlet, 2009; Lawson et al., 2013; Lawson et al., 2016; Richards et al., 2017a). Here, As mobilization seems to be affected by complex, site-specific surface-groundwater interactions as well as in-aquifer interactions which lead to a potential dual role for both surface and sedimentary organic carbon in As mobilization (Lawson et al., 2013; Lawson et al., 2016). The interpretation of the stable isotope and Cl/Br signatures of these As-bearing groundwaters allows for the characterization of recharge mechanisms and systematics, which may assist in improving the understanding of the potential controls on the nature and/or relative contributions of

organic matter affecting As mobilization (Nickson et al., 1998; Harvey et al., 2002; McArthur et al., 2004; Gault et al., 2005; Rowland et al., 2007; van Dongen et al., 2008; Neumann et al., 2009; Rowland et al., 2009; Fendorf et al., 2010; Mladenov et al., 2010; Al Lawati et al., 2012; Al Lawati et al., 2013; Lawson et al., 2013; Neumann et al., 2014; Lawson et al., 2016). The aim of this study is thus to characterize the source of As-affected groundwater in two high-resolution profiles along inferred groundwater flowpaths, with the following objectives: (i) to assess the recharge sources of the groundwater; (ii) to categorize the systematics of surface waters (ponds, rivers, precipitation); and (iii) to differentiate between groundwater bodies within the aquifer via mixing models derived from stable isotope ($\delta^{18}\text{O}$ and δD) signatures to determine the relative extent of evaporation of groundwater sources, as well as by using the conservative tracer Cl/Br.

2. Methods and Materials

2.1 Field Site Description

The field sites are located in the Kien Svay district of northern Kandal Province, Cambodia, an area heavily affected by groundwater As (Appelo and Postma, 1993; Polya et al., 2003; Polya et al., 2005; Charlet and Polya, 2006; Tamura et al., 2007; Benner et al., 2008; Kocar et al., 2008; Polizzotto et al., 2008; Rowland et al., 2008; van Dongen et al., 2008; Polya and Charlet, 2009; Lawson et al., 2013; Lawson et al., 2016; Richards et al., 2017a; Richards et al., 2017b). Field sites (**Figure 1**) are located along two distinct transects, called here “T-Sand” and “T-Clay” and which are dominated by sand and clay lithologies respectively, and both oriented to be broadly parallel to inferred major groundwater flowpaths (Richards et al., 2017a). The local geology is typical to floodplains in the Lower Mekong Basin, with elevated levees along the Mekong and Bassac River banks which retreat inland towards a seasonally saturated wetland basin (Kocar et al., 2008). Sedimentological attributes and a geomorphological framework for the study area are provided elsewhere (Magnone et al., 2017), and basic hydrogeological parameters such as hydraulic conductivities for a nearby field area are also published elsewhere (Benner et al., 2008). The annual monsoon season drives changes in the horizontal hydraulic head gradient, with groundwater flowing from the rivers inland during the monsoon season and in the opposite direction during the dry season

(Benner et al., 2008; Richards et al., 2017a). Groundwater abstraction in the area is limited and thus the field sites are representative of minimally-influenced, pre-development conditions, also noting that both population density (~ 360 people/km²) (Cambodia Investment, 2014) and sanitation coverage (~ 25 %) (Water and Sanitation Program, 2015) is relatively low.

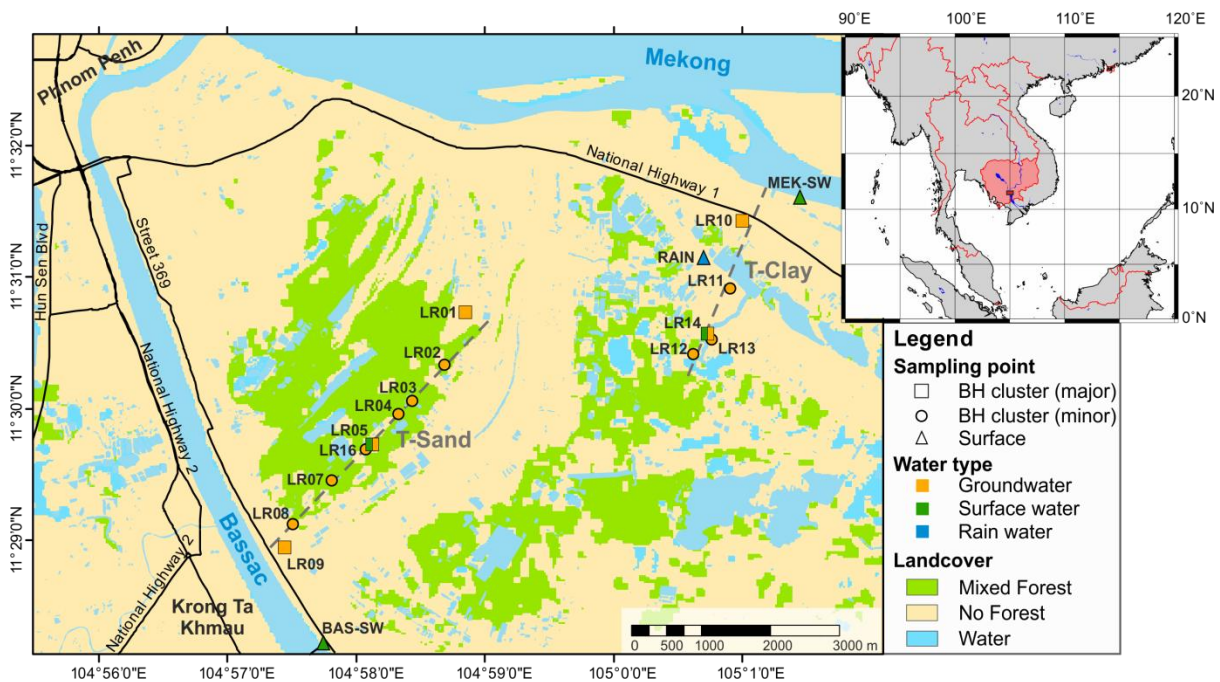


Figure 1. Map of field area and sampling locations in northern Kandal Province, Cambodia (adapted from Richards et al., 2017a; Uhlemann et al., 2017).

2.2 Sample Collection and Characterization

Groundwater from depths of 6 to 45 meters and surface waters were sampled (i) pre-monsoon in May – June 2014; and (ii) post-monsoon in November – December 2014 using methods previously described (Richards et al., 2015; Richards et al., 2017a). Samples for stable isotopes (δD and $\delta^{18}O$) were not filtered nor chemically preserved and were collected in 60 mL acid-washed and furnace-dried amber glass Schott bottles with polyseal caps, placed in field coolers within 60 minutes of collection and in refrigerated storage ($\sim 4^{\circ}C$) generally within several hours. Samples for stable isotope analysis of accumulated weekly precipitation were collected every month between July and November 2014 and stored in 500 mL amber glass bottles with polyseal caps.

Major cations (including Ca and Na) were analyzed on filtered (0.45 μm cellulose and polypropylene syringe filters, Minisart RC, UK) and acidified ($< \text{pH } 2$, trace grade nitric acid, BDH Aristar, UK) using inductively coupled plasma atomic emission spectrometry (ICP-AES, Perkin-Elmer Optima 5300 dual view) at the Manchester Analytical Geochemistry Unit (MAGU, University of Manchester, UK) with inverse variance weighted first order linear calibration models (Miller and Miller, 2010; Polya et al., 2017; Richards et al., 2017a). Chloride and bromide were measured on subsamples of un-acidified and filtered (0.45 μm cellulose and polypropylene syringe filters, Minisart RC, UK) groundwater using ion chromatography (IC; Dionex ICS5000 Dual Channel Ion Chromatograph) at MAGU (Richards et al., 2017a).

Wet sediment cores were collected at the time of drilling (Richards et al., 2015) and a subsample stored in polyethylene bags and frozen until particle size analysis. Particle size analysis was completed at the British Geological Survey (Keyworth, UK) on dried and sieved ($< 2 \text{ mm}$) sediment samples using laser diffraction (LS 13 320 Laser Diffraction Particle Size Analyzer, Beckman Coulter, UK), enabled with Polarization Intensity Differential Scattering (PIDS) to account for the sizing of non-spherical, sub-micron particles. Sediment samples were sonicated for 300 seconds prior to laser particle size analysis. Data interpretation and statistical analysis was completed using the Gradistat_v8 software package (Blott and Pye, 2001). The following particle size classifications were used: (i) clay $< 8 \mu\text{m}$ ($\phi > 7$); (ii) silt $8 \mu\text{m} - 0.063 \text{ mm}$ ($4 < \phi < 7$); and (iii) sand $0.063 - 2 \text{ mm}$ ($-1 < \phi < 4$) (Vandenberghe et al., 1997; Rawlins et al., 2009). Contour plots of grain size were produced without smoothing using OriginPro 2015 and supplemented with drilling logs where particle size analysis was not completed.

2.3 Analysis of Stable Hydrogen and Oxygen Isotopes

Stable isotope analysis (δD and $\delta^{18}\text{O}$) was conducted at the Isotope Community Support Facility (ICSF) at the Scottish Universities Environmental Research Centre (SUERC, UK). For δD analysis, 1 μL standard and sample aliquots were directly injected into a chromium furnace at 800°C , with the evolved H_2 gas subsequently analyzed on-line using mass spectrometry (VG Optima dual-inlet Mass Spectrometer) (Donnelly et al., 2001). For $\delta^{18}\text{O}$

analysis, 200 µL sample aliquots were over-gassed with 1 % CO₂-in-He for 5 minutes, followed by a 24 hour equilibration period prior to analysis with mass spectrometry (Delta V Plus Isotope Ratio Mass Spectrometer, Thermo Scientific) set at 25 °C using standard techniques (Nelson, 2000). Reproducibility was estimated to be ± 3 % and ± 0.3 % for δD and δ¹⁸O, respectively, and is based on within-run replicate analysis of international reference standards Vienna Standard Mean Ocean Water (VSMOW), Greenland Ice Sheet Precipitation (GISP) and the internal standard Lt Std.

The isotopic composition of water is reported as the per mil (‰) deviation from VSMOW, per Equation 1:

$$\delta = \left[\frac{(R_{sample} - R_{standard})}{R_{standard}} \right] \cdot 1000 \quad [1]$$

where R = ²D/¹H for hydrogen and ¹⁸O/¹⁶O for oxygen, the ratio of the heavy to light isotope. Because of the significant geographical and temporal variations in the isotopic composition of precipitation (Dansgaard, 1974; Clark and Fritz, 1997; Araguás-Araguás and Froehlich, 1998; Araguás-Araguás et al., 2000), a local meteoric water line (LWML) was derived from local precipitation to compare the isotopic composition of groundwater and surface water. The deuterium excess (d) is a way to quantify locally-dependent deviation (particularly due to humidity or mixing of different vapour masses), and is given by Equation 2 (Dansgaard, 1974; Araguás-Araguás et al., 2000):

$$d = \delta D - 8\delta^{18}O \quad [2]$$

Isotope exchange between groundwater and aquifer minerals is assumed to be negligible (Clark and Fritz, 1997).

2.4 Modelling the Estimated Relative Extent of Evaporation of Groundwater Sources

The degree of groundwater source evaporation was estimated using simple two-component mixing models with end-members representing the most enriched (e.g. 100 % evaporated compared to that of the most evaporated water observed) and most depleted (e.g. 0 % evaporated) δD and δ¹⁸O signatures observed in 2014 pond water and local precipitation,

respectively. This was calculated via Equations 3 and 4:

$$X_{GW,\delta^{18}O} = \frac{\delta^{18}O_{GW} - \delta^{18}O_{EMDepleted}}{\delta^{18}O_{EMEvaporated} - \delta^{18}O_{EMDepleted}} \quad [3]$$

$$X_{GW,\delta D} = \frac{\delta D_{GW} - \delta D_{EMDepleted}}{\delta D_{EMEvaporated} - \delta D_{EMDepleted}} \quad [4]$$

where the relative extent of source evaporation (X) of a groundwater sample based on $\delta^{18}O$ or δD is $X_{GW, \delta^{18}O}$ and $X_{GW, \delta D}$, respectively and $\delta^{18}O$ and δD of the groundwater (GW) and depleted or evaporated end-members (EM) are measured. Calculations were made for each groundwater pre- and post-monsoon sample using both the δD and $\delta^{18}O$ signatures, with the median and range reported for the δD and $\delta^{18}O$ -based results to give an estimated degree of relative source evaporation. The difference in evaporation estimate between the independent δD and $\delta^{18}O$ calculations was generally within a few percent. It was assumed that the end-member values for the 2014 sampling season were broadly similar to values typically encountered over previous years, although yearly variation in weather conditions such as rainfall and humidity can occur (Mekong River Commission, 2015). Discussion on the characterization of model end-members, model bias and limitations are found in Section 3.3.

3. Results and Discussion

3.1 Stable Oxygen and Hydrogen Isotopes

The degree of interaction between surface and groundwaters was investigated by comparing the isotopic signature (δD versus $\delta^{18}O$) of groundwaters from T-Sand and T-Clay with Mekong and Bassac River water, isolated pond waters and precipitation (**Figure 2**). The mean isotopic compositions of groundwaters, surface waters and the volumetric-weighted mean of precipitation are shown on **Table 1**. A local meteoric water line (LMWL; $\delta D = 6.4 \delta^{18}O - 1.3$, adjusted $R^2 = 0.99$) was developed from cumulative weekly samples of rainwater. The 2014 LMWL has a slope of 6.4, which is less than the global meteoric water line (GMWL)

slope of 8.17 (Rozanski et al., 1993), less than the 2009 LMWL gradient of 8.3 in the same area (Lawson et al., 2016) and also less than the 2003 – 2005 LMWL gradient of 6.82 – 7.95 for the nearby Kampong Province (Kabeya et al., 2007). The slope of any LMWL is a function of local conditions related to fluctuating weather, relative humidity or mixing of differently sourced vapour masses, and particularly in tropical regions like Cambodia, may differ substantially from the GMWL, with greater deviation reflecting more extensive evaporation (Craig and Gordon, 1965; Gat, 1971; Araguás-Araguás et al., 2000). Indeed, 2014 is the driest year on record from available data (2008 – 2015) (Mekong River Commission, 2015), which is consistent with the more evaporative LMWL observed. The deuterium excess, d , of the local precipitation ranges from 2.6 to 15.6 (relative to a slope of 8), suggesting that local surface waters contribute a kinetically controlled, re-evaporated component to the precipitation, which is characteristic of humid climates (Merlivat and Jouzel, 1979; Clark and Fritz, 1997; Pfahl and Sodemann, 2014). Seasonal differences in d have been shown to vary by more than 10 ‰ in the eastern Asian monsoon region (Kondoh and Shimada, 1997) which is the same broad range observed here.

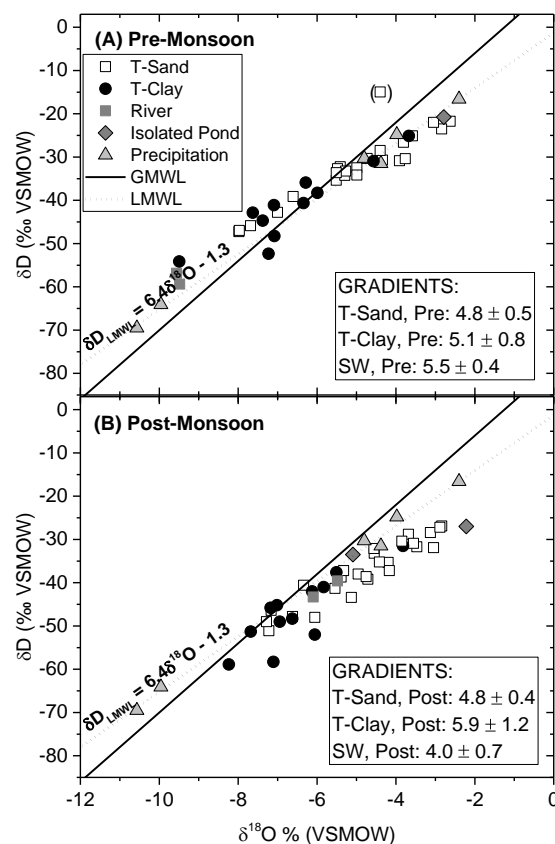


Figure 2. δD versus $\delta^{18}O$ of groundwaters (T-Sand and T-Clay), surface water and precipitation in northern Kandal Province, Cambodia. Groundwater and surface samples

were collected (A) pre-monsoon (May – June 2014) and (B) post-monsoon (November – December 2014) and local precipitation samples were collected as cumulative weekly samples taken the first week of each month from July to November 2014. The local meteoric water line is derived from the precipitation samples. The point marked in parentheses is considered an outlier as δD is beyond two standard deviations of the mean.

Table 1. Mean δD and $\delta^{18}O$ for groundwaters (GW) and surface water (SW) in northern Kandal Province, Cambodia during pre- and post-monsoon conditions and volumetric-weighted mean of precipitation. Rainfall data is from the Mekong River Commission Monitoring Station Phnom Penh Chaktomuk (Bassac) (Mekong River Commission, 2015); * indicates that only one sample was collected.

Group	δD , Mean (‰ VSMOW)			$\delta^{18}O$, Mean (‰ VSMOW)		
	Pre-Monsoon	Post-Monsoon	Overall	Pre-Monsoon	Post-Monsoon	Overall
T-Sand, GW	-32.3	-36.9	-34.7	-5.0	-4.7	-4.9
T-Clay, GW	-41.3	-46.7	-44.1	-6.6	-6.5	-6.6
River, SW	-58.0	-41.5	-49.8	-9.5	-5.8	-7.7
Ponds, SW	-21.0*	-30.3	-27.1	-2.8*	-3.7	-3.4
Precipitation		-35.7			-5.5	

Pre-monsoon groundwater (**Figure 2A**) typically falls near the LMWL, with some samples slightly enriched and some slightly depleted in comparison. Post-monsoon groundwater (**Figure 2B** and **Table 1**) typically falls on or below the LMWL, and is generally more depleted in δD (shifting to lighter, more negative values) than pre-monsoon groundwater (*e.g.* mean δD for T-Sand is -32.3 and -36.9 for pre- and post-monsoon, respectively) ; in contrast $\delta^{18}O$ becomes slightly less depleted during the post-monsoon season (*e.g.* mean $\delta^{18}O$ for T-Sand is -5.0 and -4.7 for pre- and post-monsoon, respectively). In both pre- and post-monsoon seasons, groundwater from T-Sand generally trends towards more enriched values as compared to groundwater from T-Clay. The more enriched isotopic signature of T-Sand groundwaters indicates the contribution of an evaporated source of recharge to the groundwater particularly along this transect. This evaporated source could either be from surface waters or as a result of evaporation of meteoric water during recharge. Broad comparison of the gradients of the pre-monsoon regression lines for T-Sand (slope = 4.8 ± 0.5) and T-Clay (slope = 5.1 ± 0.8) with the surface waters (5.5 ± 0.4) and LMWL (slope = 6.4 ± 0.2) suggest that surface waters are the most likely source of recharge to the groundwater prior to the onset of the monsoonal rains. In contrast, post-monsoon regression lines for T-Sand (slope = 4.8 ± 0.4) and T-Clay (slope = 5.9 ± 1.2) with the surface waters (slope = $4.0 \pm$

0.7) and LMWL (slope = 6.4 ± 0.2) suggest that contributions of both surface waters and meteoric water recharge sources may be observed in post-monsoon groundwater. The differences in the gradients of the regression lines for the different transects and seasons indicates that the recharge scenarios for the two aquifers may be different, which is feasible due to the differences in dominant lithology noted for these two transects .

The post-monsoon groundwater regression line for T-Sand intercepts the LMWL at an isotopic composition (*e.g.* at $\delta D = -54 \text{ ‰}$, $\delta^{18}O = -8.3 \text{ ‰}$) consistent with (i) precipitation which falls in between the first week in October 2014 ($\delta D = -64 \text{ ‰}$, $\delta^{18}O = -10 \text{ ‰}$) and the first week in November 2014 ($\delta D = -32 \text{ ‰}$, $\delta^{18}O = -4.4 \text{ ‰}$), as well as (ii) values of west bank Mekong water which are expected to derive from the Tonle Sap during the early post-monsoon period (Kabeya et al., 2008). This intersection point is more depleted than the volumetric-weighted mean of 2014 precipitation ($\delta D = -36 \text{ ‰}$, $\delta^{18}O = -5.5 \text{ ‰}$, shown on **Table 1**). Interestingly, the horizontal groundwater hydraulic gradient changes direction in that same time period between October and November 2014, changing from the gradient in the direction from the rivers towards inland basins before mid-October, to the opposite direction from the inland basins towards the rivers after mid-October. This is an annual effect driven by monsoonal changes in water level (Benner et al., 2008). The fact that the groundwater regression line intersects the LMWL at an isotopic signature reflecting the time that corresponds to the change in direction of groundwater gradient (October/November 2014) rather than the local volumetric precipitation peak in July 2014 (Mekong River Commission, 2015) is indicative that a significant amount of groundwater recharge may be river-derived. This provides evidence for river-groundwater connectivity which may affect the isotopic signatures of affected groundwaters, and may in part explain why a number of the post-monsoon groundwaters are more depleted than the 2014 volumetric-weighted mean of precipitation. Similarly, the LMWL intercepts the *pre*-monsoon groundwater regression lines for groundwaters along both T-Sand and T-Clay at a similar isotopic composition ($\delta D = -28 \text{ ‰}$, $\delta^{18}O = -4.2 \text{ ‰}$ for T-Sand; $\delta D = -32 \text{ ‰}$, $\delta^{18}O = -4.8 \text{ ‰}$ for T-Clay). This isotopic composition of this interception point is again similar to the local precipitation which falls in November 2014 ($\delta D = -32 \text{ ‰}$, $\delta^{18}O = -4.4 \text{ ‰}$) and similarly more depleted than the 2014 volumetric-weighted precipitation mean. Although precipitation data were not collected for the 2013 monsoon season which is what would have directly/most recently

influenced the pre-monsoon samples collected in May/June 2014, the similarity in the intersection point data with the November 2014 precipitation indicates that these interactions are likely to be annual.

The precipitation and surface waters (Mekong River, Bassac River, isolated pond near LR14 on T-Clay and isolated pond near LR05 on T-Sand) show large temporal variations over the period of May 2014 – December 2014 (**Figure 3**). These variations are largely due to (i) Rayleigh fractionation for precipitation; (ii) evaporation for pond water; and (iii) both fractionation and evaporation for river water. The isotopic signature of the precipitation shows very large temporal changes and reaches a peak in evaporative enrichment around August, corresponding to around the time when relative humidity generally also peaks (Kabeya et al., 2007). The monthly rainfall in August 2014 was unusually low as compared to previous years, contributing only ~ 8 % to the total 2014 precipitation (Mekong River Commission, 2015). Rainfall in June, July, August, September and October 2014 volumetrically contributed ~ 16 %, 36 %, 8 %, 23 % and 17 %, respectively, to the total 2014 precipitation recorded (Mekong River Commission, 2015). The isotopic signature of the rivers becomes more enriched (more positive) during the post-monsoon sampling campaign, which is consistent with the contribution of precipitation during the monsoon season and subsequent evaporation, as well as with the flood-pulse recession from the Tonle Sap (Kabeya et al., 2008). Temporal patterns in the isotopic signature of the Mekong River have been previously linked with the monsoonal changes in river water level (Lawson et al., 2013). Conversely to the rivers, the isolated ponds show the opposite overall trend during the same period. The isolated ponds become more depleted (more negative) during the post-monsoon sampling campaign, evolving toward a more groundwater-similar signature. One explanation for this trend is the contribution of precipitation to the pond water. In the period of September and October 2014, temperature decreases but rainfall remains at high volumes (Mekong River Commission, 2015) and water levels in the wetlands significantly increase (Benner et al., 2008), suggesting that dilution of the ponds from mixing with precipitation is responsible for the isotopic depletion in these waters. An alternative explanation for the increasingly depleted ponds in the post-monsoon season is that more depleted groundwater may be influenced by strong upward groundwater flow manifesting as artesian flow in areas of low topography during this time period (Benner et al., 2008;

Lawson et al., 2013), leading to a contribution of groundwater to the ponds and providing evidence for surface-groundwater connectivity.

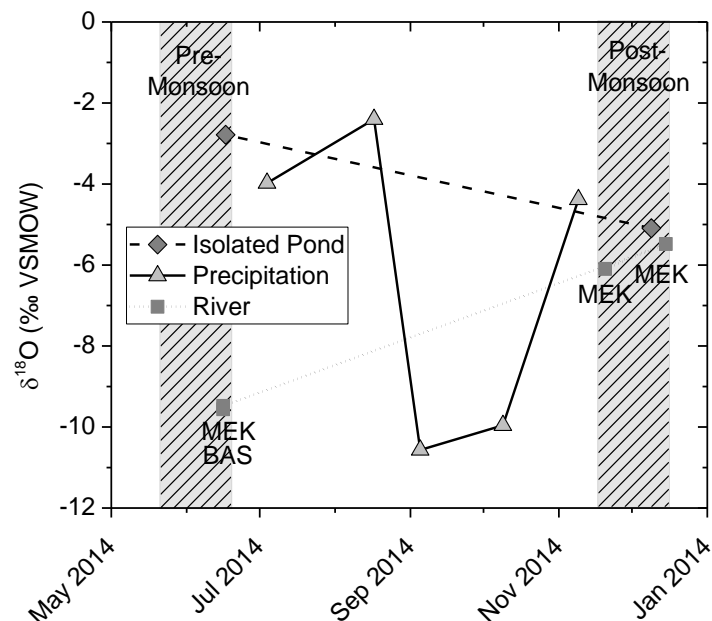


Figure 3. Temporal variability of $\delta^{18}\text{O}$ from May 2014 – December 2014 in local precipitation and surface waters in northern Kandal Province, Cambodia (River = Mekong (MEK) and Bassac (BAS) Rivers; Isolated Ponds = near site LR14 on T-Clay and another near site LR05 on T-Sand). Local precipitation samples were collected each month (as cumulative weekly samples) during the monsoon season and river and pond samples were collected during the pre- and post-monsoon water sampling campaigns, marked as grey boxes.

3.2 The Spatial Distribution of Stable Isotope Composition

The isotopic signatures of groundwater on T-Sand do not show any consistent, overall trend with depth (**Figure 4**), suggesting that the groundwater at deeper parts of the aquifer was recharged under climatic conditions which are similar to current climatic conditions. This is consistent with the relatively fast recharge rates that can be expected in an area of sand-dominated lithology. The slightly negative correlation between both δD and $\delta^{18}\text{O}$ with depth on T-Clay ($t(21) = -2.61$, $p = 0.016$ and $t(21) = -2.63$, $p = 0.016$ for δD and $\delta^{18}\text{O}$, respectively) indicates that some groundwaters on this transect may have been recharged under different, more depleted conditions. The observed differences between the two

transects are broadly consistent with differences in lithology (e.g. sand versus clay dominant) and other geochemical characterization (Lawson et al., 2013; Lawson et al., 2016).

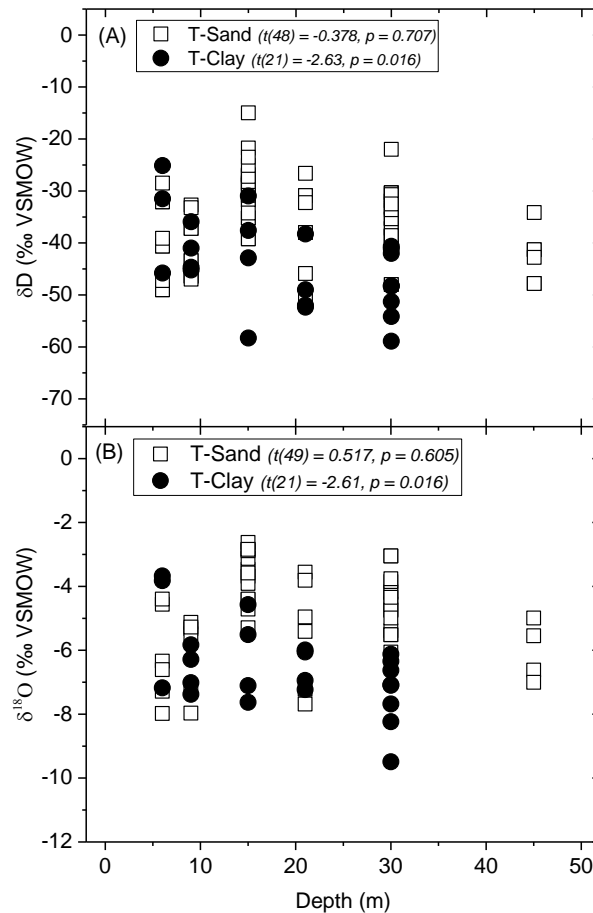


Figure 4. (A) δD and (B) $\delta^{18}O$ and Depth for T-Sand and T-Clay, northern Kandal Province, Cambodia. There is no statistically significant relationship between depth and δD nor $\delta^{18}O$ on T-Sand, suggesting that deep samples on T-Sand were recharged under similar climatic conditions which currently prevail. The slightly negative correlation for T-Clay suggests that some recharge may have occurred under different climatic conditions than currently prevail.

There are site-specific variations in isotopic signatures, with either depth or increasing distance from the river (**Figure 5**). For example, the most depleted signatures on T-Sand are observed with shallow samples located in relative proximity to the Bassac River at site LR09. Similarly the groundwater is depleted at site LR10, which is in close proximity to the Mekong River on T-Clay. The most enriched samples are located along T-Sand, particularly in the central belt of the aquifer from sites LR03 to LR07 which is dominated by sand lithology. These relatively enriched samples are indicative of an evaporated source of recharge.

Interestingly, at site LR09, the most enriched samples are found at depth indicating the possibility of depth-specific recharge sources or sources which change along groundwater flowpaths. All post-monsoon samples on T-Sand have more enriched $\delta^{18}\text{O}$ signatures than pre-monsoon signatures at the same depth and location, clearly indicating a seasonal timescale on recharge. This same observation cannot be made across T-Clay where monsoonal changes are less variable and more site-specific.

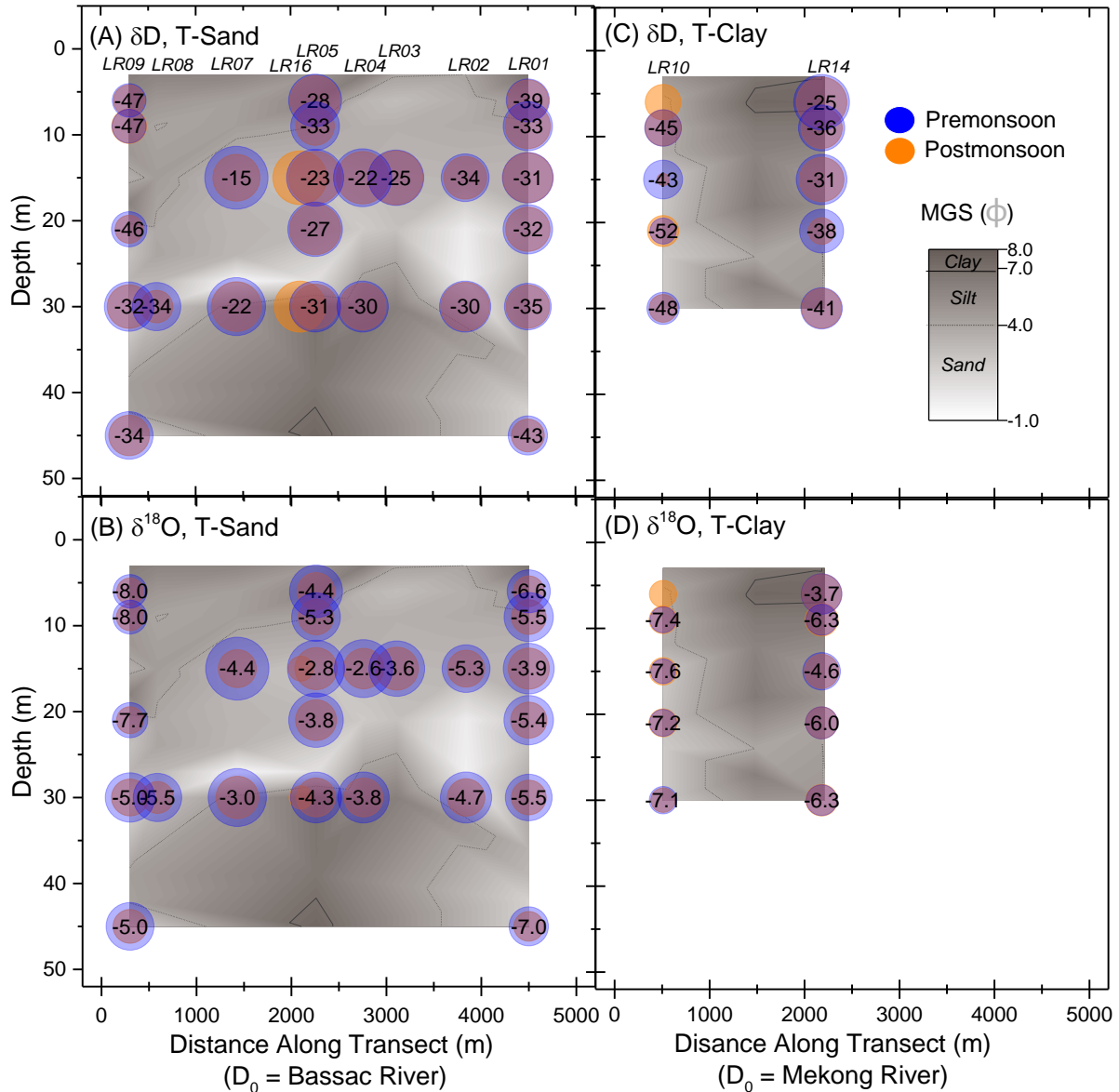


Figure 5. Distribution of (A and C) δD and (B and D) $\delta^{18}\text{O}$ across (A and B) T-Sand and (C and D) T-Clay. More negative isotopic values represent more depleted isotopic signatures and are shown by smaller size bubbles. The underlying contour represents the mean grain size (MGS) in sediments collected from the same locations within the aquifer, with darker colors

representing smaller mean particle size. Labelled datapoints represent pre-monsoon values (blue bubbles) and post-monsoon values (orange bubbles) are unlabelled.

3.3 Estimation of the Relative Extent of Evaporation of Groundwater Sources

Site-specific comparisons of the isotopic signature of various groundwaters with the signatures of isotopically enriched and depleted end-members allow for the relative extent of evaporation of recharge source to be estimated with simple two-point mixing models, and may be indicative of recharge from surface waters in some cases (**Figure 6**). Here, the end-members were assumed to be the 2014 extreme values namely (i) a pond with the most enriched signature representing 100 % relative evaporation (*e.g.* compared to that of the most evaporated water observed) ($\delta^{18}\text{O} = -2.8 \text{ ‰}$; $\delta\text{D} = -20.8 \text{ ‰}$); and (ii) meteoric water with the most depleted signature representing 0 % evaporation ($\delta^{18}\text{O} = -10.6 \text{ ‰}$; $\delta\text{D} = -69.5 \text{ ‰}$). The dashed line shown on **Figure 6** represents the modelled relative evaporation (65 %) for the 2014 annual, volumetric-weighted mean of precipitation, so anything falling to the right or left of that line is considered to be more or less evaporated, respectively, than mean precipitation. Local and small-scale variations are very important for understanding groundwater provenance and identifying recharge mechanisms. For example, at site LR09 (**Figure 6A**), which is near the Bassac River, the deeper groundwaters are more isotopically enriched (and thus have a more evaporated source) than shallow, relatively un-evaporated groundwater sources at the same location (*e.g.* approximately 70 % versus 40 % relative source evaporation, respectively). This suggests that deep and shallow groundwaters may have contributions from different recharge sources, and specifically that deeper groundwaters may be recharged by more relatively evaporated, surface-water derived sources, possibly derived from the nearby Bassac River with connectivity from a deep sand lens. A mechanism such as mixing of locally-derived recharge with relatively depleted river water (**Table 1**) in the riparian zone is plausible and modelling of groundwater mixing regimes is the subject of a separate manuscript. Site LR01 (**Figure 6B**), which is located several kilometers from the river, shows a different evaporative pattern. Here, the mid-depth LR01-15 groundwater source shows a peak in relative evaporative enrichment around 85 %, which could reflect an increasing source of

evaporated surface waters at shallow to mid depths, possibly deriving from seasonal wetlands and transporting via near-surface sand windows. The most evaporated signatures are seen at site LR05 (**Figure 6C**), which is located near a permanent pond and sand window on T-Sand. The comparatively high relative evaporative signature (averaging around 80 % with a maximum > 95 %) indicates that highly evaporated recharge is likely at this site, probably as a result of connectivity with the nearby pond. Site LR14 (data not shown) is also located near a pond and exhibits similarly high evaporative signatures. Finally, the least relative evaporative signatures overall are seen at site LR10 (**Figure 6D**), averaging around 40 %. This site is located in close proximity to the Mekong River, and the lesser extent of evaporation could foreseeably be attributed to the large contribution of precipitation to the Mekong River and subsequent surface-groundwater interaction. Trends are generally very similar between pre- and post-monsoon sample sets. Along T-Sand (**Figure 6A, B, C**), pre-monsoon isotopic signatures are typically slightly more evaporated than post-monsoon, which is consistent with a contribution of recharge occurring during the (more evaporated) dry season. The stable isotopic composition of these groundwaters is indicative of surface-groundwater interactions at sites particularly near rivers (*e.g.* LR09, LR10), ponds (*e.g.* LR05) and/or sand windows (*e.g.* LR01). When the overall dataset is considered (**Figure 7**), groundwater sources from T-Sand generally have higher relative evaporation as compared to T-Clay, and the associations with transect are more apparent than with depth.

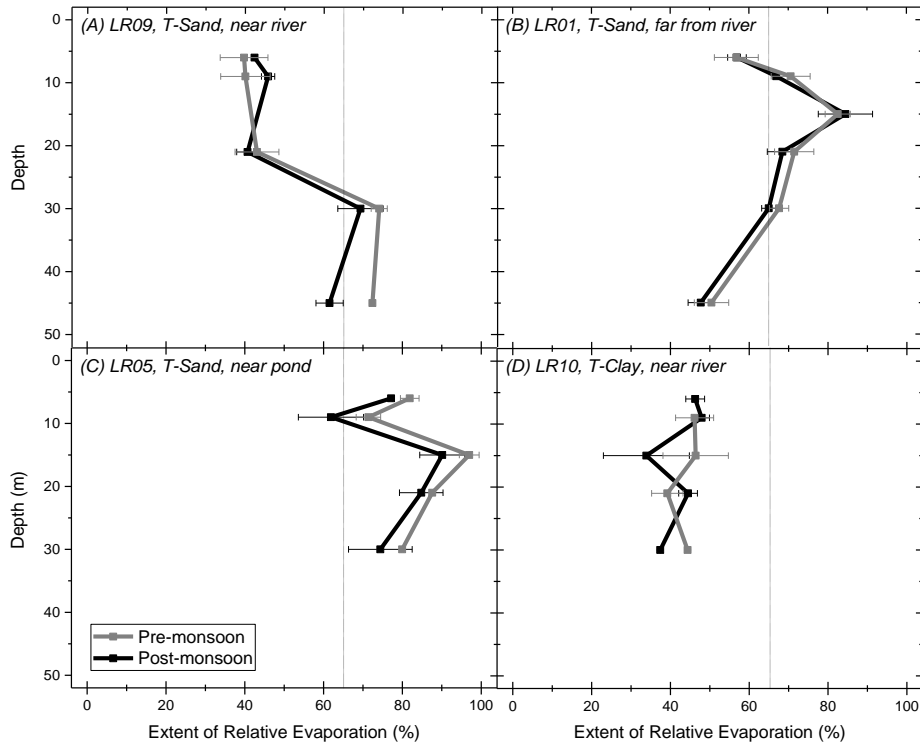


Figure 6. Estimated extent of relative recharge source evaporation with depth and site for groundwaters from northern Kandal Province, Cambodia using simple two-point mixing models assuming end-members of (i) a pond with the most enriched signature representing 100 % evaporation compared to that of the most evaporated water observed; and (ii) meteoric water with the most depleted signature from September 2014 representing 0 % evaporation. Reported values represent the mean of relative evaporation calculated from both $\delta^{18}\text{O}$ - and δD -based mixing models with error bars representing the range. The dashed line indicates the relative evaporation estimate calculated from the isotopic signature of the annual, volumetric-weighted mean of precipitation. Major well clusters on T-Sand are: (A) LR09; (B) LR01; (C) LR05; and T-Clay: (D) LR10. Sites LR09 and LR10 are located near the Bassac and Mekong rivers, respectively; site LR05 is near a pond; sites LR01 and LR05 are near sand windows.

431

432

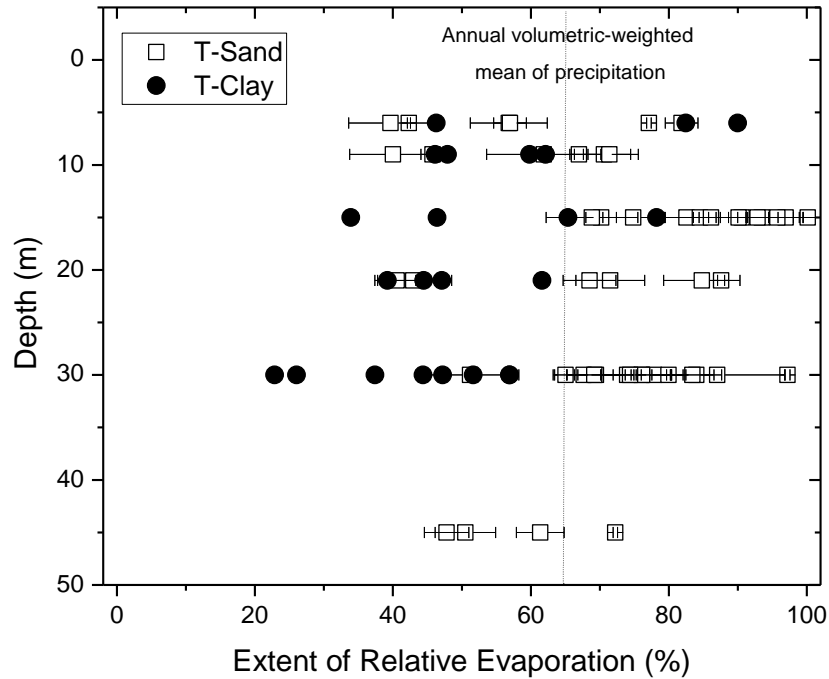


Figure 7. Estimated extent of relative source evaporation with depth and site for groundwaters from northern Kandal Province, Cambodia using simple two-point $\delta^{18}\text{O}$ - and δD -based mixing models for the overall groundwater dataset from T-Sand (open squares) and T-Clay (filled circles). The dashed line indicates the relative evaporation estimate calculated from the isotopic signature of the annual, volumetric-weighted mean of 2014 precipitation.

The modelled extent of relative groundwater source evaporation as qualitatively compared to mean, volumetric-weighted precipitation shows spatial patterns generally consistent with the proximity to surface water bodies (Figure 8). This suggests differing surface-groundwater interactions are occurring at various locations across both transects. For example, groundwater sources that are less evaporated than the mean precipitation are observed in locations near rivers (*e.g.* LR09 and LR10), whereas the majority of T-Sand has groundwater sources which are more evaporated than the mean precipitation. Some sites are variable with depth (*e.g.* LR14) which plausibly could be linked to local interactions with the nearby pond.

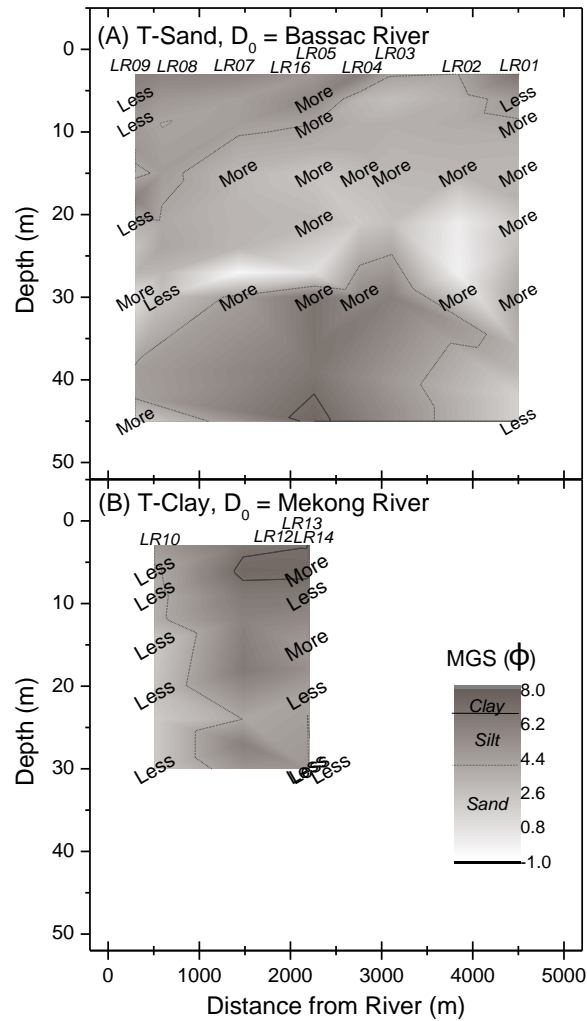


Figure 8. The modelled extent of relative groundwater source evaporation based on simple two-point $\delta^{18}\text{O}$ - and δD -based mixing models as compared to the relative extent of evaporation of the 2014 annual, volumetric-weighted mean of precipitation (65 %) for groundwater on (A) T-Sand and (B) T-Clay. “More” and “Less” refer to groundwater samples (mean of pre- and post-monsoon) with more and less evaporated sources as compared to the annual, volumetric-weighted mean of 2014 precipitation.

444

445 These comparisons should be considered indicative rather than absolute due to the

446 assumptions inherent in the mixing models, particularly since the modeled extents of

447 groundwater source evaporation are relative to the selected extreme end-members rather

448 than absolute values. The pre- and post-monsoon sampling campaigns represent two

449 “snap-shots” in time of a non-equilibrium and highly heterogeneous system, where non-

450 linear flowpaths, mixing of recharge sourced from different locations and time, and high

451 degrees of small-scale local variability are likely. The use of 2014 annual averages as mixing

452 model end-members inputs may not be sufficient. Realistically all samples will be recharged

by bulk and mixed sources over time, and thus a singular mean input for precipitation, ponds and rivers will not account for all recharge conditions. Furthermore, this mean value may not be suitable for all depths, as it assumes that recharge is the same throughout the entire depth profile and that recharge occurred under similar climatic conditions to 2014, which may not be the case particularly on T-Clay (as discussed on **Figure 4**) as well as because 2014 was the driest year in the study area from recent records (2008 – 2015) (Mekong River Commission, 2015). Regardless of these limitations, these comparative models still provide a useful tool for broadly differentiating between groundwater bodies within the aquifer.

The extent of relative groundwater source evaporation and the chloride concentration of the evaporative endmembers can be used to reconstruct a modelled chloride concentration of the groundwater samples (**Figure 9**). Distinct populations appear to be largely associated with the depth of the groundwater as well as with transect. One depth grouping, consisting of relatively deep (> 15 m depth) groundwaters, is poorly correlated with a weakly positive gradient of approximately 0.05:1 ($t(17) = 0.07$, $p = 0.95$; note this is not statistically significant). In contrast, the grouping of shallow (≤ 15 m depth) groundwaters has a weakly negative but statistically significant gradient of approximately -0.1:1 ($t(17) = -2.70$, $p = 0.02$). If the model were to reasonably describe the interactions in this system, it would be expected that the fit for all samples would be reasonably close to a 1:1 gradient. The observation that there are distinct populations, neither which is well-described by the model, suggests that other processes in addition to evaporation may also be important in some cases and/or that the selected end-members may not sufficiently describe the entire system. Evaporative processes are co-variant with the end-member parameters; for example evaporation will lead to linear changes in the concentration of the conservative tracer chloride but non-linear changes in isotopic compositions. In the case of the deep groundwater, the reconstructed chloride concentration exceeds the measured chloride in every case, which could suggest that the stable-isotope models overestimate the relative degree of source evaporation of these deeper groundwater samples. In contrast the reconstructed chloride concentration underestimates the chloride measured in shallow groundwater samples. This emphasizes the heterogeneity of the system. These differences may be attributed, in part to the co-variance of evaporation with the end-member

parameters, as well as the simplification of end-members selected to represent a complex and changing system (e.g. the end-member values selected only represent one point in time, and will change both spatially and temporally). Some small variations may be due to the presence of additional sources of chloride in the groundwater from natural and/or anthropogenic influences but this impact is likely to be minor compared to evaporative processes.

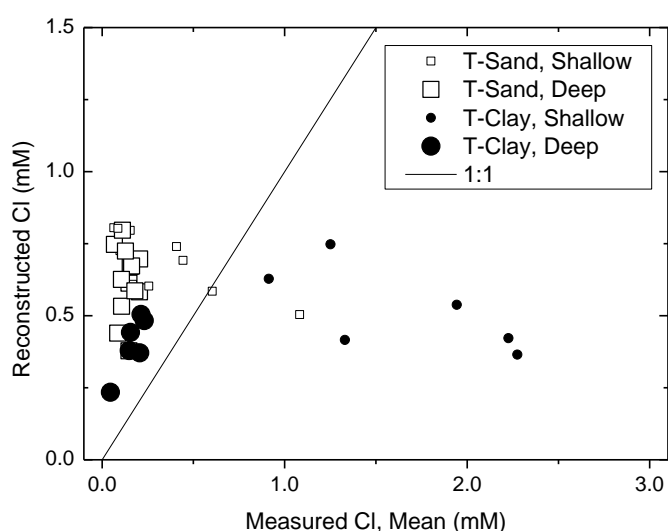


Figure 9. Calculated reconstructed chloride concentrations using the evaporative end-member chloride concentrations and relative extent of evaporation of recharge sources predicted by two-component mixing models against measured chloride (mean of post-and pre-monsoon samples) in groundwater samples from T-Sand (open square) and T-Clay (filled circle). Symbol size indicates if the groundwater is shallow (≤ 15 m depth) or deep (> 15 m depth).

The relationship between Cl/Br and chloride indicates distinct trends for T-Sand and T-Clay groundwaters (**Figure 10**). Water-rock interactions and/or leaching are indicated by a trend of higher chloride and higher Cl/Br ratios; this is particularly evident in the T-Clay groundwater samples. At sites LR10 and LR14 this might be consistent with their proximity to nearby pond and river, respectively, but the elevated chloride concentrations (**Figure 9**) are not consistent with the compositional variation being largely explained by rain water – river/pond water mixing. Instead LR10 and LR14 samples tend to fall between mixing lines calculated between the most dilute groundwater found in this study and West Bengal urine and seawater mixing as adapted from (McArthur et al., 2012). Although they tend in this

direction for these comparatively elevated (in Cl and Cl/Br) samples, the volumetric contributions of urine and/or seawater required to obtain the measured values are very small and are roughly < 0.2 % for seawater and < 2 % for urine as estimated from basic mixing models. This shows that inputs from urine or seawater are likely to be very small but still may influence the local groundwater geochemical signature in some sites. The shallow LR01-6 sample is located near a pig farm which may be plausibly associated with the relatively elevated Cl/Br and chloride observed here; similarly, though, a very small volumetric input of animal or human waste may be enough to shift the geochemical signature. The signature of the T-Clay groundwater is generally consistent with more extensive organic degradation, as organic matter preferentially concentrates Br over Cl, and more evaporation (which increases Cl but leaves Cl/Br unaffected) (McArthur et al., 2012) as compared to T-Sand. Many T-Sand groundwater samples fall along the apparent mixing line between rain and river water, with relatively low chloride and increasing Cl/Br. It is expected that rain water would have low chloride and Cl/Br and fall near the most dilute groundwater sample (Xie et al., 2012). The inverse relationship of Cl/Br with depth is apparent (**Figure 11**), with the correlation stronger for T-Clay ($t(13) = -3.23$, $p = 0.007$) than T-Sand ($t(23) = -1.82$, $p = 0.082$; note $p > \text{significance level of } 0.05$). The range of values observed are broadly consistent with other studies elsewhere in circum-Himalayan Asia, for example, in the Bengal Basin (McArthur et al., 2012; Majumder et al., 2016; McArthur et al., 2016) and China (Xie et al., 2012). Human and animal (e.g. pig) waste have been distinctively identified by Cl/Br ratios in other studies (Panno et al., 2006; McArthur et al., 2012); given that the field area has low population density and is relatively pristine, it is expected that these contributions are likely to be minimal overall but still may be locally important in some specific sites and/or samples (e.g. particularly shallow, sandy areas very near family and/or animal dwellings), which is supported by the typically relatively low Cl observed in groundwater samples here as compared to human and/or animal waste and the discussion above. On a greater regional scale, such as in the Bengal and/or Red River basins (McArthur et al., 2012) or elsewhere in the Mekong basin, it may be important to consider these impacts more broadly (McArthur et al., 2012).

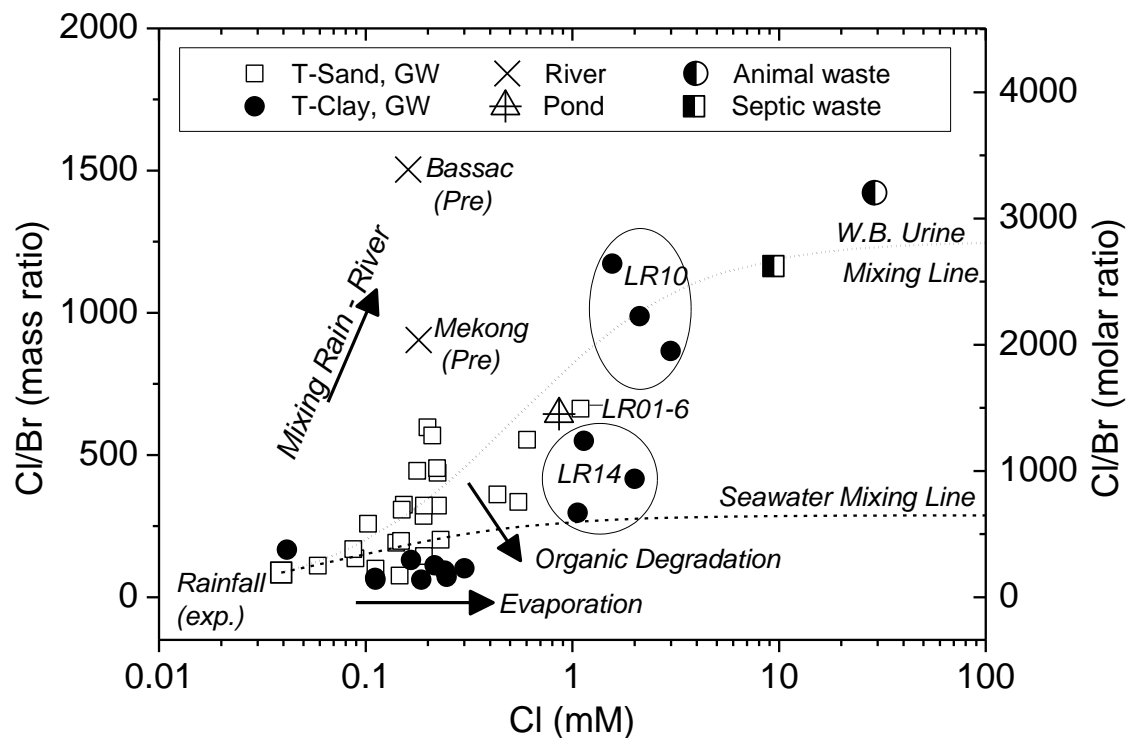


Figure 10. Cl/Br against Cl (mM, logarithmic scale) for groundwater, pond and river water and expected rainwater composition (noting that Br was not detected in the rain water sample so an exact Cl/Br for rain water could not be calculated) in northern Kandal Province, Cambodia; labels/circles are included for selected samples/sites particularly relevant to discussion. Distinct trends for T-Sand and T-Clay are observed. Mixing lines are adapted (McArthur et al., 2012) for mixing between West Bengal urine and seawater endmembers (McArthur et al., 2012) with the most dilute groundwater sample (this study, LR04-15-PRE, Cl = 0.04 mM Cl, Cl/Br = 87 by mass); septic effluent in USA and animal (hog and horse) (Panno et al., 2006) waste are shown for reference.

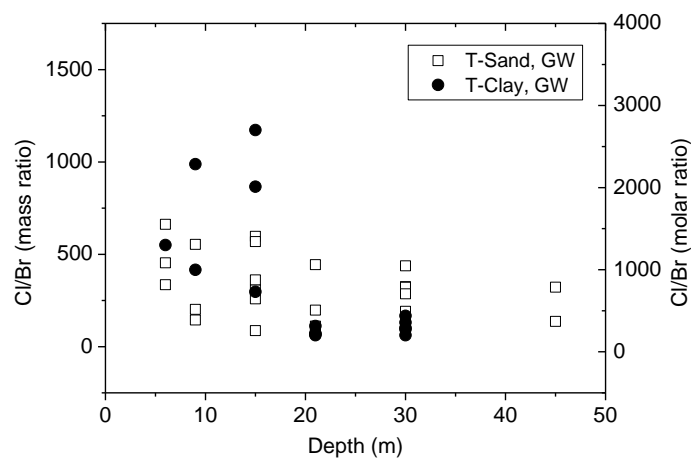


Figure 11. Cl/Br versus depth for groundwater along T-Sand (open squares) and T-Clay (filled circles).

533

534 The relationship between Cl/Br and $\delta^{18}\text{O}$ (**Figure 12**) further shows the distinction between
 535 T-Clay and T-Sand groundwater bodies, with the groundwater from LR10 approaching the
 536 high Cl/Br and low $\delta^{18}\text{O}$ observed in river samples, suggesting that there may be
 537 surface/river-groundwater connectivity near this site. Site LR09 along T-Sand, which is
 538 located near the Bassac River, also trends towards the direction of the river samples,
 539 although to a much lesser extent (particularly with regard to the Cl/Br) than the LR10
 540 groundwater. In addition, the single T-Clay sample falling on the opposite side with
 541 relatively high $\delta^{18}\text{O}$ trends towards a pond-similar signature, and is distinct from the other
 542 T-Clay samples. This groundwater sample is a shallow groundwater (6 m depth) from site
 543 LR14, which is located within meters of the nearby pond. This similarity indicates there may
 544 be surface/pond-groundwater connectivity near this site, consistent with the findings of
 545 Lawson *et al.* (2013).

546

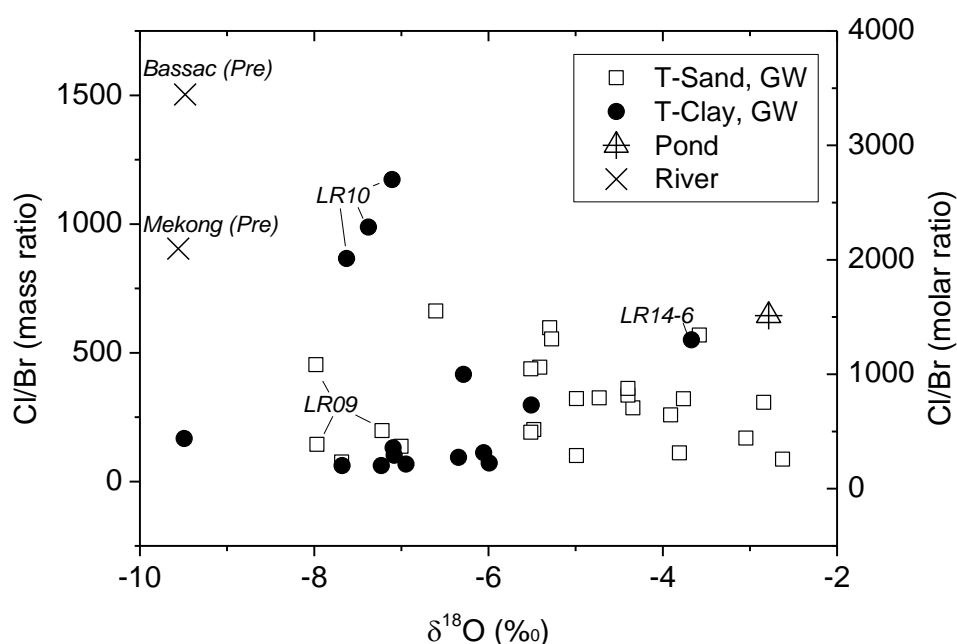


Figure 12. Cl/Br versus $\delta^{18}\text{O}$ for groundwater along T-Sand (open squares) and T-Clay (filled circles), pond (hatched triangle) and river (cross); labels/lines are included for selected samples/sites particularly relevant to discussion.

547

548 The distinct groundwater bodies and the complexity of geochemical interactions within the
 549 aquifer system are further observed when the Ca/Na mass ratio is considered alongside

stable isotope signatures (**Figure 13**). The Ca/Na ratio in natural waters is affected by weathering, sediment-water interactions and cloud type (Carroll, 1962; Khemani, 1968; Frape and Fritz, 1984). The following relative characterizations of various recharge sources and groundwaters can be observed: (i) ponds are characterized by low Ca/Na, and high $\delta^{18}\text{O}$ and δD (data not shown for δD); (ii) rivers are characterized by moderate Ca/Na and low $\delta^{18}\text{O}$ and δD ; and (iii) cumulative precipitation by high Ca/Na and moderate $\delta^{18}\text{O}$ and δD . The Ca/Na ratio of groundwater in T-Clay is generally lower than in T-Sand which could plausibly be attributed to the higher sorption capacity and ion exchange typically observed in clays as compared to sands. The deeper groundwaters in T-Clay tend to have lower $\delta^{18}\text{O}$ and δD and higher Ca/Na than shallower groundwaters, and the opposite trend is observed for T-Sand. These differences highlight that the groundwater populations from T-Clay and T-Sand are geochemically distinct. In general, more extensive water-rock interactions would be expected towards the direction of decreasing Ca/Na and $\delta^{18}\text{O}$ on **Figure 13**. The distinct trends with shallow and deep groundwater populations from both T-Sand and T-Clay indicate different recharge processes and hydrogeological conditions co-occurring within the aquifer.

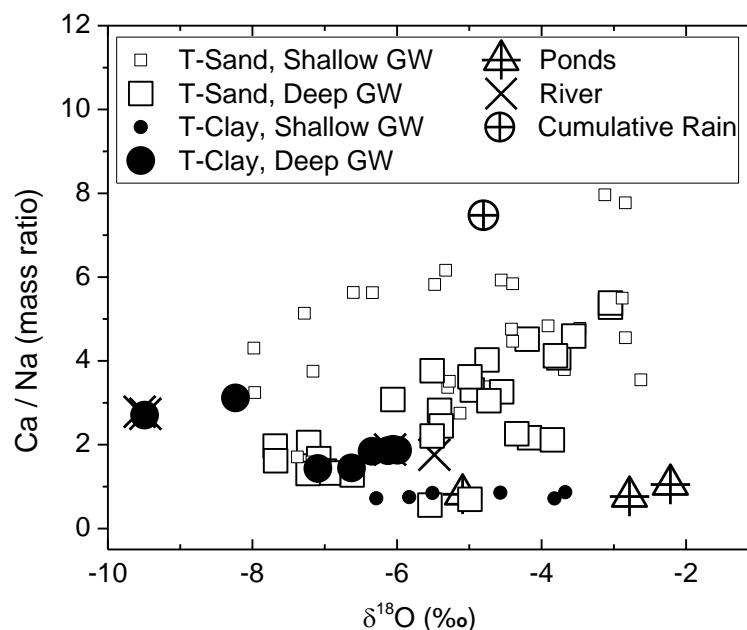


Figure 13. Ca/Na mass ratio against $\delta^{18}\text{O}$ for distinct groupings of shallow (≤ 15 m depth; smaller symbol size) and deep (> 15 m depth; larger symbol size) groundwaters from T-Clay (filled circles) and T-Sand (open squares), pond samples, river samples and cumulative

precipitation from northern Kandal Province, Cambodia. Groundwater from T-Clay typically has lower Ca/Na than groundwater from T-Sand.

3.4 Implications on Arsenic Mobilization

Groundwaters with high As (Richards et al., 2017a) show mixed trends in δD and $\delta^{18}O$ signature in comparison to the LMWL (**Figure 14A**). In a number of cases, high As groundwaters have a much more evaporated signature than the LMWL, which indicates that these groundwaters have been recharged by evaporated surface waters rather than directly by local precipitation. In other cases, high As groundwaters plot near the LMWL. Previously, high As groundwaters were shown to plot along the LMWL in West Bengal, which was used as evidence to suggest that evaporated perennial ponds were not an important source of recharge to shallow, As-affected waters (Datta et al., 2011). Our current data instead suggests that high As groundwaters can plot both near the LMWL as well as along evaporative trend lines, and thus evaporative ponds may be an important source of recharge in some circumstances, as has been suggested by Lawson *et al.* (Lawson et al., 2013; Lawson et al., 2016). The isotopic signatures reported here indicate a non-exclusive contribution of surface water to high As groundwater, consistent with but not conclusive that As release in shallow aquifers is driven in part by ingress of evaporated surface water, plausibly derived from ponds and/or wetlands. Similarly, high bulk DOC groundwaters (Richards et al., 2017a) plot both near the LMWL in some cases and, in other cases, have a much more evaporated signature than the LMWL (**Figure 14B**) indicating that high DOC groundwaters may derive from various recharge sources.

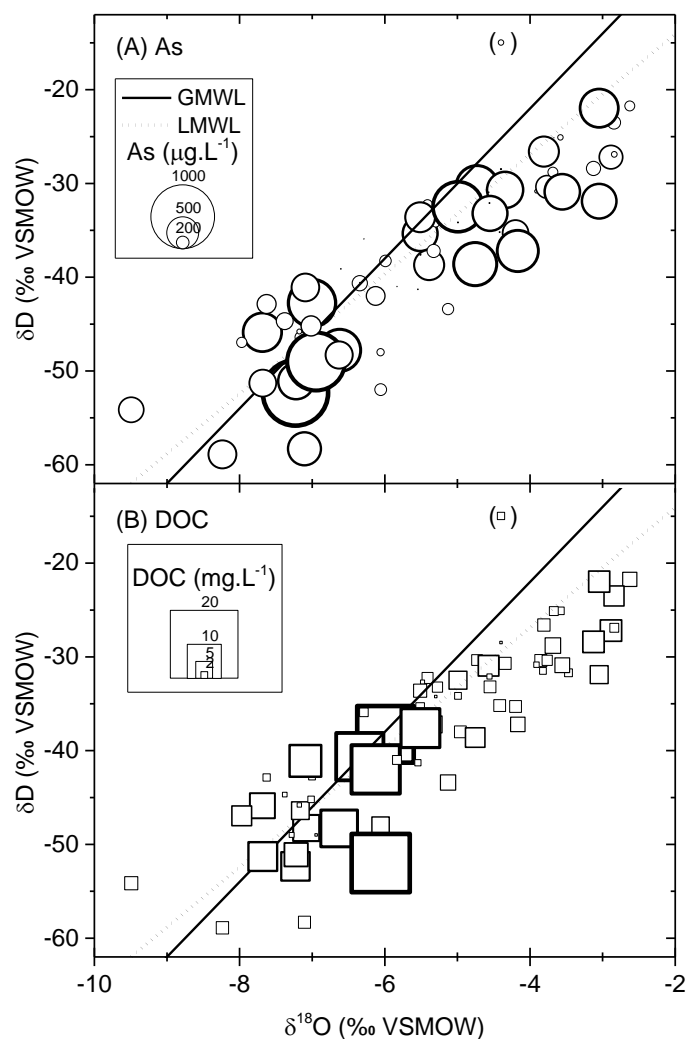


Figure 14. δD versus $\delta^{18}O$ for all groundwater samples in northern Kandal Province, Cambodia with (A) As concentrations and (B) bulk dissolved organic carbon (DOC) represented by bubble size (Richards et al., 2017a). Global Meteoric Water Line (GMWL) and Local Meteoric Water Line (LMWL) shown for comparison.

589

590 Groundwater As plotted against the modelled extent of source evaporation shows that As
 591 concentrations are very high in cases both where relative evaporation is greater or less than
 592 the annual volumetric-weighted mean of precipitation (**Figure 15**). In some cases high As is
 593 associated with evaporated surface water, likely derived from ponds and/or wetlands, and
 594 in other cases high As is associated with more precipitation-similar isotopic
 595 signatures. The high level of heterogeneity in As concentrations is likely to reflect both the
 596 inferred differing sources of organic carbon contributing to As mobilization and originating
 597 from the differing water bodies, as well as transport of released As within the aquifer. The

high heterogeneity observed is reflected also in the characterization of the aqueous inorganic geochemistry of the system (Richards et al., 2017a) and also highlights the difficulties associated with a priori extrapolation of conclusions from one site to another, even within a similar field area. For example, in general, most of the highest concentrations of As occur in more permeable sands along T-Sand, and interestingly the high As, less evaporated outliers observed on T-Clay are from a site (LR10) which is locally sandy despite being located along T-Clay (Richards et al., 2017a). Although δD and $\delta^{18}O$ do not provide direct evidence of the organic matter implicated in As release, their direct incorporation into the water molecule may be indicative of the presence of associated organic matter which is typical of a given recharge source. Thus, the data presented here speculates that mixed sources of organic matter (both surface- and sediment-derived) may be present throughout the shallow aquifers (Lawson et al., 2013; Lawson et al., 2016). The site-specific characterization of the organic matter and its role in As mobilization remains the subject of ongoing work.

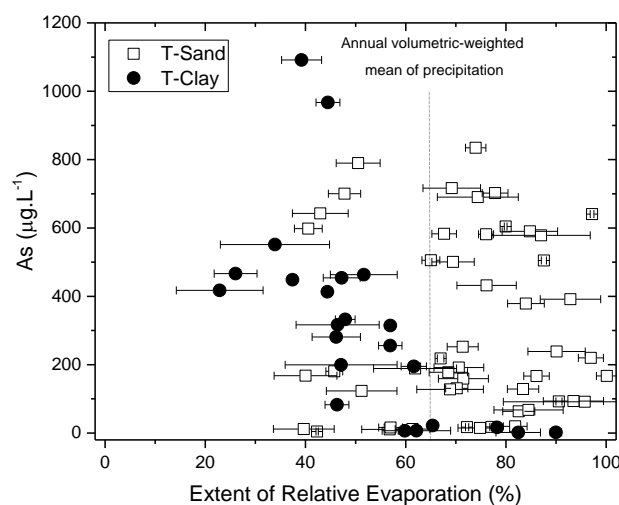


Figure 15. Groundwater As concentrations along T-Sand and T-Clay (Richards et al., 2017a) in northern Kandal Province, Cambodia with the modelled extent of relative evaporation of recharge sources. The estimated relative source evaporation is based on simple two-point mixing models assuming end-members of (i) a pond with the most enriched signature representing 100 % relative evaporation compared to that of the most evaporated water observed; and (ii) meteoric water with the most depleted signature from September 2014 representing 0 % evaporation. The dashed line indicates the relative source evaporation estimate calculated from the isotopic signature of the annual, volumetric-weighted mean of precipitation. Error bars represent the range of relative evaporation calculated using $\delta^{18}O$ - and δD -based mixing models.

4. Conclusions

The δD and $\delta^{18}O$ isotopic signature of groundwater in a heavily As-affected aquifer in Kandal Province, Cambodia in the Lower Mekong Basin was used to characterize the source of groundwater, categorize the systematics of surface waters and to differentiate between various groundwater bodies within the aquifers. Comparisons of groundwater with local precipitation and surface waters indicated varying trends with site, depth, transect and season. The relative extent of evaporation of groundwater sources was estimated based on the end-members showing the most depleted precipitation and most enriched pond signatures. Groundwaters in distinct populations were shown to have varying degrees of relative evaporation of recharge sources, consistent with lithology, locality and other geochemical observations, including the behaviour of the conservative tracer Cl/Br. High As groundwaters demonstrate varying degrees of source evaporation and plot both along the LMWL and along evaporative trend lines, indicating that high As groundwaters likely can be recharged both by local precipitation and by more evaporated surface water sources, consistent with (but not providing direct evidence for) models of a dual role of surface-derived and sedimentary organic matter in As mobilization. Such information, in conjunction with other isotopic and, particularly organic, geochemical measurements, is important to understanding the controls on As release and how As hazard may change in the future.

Acknowledgements

This research was funded by a NERC Standard Research Grant (NE/J023833/1) to DP, BvD and CB, a NERC PhD studentship (NE/L501591/1) to DM and a Leverhulme Trust Early Career Fellowship (ECF2015-657) to LR. Stable isotope analysis was supported by a NERC Isotope Geosciences Facilities award (IP-1505-1114). Sebastian Uhlemann (British Geological Survey and ETH Zurich) is thanked for adapting the site map provided. The following people are gratefully acknowledged for their contributions to the relevant field campaigns: Chansopheaktra Sovann (Royal University of Phnom Penh, Phnom Penh, Cambodia), Chivuth Kong, Pheary Meas and Yut Yann (all Royal University of Agriculture, Phnom Penh,

Cambodia), Chhengngunn Aing, Zongta Sang and Teyden Sok (all Royal University of Phnom Penh), Helen Downie (The University of Manchester) and Lee Chambers (The University of Lancaster). The support of the local landowners and drilling team led by Hok Meas was strongly appreciated. Ann Hall, Marc Hall, Lori Frees, Lori Allen and Dina Kuy (Resources Development International – Cambodia, RDI) are thanked for logistical support and the usage of laboratory facilities. Gren Turner, Barry Rawlins, Oliver Kuras (British Geological Survey) and Lee Chambers are thanked for support and/or advice regarding particle size distribution measurements. Lee Chambers also assisted with particle size measurements. We thank the reviewers whose feedback has improved the manuscript. The views expressed here do not necessarily represent those of any of the funders or individuals whose support is acknowledged.

References

- Aggarwal, P.K., Basu, A.R., Kulkarni, K.M., 2003. Comment on "Arsenic Mobility and Groundwater Extraction in Bangladesh" (I). *Science*, 300: 584b.
- Aggarwal, P.K., Basu, A.R., Poreda, R.J., Kulkarni, K.M., Froehlich, K., Tarafdar, S.A., Ali, M., Ahmed, N., Hussain, A., Rahman, M., Ahmed, S.R., 2000. Isotope hydrology of groundwater in Bangladesh: Implications for characterization and mitigation of arsenic in groundwater. In: BGD/8/016, I.-T.P.R. (Ed.). International Atomic Energy Agency, Vienna.
- Al Lawati, W.M., Jean, J.-S., Kulp, T.R., Lee, M.-K., Polya, D.A., Liu, C.-C., van Dongen, B.E., 2013. Characterisation of organic matter associated with groundwater arsenic in reducing aquifers of southwestern Taiwan. *J. Hazard. Mater.*, 262: 970 - 979.
- Al Lawati, W.M., Rizoulis, A., Eiche, E., Boothman, C., Polya, D.A., Lloyd, J.R., Berg, M., Vasquez-Aguilar, P., van Dongen, B.E., 2012. Characterisation of organic matter and microbial communities in contrasting arsenic-rich Holocene and arsenic-poor Pleistocene aquifers, Red River Delta, Vietnam. *Appl. Geochem.*, 27: 315 - 325.
- Alcalá, F.J., Custodio, R., 2005. Use of the Cl/Br ratio as a tracer to identify the origin of salinity in some coastal aquifers of Spain, 18th Salt Water Intrusion Meeting IGME y IAH, Cartagena, pp. 481 - 497.
- Appelo, C.A.J., Postma, D., 1993. *Geochemistry, groundwater and pollution*. Balkema.
- Araguás-Araguás, L., Froehlich, K., 1998. Stable isotope composition of precipitation over southeast Asia. *J. Geophys. Res.*, 103(D22): 28721 - 28742.
- Araguás-Araguás, L., Froehlich, K., Rozanski, K., 2000. Deuterium and oxygen-18 isotope composition of precipitation and atmospheric moisture. *Hydrol. Proc.*, 14: 1341 - 1355.
- Benner, S.G., Polizzotto, M.L., Kocar, B.D., Ganguly, S., Phan, K., Ouch, K., Sampson, M., Fendorf, S., 2008. Groundwater flow in an arsenic-contaminated aquifer, Mekong Delta, Cambodia. *Appl. Geochem.*, 23(11): 3072-3087.
- Berg, M., Trang, P.T.K., Stengel, C., Buschmann, J., Viet, P.H., Van Dan, N., Giger, W., Stüben, D., 2008. Hydrological and sedimentary controls leading to arsenic contamination of groundwater in the Hanoi area, Vietnam: The impact of iron-arsenic ratios, peat, river bank deposits, and excessive groundwater abstraction. *Chem. Geol.*, 249(1-2): 91-112.
- Bhattacharya, P., Chatterjee, D., Jacks, G., 1997. Occurrence of arsenic contaminated groundwater in alluvial aquifers from delta plains, Eastern India: Options for safe drinking water supply. *Wat. Res. Dev.*, 13: 79-92.
- Blott, S.J., Pye, K., 2001. GRADISTAT: A grain size distribution and statistics package for the analysis of unconsolidated sediments. *Eart. Surf. Proc. Land.*, 26: 1237 - 1248.
- Cambodia Investment, 2014. Municipality and Province Investment Information: Kandal Province (http://www.cambodiainvestment.gov.kh/wp-content/uploads/2014/03/Kandal-Province_eng.pdf, accessed Oct 2017).
- Carroll, D., 1962. Rainwater as a Chemical Agent of Geologic Processes - A Review. Geological Survey Water-Supply Paper 1535-G, U.S. Department of the Interior.
- Cartwright, I., Weaver, T.R., Fifield, L.K., 2006. Cl/Br ratios and environmental isotopes as indicators of recharge variability and groundwater flow: An example from the southeast Murray Basin, Australia. *Chem. Geol.*, 231: 38 - 56.

- Charlet, L., Polya, D.A., 2006. Arsenic in Shallow, Reducing Groundwaters in Southern Asia: An Environmental Health Disaster. *Elements*, 2: 91 - 96.
- Clark, I., Fritz, P., 1997. *Environmental Isotopes in Hydrogeology*. Lewis Publishers, New York.
- Craig, H., 1961. Isotopic Variations in Meteoric Waters. *Science*, 133(3465): 1702 - 1703.
- Craig, H., Gordon, L.I., 1965. Deuterium and oxygen 18 variations in the ocean and the marine atmosphere. 277 -374.
- Dansgaard, W., 1974. Stable isotopes in precipitation. *Tellus*, XVI(4).
- Datta, S., Neal, A.W., Mohajerin, T.J., Ocheltree, T., Rosenheim, B.E., White, C.D., Johannesson, K.H., 2011. Perennial ponds are not an important source of water or dissolved organic matter to groundwaters with high arsenic concentrations in West Bengal, India. *Geophysical Research Letters*, 38(L20404).
- Davis, S.N., Whittemore, D.O., Fabryka-Martin, J., 1998. Uses of Chloride/Bromide Ratios in Studies of Potable Water. *Groundwater*, 36(2): 338 - 350.
- Donnelly, T., Waldron, S., Tait, A., Dougans, J., Bearhop, S., 2001. Hydrogen isotope analysis of natural abundance and deuterium-enriched waters by reduction over chromium on-line to a dynamic dual inlet isotope-ratio mass spectrometer. *Rapid Commun. Mass Spectrom.*, 15: 1297-1303.
- Fendorf, S., Michael, H.A., van Geen, A., 2010. Spatial and temporal variations of groundwater arsenic in south and southeast Asia. *Science*, 328: 1123-1127.
- Frape, S.K., Fritz, P., 1984. Water-rock interaction and chemistry of groundwaters from the Canadian Shield. *Geochim. Cosmochim. Acta*, 48: 1617 - 1627.
- Gat, J.R., 1971. Comments on the Stable Isotope Method in Regional Groundwater Investigations. *Water Resour. Res.*, 7(4): 980 - 993.
- Gault, A.G., Islam, F.S., Polya, D.A., Charnock, J.M., Boothman, C., Chatterjee, D., Lloyd, J.R., 2005. Microcosm depth profiles of arsenic release in a shallow aquifer, West Bengal. *Mineralogical Magazine*, 69(5): 855-863.
- Harvey, C.F., Swartz, C.H., Badruzzaman, A.B.M., Keon-Blute, N., Ali, M.A., Jay, J., Beckie, R., Oates, P.M., Ashfaq, K.N., Islam, S., Hemond, H.F., Ahmed, M.F., 2003. Response to comments on "Arsenic mobility and groundwater extraction in Bangladesh". *Science*, 300: 584d.
- Harvey, C.F., Swartz, C.H., Badruzzaman, A.B.M., Keon-Blute, N., Yu, W., Ali, M.A., Jay, J., Beckie, R., Niedan, V., Brabander, D., Oates, P.M., Ashfaq, K.N., Islam, S., Hemond, H.F., Ahmed, M.F., 2005. Groundwater arsenic contamination on the Ganges Delta: biogeochemistry, hydrology, human perturbations, and human suffering on a large scale. *Comp. Rend. Geos.*, 337(1-2): 285-296.
- Harvey, C.F., Swartz, C.H., Badruzzaman, A.B.M., Keon-Blute, N., Yu, W., Ashraf Ali, M., Jay, J., Beckie, R., Niedan, V., Brabander, D., Oates, P.M., Ashfaq, K.N., Islam, S., Hemond, H.F., Ahmed, M.F., 2002. Arsenic mobility and groundwater extraction in Bangladesh. *Science*, 298: 1602-1606.
- Islam, F.S., Gault, A.G., Boothman, C., Polya, D.A., Charnock, J.M., Chatterjee, D., Lloyd, J.R., 2004. Role of metal-reducing bacteria in arsenic release from Bengal delta sediments. *Nature*, 430: 68-71.
- Kabeya, N., Kubota, T., Shimizu, A., Nobuhiro, T., Tsuboyama, Y., Chann, S., Tith, N., 2008. Isotopic investigation of river water mixing around the confluence of the Tonle Sap and Mekong rivers. *Hydrol. Proc.*, 22(0): 1351 - 1358.

- Kabeya, N., Shimizu, A., Chann, S., Tsuboyama, Y., Nobuhiro, T., Keth, N., Tamai, K., 2007. Stable Isotope Studies of Rainfall and Stream Water in Forest Watersheds in Kampong Thom, Cambodia, Forest Environments in the Mekong River Basin, pp. 125 - 134.
- Khemani, L.T., 1968. Chemical composition of rain water and rain characteristics of Delhi. *Tellus*, 20(2): 284 - 292.
- Klump, S., Kipfer, R., Cirpka, O.A., Harvey, C.F., Brennwald, M.S., Ashfaq, K.N., Badruzzaman, A.B.M., Hug, S.J., Imboden, D.M., 2006. Groundwater dynamics and arsenic mobilization in Bangladesh assessed using noble gases and tritium. *Environ. Sci. Technol.*, 40: 243-250.
- Kocar, B.D., Polizzotto, M.L., Benner, S.G., Ying, S.C., Ung, M., Ouch, K., Samreth, S., Suy, B., Phan, K., Sampson, M., Fendorf, S., 2008. Integrated biogeochemical and hydrologic processes driving arsenic release from shallow sediments to groundwaters of the Mekong delta. *Appl. Geochem.*, 23(11): 3059-3071.
- Kondoh, A., Shimada, J., 1997. The Origin of Precipitation in Eastern Asia by Deuterium Excess. *J. Jap. Soc. Hydrol. Wat. Res.*, 10(6): 627 - 629.
- Lawson, M., Polya, D.A., Boyce, A.J., Bryant, C., Ballentine, C.J., 2016. Tracing organic matter composition and distribution and its role on arsenic release in shallow Cambodian groundwaters. *Geochim. Cosmochim. Acta*, 178: 160 - 177.
- Lawson, M., Polya, D.A., Boyce, A.J., Bryant, C., Mondal, D., Shantz, A., Ballentine, C.J., 2013. Pond-derived organic carbon driving changes in arsenic hazard found in Asian groundwaters. *Environ. Sci. Technol.*, 47: 7085 - 7094.
- Magnone, D., Richards, L.A., Polya, D.A., Bryant, C., Jones, M., van Dongen, B.E., 2017. Biomarker-indicated extent of oxidation of plant-derived organic carbon (OC) in relation to geomorphology in an arsenic contaminated Holocene aquifer, Cambodia. *Sci. Rep.*, 7(13093): DOI:10.1038/s41598-017-13354-8.
- Mailloux, B.J., Trembath-Reichert, E., Cheung, J., Watson, M., Stute, M., Freyer, G.A., Ferguson, A.S., Ahmed, K.M., Alam, M.J., Buchholz, B.A., Thomas, J., Layton, A.C., Zheng, Y., Bostick, B.C., van Geen, A., 2013. Advection of surface-derived organic carbon fuels microbial reduction in Bangladesh groundwater. *PNAS*, 110(13): 5331 - 5335.
- Majumder, S., Datta, S., Nath, B., Neidhardt, H., Sarkar, S., Roman-Ross, G., Berner, Z., Hidalgo, M., Chatterjee, D., 2016. Monsoonal influence on variation of hydrochemistry and isotopic signatures: Implications for associated arsenic release in groundwater. *J. Hydrol.*, 535: 407 - 417.
- McArthur, J., Ravenscroft, P., Safiulla, S., Thirwall, M.F., 2001. Arsenic in groundwater: Testing pollution mechanisms for sedimentary aquifers in Bangladesh. *Water Resour. Res.*, 37(1): 109-117.
- McArthur, J.M., Banerjee, D.M., Hudson-Edwards, K.A., Mishra, R., Purohit, R., Ravenscroft, P., Cronin, A., Howarth, R.J., Chatterjee, A., Talukder, T., Lowry, D., Houghton, S., Chadha, D.K., 2004. Natural organic matter in sedimentary basins and its relation to arsenic in anoxic ground water: the example of West Bengal and its worldwide implications. *Appl. Geochem.*, 19(8): 1255-1293.
- McArthur, J.M., Ghosal, U., Sikdar, P.K., Ball, J.D., 2016. Arsenic in Groundwater: The Deep Late Pleistocene Aquifers of the Western Bengal Basin. *Environ. Sci. Technol.*, 50(7): 3469 - 3476.

792 McArthur, J.M., Ravenscroft, P., Sracek, O., 2011. Aquifer arsenic source. *Nat. Geos.*, 4(10):
793 655 - 656.

794 McArthur, J.M., Sikdar, P.K., Hoque, M.A., Ghosal, U., 2012. Waste-water impacts on
795 groundwater: Cl/Br ratios and implications for arsenic pollution of groundwater in
796 the Bengal Basin and Red River Basin, Vietnam. *Sci. Total Environ.*, 437: 390 - 402.

797 Mekong River Commission, 2015. Historical Records
798 (http://ffw.mrcmekong.org/historical_rec.htm, last accessed 20 October 2015).

799 Merlivat, L., Jouzel, J., 1979. Global Climatic Interpretation of the Deuterium-Oxygen 18
800 Relationship for Precipitation. *J. Geophys. Res.*, 84(C8): 5029 - 5033.

801 Miller, J.N., Miller, J.C., 2010. Chapter 5: Calibration methods in instrumental analysis:
802 regression and correlation, *Statistics and Chemometrics for Analytical Chemistry*.
803 Pearson Education.

804 Mladenov, N., Zheng, Y., Miller, M.P., Nemergut, D.R., Legg, T., Simone, B., Hageman, C.,
805 Rahman, M.M., Ahmed, K.M., McKnight, D.M., 2010. Dissolved Organic Matter
806 Sources and Consequences for Iron and Arsenic Mobilization in Bangladesh Aquifers.
807 *Environ. Sci. Technol.*, 44(1): 123 - 128.

808 Mukherjee, A., Fryar, A.E., Rowe, H.D., 2007. Regional-scale stable isotopic signatures of
809 recharge and deep groundwater in the arsenic affected areas of West Bengal, India.
810 *J. Hydrol.*, 334(1-2): 151-161.

811 Nelson, S.T., 2000. A simple, practical methodology for routine VSMOW/SLAP normalization
812 of water samples analyzed by continuous flow methods. *Rapid Commun. Mass*
813 *Spectrom.*, 14: 1044 - 1046.

814 Neumann, R.B., Ashfaq, K.N., Badruzzaman, A.B.M., Ali, M.A., Shoemaker, J.K., Harvey,
815 C.F., 2010. Anthropogenic influences on groundwater arsenic concentrations in
816 Bangladesh. *Nat. Geos.*, 3(1): 46-52.

817 Neumann, R.B., Ashfaq, K.N., Badruzzaman, A.B.M., Ali, M.A., Shoemaker, J.K., Harvey,
818 C.F., 2011. Aquifer arsenic source reply. *Nat. Geos.*

819 Neumann, R.B., Polizzotto, M.L., Badruzzaman, A.B.M., Ali, M.A., Zhang, Z.Y., Harvey, C.F.,
820 2009. Hydrology of a groundwater-irrigated rice field in Bangladesh: Seasonal and
821 daily mechanisms of infiltration. *Water Resour. Res.*, 45: 14.

822 Neumann, R.B., Pracht, L.E., Polizzotto, M.L., Badruzzaman, A.B.M., Ashraf Ali, M., 2014.
823 Biodegradable Organic Carbon in Sediments of an Arsenic-Contaminated Aquifer in
824 Bangladesh. *Environmental Science and Technology Letters*, 1: 221 - 225.

825 Nickson, R.T., McArthur, J.M., Burgess, W.G., Ahmed, K.M., Ravenscroft, P., Rahman, M.,
826 1998. Arsenic poisoning of Bangladesh groundwater. *Nature*, 395: 338.

827 Panno, S.V., Hackley, K.C., Hwang, H.H., Greenberg, S.E., Krapac, I.G., Landsberger, S.,
828 O'Kelly, D.J., 2006. Characterization and Identification of Na-Cl Sources in
829 Groundwater. *Groundwater*, 44(2): 176 - 187.

830 Papacostas, N.C., Bostick, B., Quicksall, A.N., Landis, J.D., Sampson, M., 2008. Geomorphic
831 controls on groundwater arsenic distribution in the Mekong River Delta, Cambodia.
832 *Geology*, 36(11): 891-894.

833 Pfahl, S., Sodemann, H., 2014. What controls deuterium excess in global precipitation? *Clim.*
834 *Past*, 10: 771 - 781.

835 Polizzotto, M.L., Kocar, B.D., Benner, S.G., Sampson, M., Fendorf, S., 2008. Near-surface
836 wetland sediments as a source of arsenic release to ground water in Asia. *Nature*,
837 454: 505-508.

838 Poly, D.A., Charlet, L., 2009. Rising arsenic risk? *Nat. Geos.*, 2(6): 383-384.

839 Polya, D.A., Gault, A.G., Bourne, N.J., Lythgoe, P.R., Cooke, D.A., 2003. Coupled HPLC-ICP-MS
840 analysis indicates highly hazardous concentrations of dissolved arsenic species in
841 Cambodian groundwaters. *Royal Society of Chemistry Special Publication*, 288: 127 -
842 140.

843 Polya, D.A., Gault, A.G., Diebe, N., Feldman, P., Rosenboom, J.W., Gilligan, E., Fredericks, D.,
844 Milton, A.H., Sampson, M., Rowland, H.A.L., Lythgoe, P.R., Jones, J.C., Middleton, C.,
845 Cooke, D.A., 2005. Arsenic hazard in shallow Cambodian groundwaters.
846 *Mineralogical Magazine*, 69(5): 807-823.

847 Polya, D.A., Richards, L.A., Al Bualy, A.N., Sovann, C., Magnone, D., Lythgoe, P.R., 2017.
848 Chapter A14: Groundwater sampling, arsenic analysis and risk communication:
849 Cambodia Case Study. In: Bhattacharya, P., Polya, D.A., Jovanovic, D. (Eds.), *Best*
850 *Practice Guide for the Control of Arsenic in Drinking Water*. IWA Publishing.

851 Postma, D., Larsen, F., Minh Hue, N.T., Duc, M.T., Viet, P.H., Nhan, P.Q., Jessen, S., 2007.
852 Arsenic in groundwater of the Red River floodplain, Vietnam: Controlling
853 geochemical processes and reactive transport modeling. *Geochim. Cosmochim. Acta*,
854 71(21): 5054-5071.

855 Ravenscroft, P., Brammer, H., Richards, K., 2009. Arsenic pollution - A global synthesis. *Royal*
856 *Geographical Society with IBG. Wiley-Blackwell*, Chichester, 588 pp.

857 Rawlins, B.G., Webster, R., Tye, A.M., Lawley, R., O'Hara, S.L., 2009. Estimating particle-size
858 fractions of soil dominated by silicate minerals from geochemistry. *European Journal*
859 *of Soil Science*, 60: 116 - 126.

860 Richards, L.A., Magnone, D., Sovann, C., Kong, C., Uhlemann, S., Kuras, O., van Dongen, B.E.,
861 Ballentine, C.J., Polya, D.A., 2017a. High Resolution Profile of Inorganic Aqueous
862 Geochemistry and Key Redox Zones in an Arsenic Bearing Aquifer in Cambodia. *Sci.*
863 *Total Environ.*, 590 - 591: 540 - 553.

864 Richards, L.A., Magnone, D., van Dongen, B.E., Ballentine, C.J., Polya, D.A., 2015. Use of
865 Lithium Tracers to Quantify Drilling Fluid Contamination for Groundwater Monitoring
866 in Southeast Asia. *Appl. Geochem.*, 63: 190 - 202.

867 Richards, L.A., Sültenfuß, J., Ballentine, C.J., Magnone, D., van Dongen, B.E., Sovann, C.,
868 Polya, D.A., 2017b. Tritium Tracers of Rapid Surface Water Ingression into Arsenic-
869 Bearing Aquifers in the Lower Mekong Basin, Cambodia. *Procedia Earth and*
870 *Planetary Science*, 17C: 849 - 852.

871 Rowland, H.A.L., Boothman, C., Pancost, R.D., Gault, A.G., Polya, D.A., Lloyd, J.R., 2009. The
872 role of indigenous microorganisms in the biodegradation of naturally occurring
873 petroleum, the reduction of iron, and the mobilization of arsenite from West Bengal
874 aquifer sediments. *J. Env. Qual.*, 38(4): 1598 - 1607.

875 Rowland, H.A.L., Gault, A.G., Lythgoe, P., Polya, D.A., 2008. Geochemistry of aquifer
876 sediments and arsenic-rich groundwaters from Kandal Province, Cambodia. *Appl.*
877 *Geochem.*, 23(11): 3029-3046.

878 Rowland, H.A.L., Pederick, R.L., Polya, D.A., Pancost, R.D., Van Dongen, B.E., Gault, A.G.,
879 Vaughan, D.J., Bryant, C., Anderson, B., Lloyd, J.R., 2007. The control of organic
880 matter on microbially mediated iron reduction and arsenic release in shallow alluvial
881 aquifers, Cambodia. *Geobio.*, 5: 281-292.

882 Rozanski, K., Araguás-Araguás, L., Gonfiantini, R., 1993. *Isotopic Patterns in Modern Global*
883 *Precipitation. Climate Change in Continental Isotopic Records, Geochemical*
884 *Monograph 78(American Geophysical Union).*

- Schaefer, M.V., Ying, S.C., Benner, S.G., Duan, Y., Wang, Y., Fendorf, S., 2016. Aquifer Arsenic Cycling Induced by Seasonal Hydrologic Changes within the Yangtze River Basin. *Environ. Sci. Technol.*, 50(7): 3521 - 3529.
- Sengupta, S., McArthur, J., Sarkar, A., Leng, M.J., Ravenscroft, P., Howarth, R.J., Banerjee, D.M., 2008. Do Ponds Cause Arsenic-Pollution of Groundwater in the Bengal Basin? An Answer from West Bengal. *Environ. Sci. Technol.*, 42: 5156 - 5164.
- Smedley, P.L., Kinniburgh, D.G., 2002. A review of the source, behaviour and distribution of arsenic in natural waters. *Appl. Geochem.*, 17(5): 517-568.
- Stuben, D., Berner, Z., Chandrasekharam, D., Karmaker, J., 2003. Arsenic enrichment in groundwater of West Bengal, India: geochemical evidence for mobilization of As under reducing conditions. *Appl. Geochem.*, 18: 1417-1434.
- Stuckey, J.W., Schaefer, M.V., Kocar, B.D., Benner, S.G., Fendorf, S., 2016. Arsenic release metabolically limited to permanently water-saturated soil in Mekong Delta. *Nat. Geos.*, 9: 70 - 76.
- Tamura, T., Saito, Y., Sieng, S., Ben, B., Kong, M., Choup, S., Tsukawaki, S., 2007. Depositional facies and radiocarbon ages of a drill core from the Mekong River lowland near Phnom Penh, Cambodia: Evidence for tidal sedimentation at the time of Holocene maximum flooding. *J. Asia. Ear. Sci.*, 29(5-6): 585-592.
- Uhlemann, S., Kuras, O., Richards, L.A., Naden, E., Polya, D.A., 2017. Electrical Resistivity Tomography determines the spatial distribution of clay layer thickness and aquifer vulnerability, Kandal Province, Cambodia. *J. Asia. Ear. Sci.*, 147: 402 - 414.
- van Dongen, B., Rowland, H.A.L., Gault, A.G., Polya, D.A., Bryant, C., Pancost, R.D., 2008. Hopane, sterane and n-alkane distributions in shallow sediments hosting high arsenic groundwaters in Cambodia. *Appl. Geochem.*, 23: 3047 - 3058.
- van Geen, A., Rose, J., Thorai, S., Garnier, J.M., Zheng, Y., Bottero, J.Y., 2004. Decoupling of As and Fe release to Bangladesh groundwater under reducing conditions. Part II: Evidence from sediment incubations. *Geochim. Cosmochim. Acta*, 68(17): 3475-3486.
- van Geen, A., Zheng, Y., Stute, M., Ahmed, K.M., 2003. Comment on "Arsenic mobility and groundwater extraction in Bangladesh" (II). *Science*, 300: 584c.
- Vandenbergh, J., Zhisheng, A., Nugteren, G., Huary, L., Van Huissteden, K., 1997. New absolute time scale for the Quaternary climate in the Chinese loess region by grain-size analysis. *Geology*, 25(1): 35 - 38.
- Water and Sanitation Program, 2015. Water Supply and Sanitation in Cambodia: Turning Finance into Services for the Future (<https://www.wsp.org/sites/wsp.org/files/publications/WSP-Cambodia-WSS-Turning-Finance-into-Service-for-the-Future.pdf>, accessed Oct 2017).
- World Health Organization, 2011. Guidelines for Drinking-water Quality: Fourth Edition, Geneva.
- Xie, X., Wang, Y., Su, C., Li, J., Li, M., 2012. Influence of irrigation practices on arsenic mobilization: Evidence from isotope composition and Cl/Br ratios in groundwater from Datong Basin, northern China. *J. Hydrol.*, 424 - 426: 37 - 47.
- Zheng, Y., van Geen, A., Stute, M., Dhar, R., Mo, Z., Cheng, Z., Horneman, A., Gavrieli, I., Simpson, H.J., Versteeg, R., Steckler, M., Grazioli-Venier, A., Goodbred, S., Shahnewaz, M., Shamsudduha, M., Hoque, M.A., Ahmed, K.M., 2005. Geochemical and hydrogeological contrasts between shallow and deeper aquifers in two villages

931 of Araihasar, Bangladesh: Implications for deeper aquifers as drinking water sources.
932 Geochim. Cosmochim. Acta, 69(22): 5203-5218.

933

934

List of Figures

Figure 1. Map of field area and sampling locations in northern Kandal Province, Cambodia (adapted from Richards et al., 2017a; Uhlemann et al., 2017).

Figure 2. δD versus $\delta^{18}O$ of groundwaters (T-Sand and T-Clay), surface water and precipitation in northern Kandal Province, Cambodia. Groundwater and surface samples were collected (A) pre-monsoon (May – June 2014) and (B) post-monsoon (November – December 2014) and local precipitation samples were collected as cumulative weekly samples taken the first week of each month from July to November 2014. The local meteoric water line is derived from the precipitation samples.

Figure 3. Temporal variability of $\delta^{18}O$ from May 2014 – December 2014 in local precipitation and surface waters in northern Kandal Province, Cambodia (River = Mekong (MEK) and Bassac (BAS) Rivers; Isolated Ponds = near site LR14 on T-Clay and another near site LR05 on T-Sand). Local precipitation samples were collected each month (as cumulative weekly samples) during the monsoon season and river and pond samples were collected during the pre- and post-monsoon water sampling campaigns, marked as grey boxes.

Figure 4. (A) δD and (B) $\delta^{18}O$ and Depth for T-Sand and T-Clay, northern Kandal Province, Cambodia. There is no statistically significant relationship between depth and δD nor $\delta^{18}O$ on T-Sand, suggesting that deep samples on T-Sand were recharged under similar climatic conditions which currently prevail. The slightly negative correlation for T-Clay suggests that some recharge may have occurred under different climatic conditions than currently prevail.

Figure 5. Distribution of (A and C) δD and (B and D) $\delta^{18}O$ across (A and B) T-Sand and (C and D) T-Clay. More negative isotopic values represent more depleted isotopic signatures and are shown by smaller size bubbles. The underlying contour represents the mean grain size (MGS) in sediments collected from the same locations within the aquifer, with darker colors representing smaller mean particle size.

Figure 6. Estimated extent of relative recharge source evaporation with depth and site for groundwaters from northern Kandal Province, Cambodia using simple two-point mixing models assuming end-members of (i) a pond with the most enriched signature representing 100 % evaporation compared to that of the most evaporated water observed; and (ii) meteoric water with the most depleted signature from September 2014 representing 0 % evaporation. Reported values represent the mean of relative evaporation calculated from both $\delta^{18}O$ - and δD -based mixing models with error bars representing the range. The dashed line indicates the relative evaporation estimate calculated from the isotopic signature of the annual, volumetric-weighted mean of precipitation. Major well clusters on T-Sand are: (A) LR09; (B) LR01; (C) LR05; and T-Clay: (D) LR10. Sites LR09 and LR10 are located near the Bassac and Mekong rivers, respectively; site LR05 is near a pond; sites LR01 and LR05 are near sand windows.

Figure 7. Estimated extent of relative source evaporation with depth and site for groundwaters from northern Kandal Province, Cambodia using simple two-point $\delta^{18}\text{O}$ - and δD -based mixing models for the overall groundwater dataset from T-Sand (open squares) and T-Clay (filled circles). The dashed line indicates the relative evaporation estimate calculated from the isotopic signature of the annual, volumetric-weighted mean of 2014 precipitation.

Figure 8. The modelled extent of relative groundwater source evaporation based on simple two-point $\delta^{18}\text{O}$ - and δD -based mixing models as compared to the relative extent of evaporation of the 2014 annual, volumetric-weighted mean of precipitation (65 %) for groundwater on (A) T-Sand and (B) T-Clay. “More” and “Less” refer to groundwater samples (mean of pre- and post-monsoon) with more and less evaporated sources as compared to the annual, volumetric-weighted mean of 2014 precipitation.

Figure 9. Calculated reconstructed chloride concentrations using the evaporative end-member chloride concentrations and relative extent of evaporation of recharge sources predicted by two-component mixing models against measured chloride (mean of post-and pre-monsoon samples) in groundwater samples from T-Sand (open square) and T-Clay (filled circle). Symbol size indicates if the groundwater is shallow (≤ 15 m depth) or deep (> 15 m depth).

Figure 10. Cl/Br against Cl (mM, logarithmic scale) for groundwater, pond and river water and expected rainwater composition (noting that Br was not detected in the rain water sample so an exact Cl/Br for rainwater could not be calculated) in northern Kandal Province, Cambodia; labels/circles are included for selected samples/sites particularly relevant to discussion. Distinct trends for T-Sand and T-Clay are observed. Mixing lines are adapted (McArthur et al., 2012) for mixing between West Bengal urine and seawater endmembers (McArthur et al., 2012) with the most dilute groundwater sample (this study, LR04-15-PRE, $\text{Cl} = 0.04$ mM Cl , $\text{Cl}/\text{Br} = 87$ by mass); septic effluent in USA and animal (hog and horse) (Panno et al., 2006) waste are shown for reference.

Figure 11. Cl/Br versus depth for groundwater along T-Sand (open squares) and T-Clay (filled circles).

Figure 12. Cl/Br versus $\delta^{18}\text{O}$ for groundwater along T-Sand (open squares) and T-Clay (filled circles), pond (hatched triangle) and river (cross); labels/lines are included for selected samples/sites particularly relevant to discussion.

Figure 13. Ca/Na mass ratio against $\delta^{18}\text{O}$ for distinct groupings of shallow (≤ 15 m depth; smaller symbol size) and deep (> 15 m depth; larger symbol size) groundwaters from T-Clay (filled circles) and T-Sand (open squares), pond samples, river samples and cumulative precipitation from northern Kandal Province, Cambodia. Groundwater from T-Clay typically has lower Ca/Na than groundwater from T-Sand.

Figure 14. δD versus $\delta^{18}O$ for all groundwater samples in northern Kandal Province, Cambodia with (A) As concentrations and (B) bulk dissolved organic carbon (DOC) represented by bubble size (Richards et al., 2017a). Global Meteoric Water Line (GMWL) and Local Meteoric Water Line (LMWL) shown for comparison.

Figure 15. Groundwater As concentrations along T-Sand and T-Clay (Richards et al., 2017a) in northern Kandal Province, Cambodia with the modelled extent of relative evaporation of recharge sources. The estimated relative source evaporation is based on simple two-point mixing models assuming end-members of (i) a pond with the most enriched signature representing 100 % relative evaporation compared to that of the most evaporated water observed; and (ii) meteoric water with the most depleted signature from September 2014 representing 0 % evaporation. The dashed line indicates the relative source evaporation estimate calculated from the isotopic signature of the annual, volumetric-weighted mean of precipitation. Error bars represent the range of relative evaporation calculated using $\delta^{18}O$ - and δD -based mixing models.

1026 **List of Tables**

1027 **Table 1.** Mean δD and $\delta^{18}O$ for groundwaters (GW) and surface water (SW) in northern
1028 Kandal Province, Cambodia during pre- and post-monsoon conditions and volumetric-
1029 weighted mean of precipitation. Rainfall data is from the Mekong River Commission
1030 Monitoring Station Phnom Penh Chaktomuk (Bassac) (Mekong River Commission, 2015);
1031 * indicates that only one sample was collected.

1032